



8-2007

Characterization of the Role of Mouse *Nell1* Gene in Osteogenesis and Chondrogenesis During Mammalian Fetal Development

Jayashree Basavaraj Desai
University of Tennessee - Knoxville

Recommended Citation

Desai, Jayashree Basavaraj, "Characterization of the Role of Mouse *Nell1* Gene in Osteogenesis and Chondrogenesis During Mammalian Fetal Development." PhD diss., University of Tennessee, 2007.
https://trace.tennessee.edu/utk_graddiss/153

This Dissertation is brought to you for free and open access by the Graduate School at Trace: Tennessee Research and Creative Exchange. It has been accepted for inclusion in Doctoral Dissertations by an authorized administrator of Trace: Tennessee Research and Creative Exchange. For more information, please contact trace@utk.edu.

To the Graduate Council:

I am submitting herewith a dissertation written by Jayashree Basavaraj Desai entitled "Characterization of the Role of Mouse *Nell1* Gene in Osteogenesis and Chondrogenesis During Mammalian Fetal Development." I have examined the final electronic copy of this dissertation for form and content and recommend that it be accepted in partial fulfillment of the requirements for the degree of Doctor of Philosophy, with a major in Life Sciences.

Cymbeline T. Culiati, Major Professor

We have read this dissertation and recommend its acceptance:

Bruce McKee, Brynn Voy, Yisong Wang

Accepted for the Council:

Dixie L. Thompson

Vice Provost and Dean of the Graduate School

(Original signatures are on file with official student records.)

To the Graduate Council:

I am submitting herewith a dissertation written by Jayashree Basavaraj Desai entitled “Characterization of the Role of Mouse *Nell1* Gene in Osteogenesis and Chondrogenesis During Mammalian Fetal Development.” I have examined the final electronic copy of this dissertation for form and content and recommend that it be accepted in partial fulfillment of the requirements for the degree of Doctor of Philosophy, with a major in Life Sciences.

Cymbeline T. Culiati

Major Professor

We have read this dissertation
And recommend its acceptance:

Bruce McKee

Brynn Voy

Yisong Wang

Accepted for the Council:

Carolyn R. Hodges

Vice Provost and Dean
of the Graduate School

(Original signatures are in the file with official student records)

**Characterization Of The Role Of Mouse *Nell1* Gene In
Osteogenesis And Chondrogenesis During Mammalian
Fetal Development**

A Dissertation Presented for the
Doctor of Philosophy
Degree
The University of Tennessee, Knoxville

Jayashree Basavaraj Desai

August 2007

Copyright© 2007 by Jayashree Desai
All rights reserved

DEDICATION

This dissertation is dedicated to my family, my grandparents, Basavantrao and Laxmi Desai for raising me and for their endless love and support; to my parents, Jagadevrao and Uma Deshmukh for their love and for instilling in me the importance of higher education; to my wonderful sister, Sheela Prathap for always being there for me and to my beautiful nieces, Tejesvini, Prarthana and Prerana for their love and the joy they have given me.

ACKNOWLEDGEMENTS

I would like to thank the people who helped me to make this research and degree possible. First I would like to thank my advisor Dr. Cymbeline Culiat for her guidance, support, patience, and for introducing me to the world of mouse genetics. I would like to thank Dr. Bruce McKee, Dr. Brynn Voy, and Dr. Yisong Wang for their willingness to serve on my committee and for their invaluable input, advice and support. I like to especially thank Dr. Voy for her kindness, encouragement and positive attitude. Special thanks to Dr. Donald Torry, my previous mentor, for teaching me how to be a better graduate student and a scientist. Without his guidance and training I would not be here today. Also I would like to thank Dr. Jeffery Becker, the head of the department of Microbiology and the former director of graduate school of Genome Science and Technology for always believing in me and for his help, support and advice on countless occasions.

I would like to thank my lab mates, Beverley Stanford, Marilyn Kerley and Lori Hughes for their friendship, support and help all through this journey. Lori, I especially thank you for teaching me how to do the animal work and helping me with the project. I would also like to thank all the members of the Mammalian Genetics and Functional Genomics Group (Oak Ridge 'Mouse House') for their technical support.

Ingrid and Pushan, thank you for everything. Ingrid, I cannot thank you enough for your friendship, support and believing in me and above all being in my life and for just being who you are. Last but not least, my husband Raj, thank you for your support. Without you I would not have been able to achieve this goal. I would also like to thank my and Raj's family in India for their love and support.

ABSTRACT

The mammalian *Nell1* gene encodes a PKC- β 1 binding protein that belongs to a new class of cell-signaling molecules controlling cell growth and differentiation. Overexpression of *NELLI/Nell1* in the developing cranial sutures in both human and mouse induces craniosynostosis, the premature fusion of cranial sutures. This study describes the characterization of *Nell1*^{6R} (102DSJ), a recessive, neonatal-lethal point mutation in the mouse *Nell1* gene, induced by N-ethyl-N-nitrosourea (ENU). The generation and sequencing of the mouse full-length cDNA (2862 bp) revealed that the *Nell1* gene has an open reading frame of 2433 bp and encodes an 810 amino acid protein which is highly homologous to human and rat *NELLI*. *Nell1*^{6R} has a T→A base change that converts a codon for cysteine into a premature stop codon, resulting in severe truncation of the predicted protein product and marked reduction in steady state levels of the transcript. Immuno-histochemical analysis indicates that *Nell1* is expressed in the vertebral column and is involved in osteoblast and chondrocyte differentiation. In addition to the expected alteration of cranial morphology, *Nell1*^{6R} mutants manifest skeletal defects in the vertebral column and ribcage, revealing a hitherto undefined role for *Nell1* in signal transduction in endochondral ossification. Real-time quantitative RT-PCR assays of 219 genes showed an association between the loss of *Nell1* function and reduced expression of genes for extracellular matrix proteins critical for chondrogenesis and osteogenesis. Several affected genes are involved in the human cartilage disorder known as Ehlers-Danlos Syndrome (EDS) and other disorders associated with spinal curvature anomalies. *Nell1*^{6R} mutant mice are a new tool for elucidating basic mechanisms in osteoblast and chondrocyte differentiation in the developing skull and vertebral column and understanding how perturbations in the production of extracellular matrix proteins can lead to anomalies in these structures. The characterization of *Nell1* functions using the *Nell1*^{6R} mouse model may further provide insights into the pathology of craniofacial defects like CS, cartilage diseases such as EDS as well as other bone and cartilage diseases.

TABLE OF CONTENTS

Chapter	Page
Chapter 1	1
Introduction	1
Chapter 2	5
Literature review	5
Vertebrate skeleton	5
Bone	5
Cartilage	7
Skeletogenesis	8
Intramembranous ossification	11
Endochondral ossification	13
Development of axial skeleton	15
Molecular basis for bone and cartilage formation	16
Transcription factors	17
Osteoblast specific factor (Osf-2)	17
Msx-2	19
Extracellular matrix (ECM) proteins	20
Collagens	20
Non-Collagenous extracellular matrix proteins	24
Bone morphogenetic proteins (BMP) and BMP receptors	34
<i>NELLI</i> : a novel cell differentiation signaling protein in bone and cartilage development	36
Gene and protein structure	36
Expression profile in humans and mouse	37
Gene regulation and associated pathway(s)	38
Functions	39

Chapter	Page
Protein kinase C signaling pathways and its relationship to <i>NELLI</i>	41
Protein kinase C (PKC)	41
Bone and cartilage disorders associated with <i>NELLI</i> -mediated pathways	44
Craniosynostosis (CS)	44
Ehlers-Danlos syndrome (EDS)	47
N-ethyl-N-nitrosourea (ENU) mutagenesis	48
Chapter 3	50
Materials and methods	50
Mouse breeding and maintenance	50
Generation of mutant hemizygotes and homozygotes for DSJ line	50
Collection mouse embryos	51
Genotyping of wild-type and <i>l7R^{6R}</i> mutants	54
Isolation of total and mRNA	54
<i>Nell1</i> gene profiling by northern blot and RT-PCR	55
Generation and sequencing of <i>Nell1</i> cDNA	57
Identification of mutation in <i>Nell1^{6R}</i>	58
Body and head measurements	59
Skeletal analysis	59
Histological analysis	62
Immunohistochemistry	63
High-throughput Real-Time qRT-PCR assays	63
Multiplex pre-amplification of cDNA targets	64
Real-time PCR reactions	64
Data analysis	65
Chapter 4	66
Results	66
Characterization of molecular basis of <i>Nell1^{6R}</i> mutations	66
Expression analysis of mouse <i>Nell1</i> gene	66

Chapter	Page
Sequencing of mouse <i>Nell1</i> cDNA	71
Identification of <i>Nell1</i> mutation in <i>Nell1</i> ^{6R} mice	71
Determination of the gross morphological and skeletal defects in <i>Nell1</i> ^{6R} mutant mice	74
Gross phenotypes	75
Morphometric analysis	75
<i>Nell1</i> ^{6R} mutant mice have skeletal defects in the skull and vertebral column	75
Examination of the role of <i>Nell1</i> in osteoblast and chondrocyte differentiation in the vertebral column	84
Localization of <i>Nell1</i> expression in wild-type and mutant <i>Nell1</i> ^{6R} fetal vertebral column	84
Effect of <i>Nell1</i> ^{6R} mutation on differentiation of osteoblasts and chondrocytes in the developing vertebral column	89
Determination of the biological pathway(s) perturbed by the <i>Nell1</i> ^{6R} mutation	91
High-throughput qRT-PCR	91
Chapter 5	95
Conclusion and future directions for elucidating the role of <i>Nell1</i> in craniofacial and vertebral column development	95
Summary of results and conclusion	95
<i>Nell1</i> gene structure, wild-type Vs <i>Nell1</i> ^{6R}	96
<i>Nell1</i> RNA and protein expression	96
Phenotypic consequences of <i>Nell1</i> loss of function	97
<i>Nell1</i> in cell differentiation pathways	98
<i>Nell1</i> controls cell differentiation via ECM pathways	99
Regulators of <i>Nell1</i>	100
Model for <i>Nell1</i> -mediated pathways	101
Future directions and recommendations	105
List of references	109

Chapter

Page

Vita 127

LIST OF TABLES

Table	Page
Table. 2.1. Tissue-specific expression of Protein kinase C (PKC) isoforms	43
Table. 3.1. Primers used to synthesize and sequence mouse <i>Nell1</i> cDNA	58
Table. 3.2. Primers used to amplify mouse <i>Nell1</i> genomic DNA	60
Table. 4.1. Quantitative analysis of changes in body length and head size of <i>Nell1</i> ^{6R} homogygous mutants compared to wild-type littermates (in mm) at E18 days of gestation	77

LIST OF FIGURES

Figure	Page
Figure. 2.1. Embryonic cell lineages and early steps in the development of vertebrate skeleton	6
Figure. 2.2. Intramembranous and endochondral ossification	9
Figure. 2.3. Regulation of osteoblast proliferation and differentiation by growth factors and transcription factors	12
Figure. 2.4. Regulation of chondrocyte proliferation and differentiation by growth factors and transcription factors	14
Figure. 2.5. Calvarial bones and sutures	45
Figure. 2.6. Human craniosynostosis	46
Figure. 3.1. Breeding protocol used to generate hemizygous and homozygous <i>l7R6^{6R}</i> (102DSJ) mice	52
Figure. 4.1. Complementation analysis	67
Figure. 4.2. Expression of the mouse <i>Nell1</i> gene	69
Figure. 4.3. Aberrant expression of <i>Nell1</i> in <i>l7R6</i> mutants	70
Figure. 4.4. Identification of the <i>Nell1^{6R}</i> mutation	72
Figure. 4.5. Phenotypes of <i>l7R6</i> mutants	76
Figure. 4.6. Skeletal analysis of <i>l7R6</i> neonates	79
Figure. 4.7. Skeletal phenotype of <i>Nell1^{6R}</i> homozygote mutant mouse	80
Figure. 4.8. Cranial defects in <i>Nell1^{6R}</i> homozygote mutant mouse	81
Figure. 4.9. Skeletal defects in <i>Nell1^{6R}</i> homozygote mutant mouse	83
Figure. 4.10. Histological analysis of fetal vertebral column	85
Figure. 4.11. Expression of <i>Nell1</i> in fetal vertebral column	87
Figure. 4.12. Expression of <i>Nell1</i> in fetal skin	88
Figure. 4.13. Expression of <i>col X</i> in fetal vertebral column	90
Figure. 4.14. van Kossa staining of vertebral column and parietal bone	92

Figure	Page
Figure. 4.15. Gene expression profile of <i>Nell1</i> ^{6R} mutants compared with wild-type fetuses (E18.5)	94
Figure. 5.1. The hypothetical model of <i>Nell1</i> signaling pathway	102

CHAPTER 1

INTRODUCTION

Bone and cartilage constitute the primary structural support of the vertebrate organism. The formation of bone (osteogenesis) and cartilage (chondrogenesis) are complex processes involving several stages: a) commitment of the precursor cells, b) the proliferation of the osteoprogenitor/chondroprogenitor cells, c) differentiation of osteoblasts and chondrocytes and d) the formation of cartilage or a calcified bone matrix. In the developing skull, calvarial bones are formed by intramembranous ossification, in which mesenchymal cells differentiate into osteoblasts and the production of bone matrix occurs directly without previous cartilage formation. Other bones in the body are formed by endochondral ossification, in which mesenchymal cells differentiate into chondrocytes and the formation of cartilage models occurs first, followed by replacement of the models by bone. (Erlebacher et al. 1995; Hall et al. 2000). Normal bone formation involves a delicate balance between proliferation, differentiation and apoptosis in osteoblasts and chondrocytes. Disruption of this balance leads to many serious human birth defects and diseases like craniosynostosis, osteochondrodysplasias, epiphyseal dysplasia, arthritis, and osteoarthritis etc.

Understanding of the mechanisms underlying osteogenesis and chondrogenesis has progressed considerably by studying mutations in humans and mice. Some of the craniofacial and other bone diseases are due to known mutations in growth factors, transcription factors and other proteins which are known to regulate osteoblast and chondrocyte proliferation, differentiation and survival. However, the genetic and molecular bases of many bone and cartilage diseases are still unknown, thus it is possible that perturbations in other genes may be responsible for these disease processes.

In this dissertation research, a new mouse mutation generated at Oak Ridge National Laboratory (ORNL) was characterized. This loss of function mutation was associated with bone and cartilage defects. The characterization of genetic and functional bases of this mutation will further contribute to the current understanding of the mechanisms underlying osteogenesis and chondrogenesis.

Large-scale mouse mutagenesis, conducted at ORNL, using the chemical mutagen, N-ethyl-N-nitrosourea (ENU) has generated the mutations mapping to a small segment of mouse chromosome 7, proximal to the pink-eyed gene (*p*) (Rinchik et al. 2002). One locus mutated in these experiments was designated as *l7R6* and has yielded eight recessive neonatally-lethal alleles. Homozygotes manifested abnormal head-shape and body curvature of late gestation fetuses and neonates. High-resolution genetic and molecular mapping indicated that *l7R6* maps to a ~ 1 Mb interval homologous to a segment of human 11p15 where the *NELLI* gene is located. Initially six genes were tested as candidates for the *l7R6* locus. However, none of these genes were associated with the skeletal defects and the gross and skeletal phenotypes observed in *l7R6* mutant mice. The preliminary molecular and phenotype analysis of four mutant alleles of *l7R6* done in this study, along with the previously published data, further supported the hypothesis that *l7R6* is the *Nelli* gene.

Earlier studies have demonstrated that *Nelli* is a gene whose overexpression in human and mouse leads to craniosynostosis (CS), premature closure of the cranial sutures in the developing skull (Ting et al. 1999; Zhang et al. 2002). CS affects 1 in 3000 infants and is one of the most common human congenital craniofacial deformities (Wilkie 1997; Cohen 2000). In CS, constrained brain growth due to the cessation of skull growth leads to a severe cranial dysmorphism, often resulting in increased intracranial pressure, impaired cerebral flow, airway obstruction and impaired vision and hearing. A series of major cranial surgeries in infants or young children are necessary to correct CS. (Wilkie 1997; Carver et al. 2002). Additionally, certain types of CS are associated with defects in the limb and spine development (Anderson et al. 1996; Anderson et al. 1997). Zhang et al (Zhang et al. 2002) further characterized the role of *Nelli* in suture fusion by creating an overexpressing transgenic mouse model. The transgenic mice exhibited CS and no apparent defects in other organ systems. The results of their study suggest that overexpression of *Nelli* stimulates osteoblast differentiation at the growing fronts of the calvarial bones leading to rapid mineralization and premature fusion of the sutures. Another study by Zhang et al (Zhang et al. 2003) indicates that *Nelli* modulates calvarial osteoblast differentiation and apoptosis pathways during intramembranous ossification of

the developing skull. Moreover, both *in vitro* and *in vivo* studies showed that this gene plays a role in osteoblast differentiation (Zhang et al. 2002; Zhang et al. 2003). Additionally, Cowan et al (Cowan et al. 2006) reported that *Nell1* accelerates chondrocyte hypertrophy and endochondral bone formation within the distracted maxillary suture. It also induced premature hypertrophy and increased apoptosis of chondrocytes, which in turn leads to distortion of chondrocranium and subsequent cranial deformity during mouse development (Zhang et al. 2006). The present study further corroborates these reports; *Nell1* is expressed in vertebral column and is involved in both osteoblast and chondrocyte differentiation.

The preliminary molecular and phenotype analysis of four mutant alleles of *I7R6* locus revealed that loss of function mutation at this locus leads to varying degrees of skeletal defects in mutant mice ranging from mild to severe. In one of these *I7R6* alleles, designated as the 102DSJ stock, homozygote mutants exhibited marked cranial and vertebral column defects and had severely reduced levels of *Nell1* gene expression. As such this severely affected allele became a focus of this dissertation research and the *Nell1*^{6R} mutant allele was further characterized to study the consequences of *Nell1* mutation in cranial and vertebral column development in mouse. The main goal of this project is to determine the molecular/cellular and functional basis of the craniofacial and axial skeleton (vertebral column) defects found in *Nell1*^{6R} allele.

Mutation in *Nell1*^{6R} was evaluated by examining gross morphological traits, conducting detailed skeletal analysis and by using chemical stains specific for bone and cartilage, and morphometric analysis of formalin fixed embryos. To characterize the molecular basis of *Nell1*^{6R} mutation, expression profile of *Nell1* gene during the mouse development and impact of its mutation on the expression of *Nell1* gene was investigated by Northern blot, RT-PCR and immunohistochemistry. Additionally, the complete coding sequence of the gene was sequenced along with identification of the *Nell1*^{6R} mutation. In order to determine cellular functions of *Nell1*^{6R}, the expression of *Nell1* in mutant fetal vertebral columns and effects of its loss of function mutation on both chondrocyte and osteoblast differentiation was examined by histochemical staining as well as immunohistochemistry. In order to define the genes and pathways that are perturbed by

the *Nell1*^{6R} mutation, expression profile of 219 genes, which are associated with craniosynostosis, osteogenesis/chondrogenesis and, growth and differentiation was examined by Real-Time qRT-PCR analysis.

The results of this study suggested an association between the loss of *Nell1* function and defects in the development of the skull and vertebral column. The *Nell1*^{6R} mutants exhibit skeletal defects in the vertebral column and ribcage in addition to the expected alteration in cranial morphology. These observations indicate that *Nell1* may play a yet undetermined role in endochondral ossification.

The impact of *Nell1* on the formation of the vertebral column was a novel finding and unexpected based on observations on the overexpressing transgenic mouse model. This study also demonstrated that in the *Nell1*^{6R} mutation, there is a reduced expression of numerous extracellular matrix proteins that are critical for chondrogenesis and osteogenesis. Several affected genes are implicated in the pathophysiology of human cartilage/connective tissue disorder, Ehlers-Danlos Syndrome (EDS) and other disorders associated with skeletal defects in the vertebral column. EDS, a severe cartilage defect, which affects 1 in 5000 individuals, is characterized by hyperextensibility of the skin and extreme flexibility of joints (Beighton et al. 1998; Mao et al. 2001). Individuals with EDS do not have the ability to make certain components of the connective tissue, particularly fibrillar collagens, or they have defective regulation of collagen synthesis and deposition (Mao et al. 2001; Mao et al. 2002). One particular form of EDS, EDS-type VI is characterized by abnormal curvature of the spine, hypotonia, joint laxity and ocular fragility (Beighton et al. 1998; Mao et al. 2001). The data generated from this study suggests that, in addition to its role in intramembranous ossification in the skull, *Nell1* plays a critical role in endochondral ossification and chondrogenesis in the developing vertebral skeleton. The characterization of *Nell1* functions using the *Nell1*^{6R} mutation is a unique opportunity to further elucidate the basic mechanisms of osteogenesis and chondrogenesis. It will provide insights into the pathology of craniofacial defects like CS, as well as other bone and cartilage diseases such as EDS.

CHAPTER 2

LITERATURE REVIEW

VERTEBRATE SKELETON

Forget the great human heart and the brain, the eyes that see sweeping vistas, the lips that declare, "I am". The real thing standing between us and the primordial ooze is the human skeleton. Built of 206 bones, the skeleton is a living cathedral of ivory vaults, ribs and buttresses- a structure at once light and strong, flexible and firm. (Angier 1994).

The vertebrate skeleton, which is composed of cartilage and bone, develops from cells from three embryonic lineages: neural crest, paraxial mesoderm and lateral plate mesoderm. Neural crest cells give rise to most of the craniofacial skeleton. The axial skeleton consisting of the vertebrae and ribs is derived from the paraxial mesoderm (somites) and the appendicular (limb) skeleton originates from the lateral plate mesodermal cells. Cells from these lineages migrate to the sites in the developing embryo where future skeletal elements will emerge and form mesenchymal osteogenic/chondrogenic condensations and differentiate into specialized cells called the osteoblasts and chondrocytes (Hall et al. 1995) (Fig.2.1).

BONE: Bone is a highly complex and specialized tissue that forms a supporting framework for the vertebrate body. It supports and protects many delicate organs in the body, supports hematopoiesis in the bone marrow and participates in calcium homeostasis (Cohen 2006). Bone is made up of osteoblasts, which are responsible for secreting the matrix. Once these cells fully differentiate and are surrounded by calcified matrix, they become quiescent and are known as osteocytes. Bone is composed of an organic matrix (95% *COL-1*, 5% proteoglycans and non-collagenous proteins) that is strengthened by inorganic salts (mainly calcium phosphate in the form of hydroxyapatite) (Anderson, 1995). There are two varieties of bone tissue, cortical and cancellous. Cortical or compact bone is dense and extremely hard due to the densely packed collagen fibrils

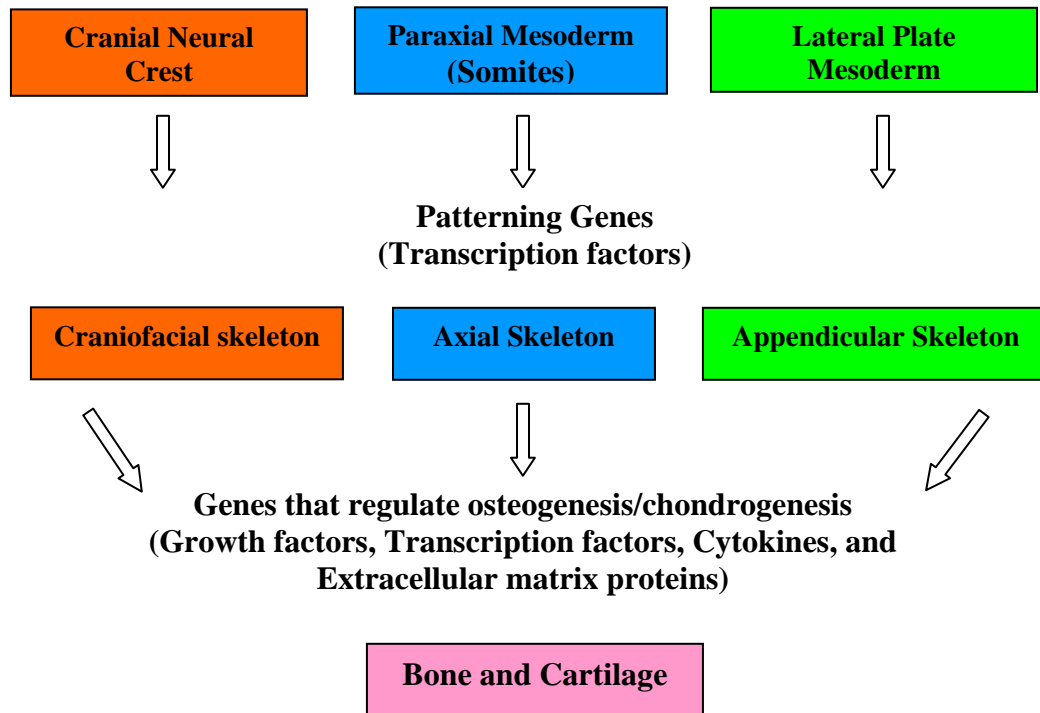


Figure. 2.1: Embryonic Cell Lineages and Early Steps in the Development of Vertebrate Skeleton. Osteoblasts deposit bone matrix while chondrocytes form cartilage. A third cell type of the skeletal system, called osteoclasts resorb bone. Osteoblasts and chondrocytes originate from mesenchymal cells whereas osteoclasts arise from the hematopoietic system (Cohen 2006).

that form concentric lamellae. The blood vessels in the cortical bone occupy small tube like spaces called Haversian canals. Each canal is surrounded by several lamellae, and forms a cylindrical block of bone called a Haversian system. The diaphysis (shaft) of typical long bones such as femur and humerus consists of a thick walled hollow cylinder of compact bone and a central marrow cavity. Cortical bone provides protection and mechanical support. Cancellous bone is light and spongy and consists of a three dimensional lattice of bony spicules or trabeculae that create many large intercommunicating spaces that are filled by bone marrow. It lies deep within the cortical bone and provides metabolic functions. The two forms of bone merge (abrupt transition) into one another without a sharp boundary. (Gillison 1962; Fawcett 1994).

CARTILAGE: Cartilage is a unique connective tissue found in the structures of certain organs that forms a close association with the bone and plays numerous important roles during vertebrate prenatal and postnatal development. Cartilage provides a template for the developing bones, a structural support for the developing embryo, factors for postnatal growth of the skeleton, cushion for the joints, flexibility to facial structure, and repair mechanisms for fractured bones. Furthermore, cartilage in airways, joints and ears are crucial for breathing, locomotion and hearing because it allows for movements without interfering with function. (Shum et al. 2002; Lefebvre et al. 2005).

Cartilage is made up of chondrocytes, which occupy small cavities called lacunae within the extracellular matrix they secrete. There are three types of cartilage: hyaline, elastic and fibrocartilage. Hyaline cartilage forms the temporary cartilage of the skeletal system and is gradually replaced by bone. In fully developed bones, hyaline cartilage persists as a covering for the articular surfaces. This articular cartilage allows for the smooth movements of joints and acts as a shock absorber. Ribs are attached to the sternum by hyaline cartilage and the cartilage increases the mobility and the flexibility of the thorax, which is crucial for respiration. Hyaline cartilage is also found in the respiratory passages such as trachea, bronchi, larynx and tip of the nose. Elastic cartilage is more flexible and resilient than the other cartilages. It is only found in a few parts of the body where flexibility is required, as in the pinna of the ear, auditory tube, epiglottis

and parts of the larynx. Fibrocartilage is always found in conjunction with hyaline cartilage or other fibrous tissue. It is much less flexible and resilient than hyaline cartilage but is very dense, tough and resistant to stretching. It is associated with the capsules and ligaments of joints such as temporo-mandibular, sterno-clavicular, shoulder, hip and knee joints. Intervertebral discs are made up of fibrocartilage and the cartilage allows limited compression or torsion and allows limited movement between adjacent vertebrae. The discs also act as shock absorbers preventing excessive jarring of the spine and head. (Gillison 1962; Fawcett 1994).

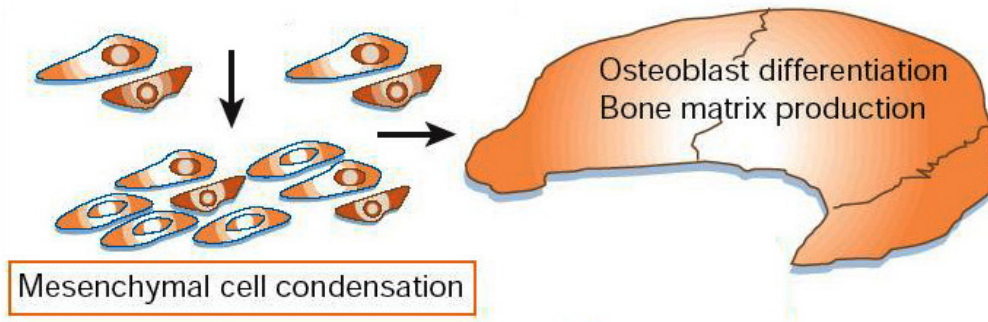
SKELETOGENESIS

The formation of bone (osteogenesis) and cartilage (chondrogenesis) are complex processes involving several stages: a) commitment of precursor cells, b) proliferation of the osteoprogenitor/chondroprogenitor cells, c) differentiation of osteoblasts and chondrocytes, and d) the formation of cartilage or a calcified bone matrix. The earliest event in skeletal morphogenesis is the migration of mesenchymal cells to the locations of future skeletal elements, where they form dense condensation at the sites of future bones. Condensations are either osteogenic or chondrogenic, depending on the skeletal elements they initiate (Erlebacher et al. 1995; Hall et al. 2000). This event is followed by differentiation to chondrocytes or osteoblasts within the condensation. The subsequent growth during the organogenesis phase generates cartilage models (anlagen) of future bones as in limb bones or membranous bones as in the cranial vault. The craniofacial skeleton is constructed by membranous ossification, wherein differentiation of mesenchymal cells to osteoblasts and the production of bone matrix occurs directly without cartilage formation (Erlebacher et al. 1995; Hall et al. 2000) (Fig. 2.2A). The axial and limb skeletal systems are developed by endochondral ossification, where differentiation of mesenchymal cells to chondrocytes, and formation of cartilage model occurs first, followed by the replacement of the models by bone (Fig. 2.2B).

Figure 2.2: Intramembranous and Endochondral Ossification. (A). Mesenchymal cells from neural crest differentiate into osteoblast and production of bone matrix occurs directly without formation of cartilage. (B). Mesenchymal cells from somites differentiate into chondrocytes to form a cartilage model (anlagen). In the center of the anlage chondrocytes mature, hypertrophy and begin to express high levels of Vascular Endothelial Factor (VEGF), which facilitates invasion of capillaries into the anlage with subsequent recruitment of osteoblasts. Osteoblasts produce bone matrix to generate the collar of bone and growth plates (green area). Hypertrophic cartilage is subsequently degraded and eventually replaced by cancellous bone and bone marrow. [Modified from ((Zelzer et al. 2003)].

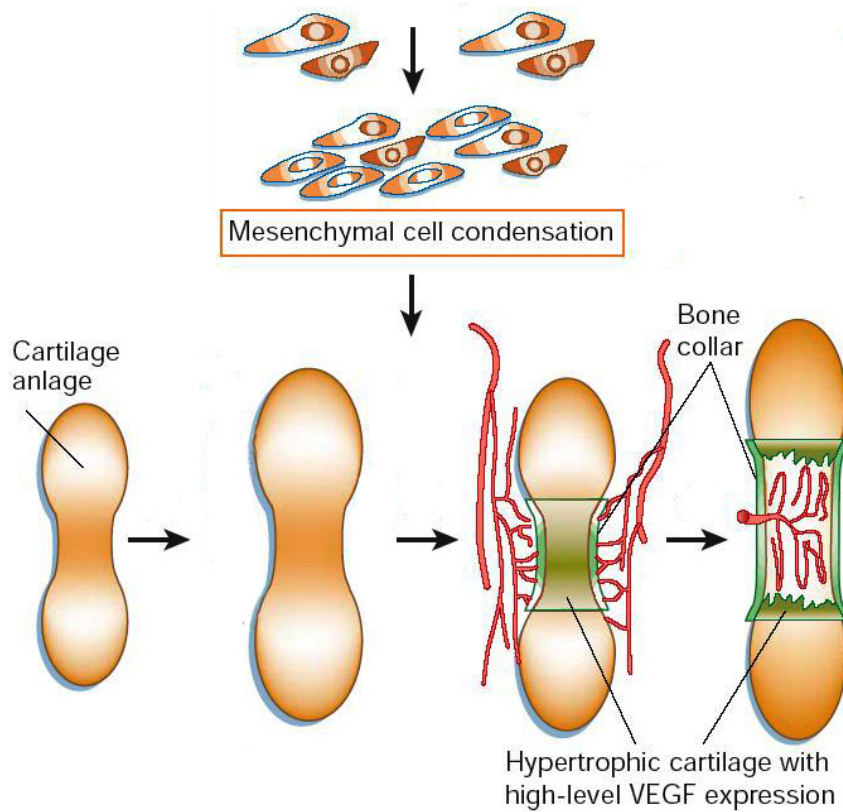
A.

Cells from cranial neural crest



B.

Cells from somites and lateral plate mesoderm



INTRAMEMBRANOUS OSSIFICATION: In the developing skull, calvarial bones, mandibles, and clavicles are formed by intramembranous ossification (Zelzer et al. 2003). Formation of these bones involve the migration of undifferentiated mesenchymal cells from the neural crest into areas destined to become bone, where they condense and proliferate in response to the signals from the underlying neural tissue. Molecular signals from growth factors like Bone Morphogenetic Proteins (BMPs), Fibroblast Growth Factors (FGFs), Epidermal Growth Factor (EGF), Insulin like growth factors (IGFs) and transcription factors trigger differentiation into osteoprogenitor cells and subsequently into osteoblasts. Osteoblasts secrete a mineralized matrix in the ossification centers. At the end of the formation period, osteoblasts die by apoptosis or are embedded in the matrix, becoming osteocytes, which then undergo apoptosis at the end of their life. The flat calvarial bones of the skull grow towards each other from the primary ossification centers and meet at sutures. Then the calvarial bones grow at the sutures in concert with the expanding brain. The center of the suture contains proliferatory pre-osteoblast population, which eventually differentiates and moves toward adjacent bone surfaces, becoming osteoblasts. (Wilkie 1997; Zelzer et al. 2003).

Based on morphological and histological studies, osteoblastic cells *in vivo* are believed to follow a linear developmental progression from proliferating osteoprogenitors to proliferating pre-osteoblasts to mature osteoblasts to osteocytes (Stein et al. 1993) (Fig. 2.3). As the osteoblasts progress through these stages, there is a sequential expression of cell growth, tissue and stage specific genes. During the proliferative stage, the prominently expressed genes are FGF, EGF, Platelet Derived Growth Factor (PDGF) and IGFs. During the differentiation process, specific genes and extracellular matrix (ECM) biosynthesis associated factors, like BMPs, Transforming growth factor- β (TGF- β), FGF-3 and type I collagen (COL-1) are expressed (Stein et al. 1993). Alkaline phosphatase (AP) and Bone Sialoprotein (BSP) expression are relatively high during the matrix modulation stage. These differentiation-specific genes that are associated with maturation and organization of the bone ECM are essential for preparing the matrix for mineralization. During bone mineralization, osteopontin (OPN) and osteocalcin (OCN) are maximally expressed (Stein et al. 1993). Mineralization of ECM marks the final

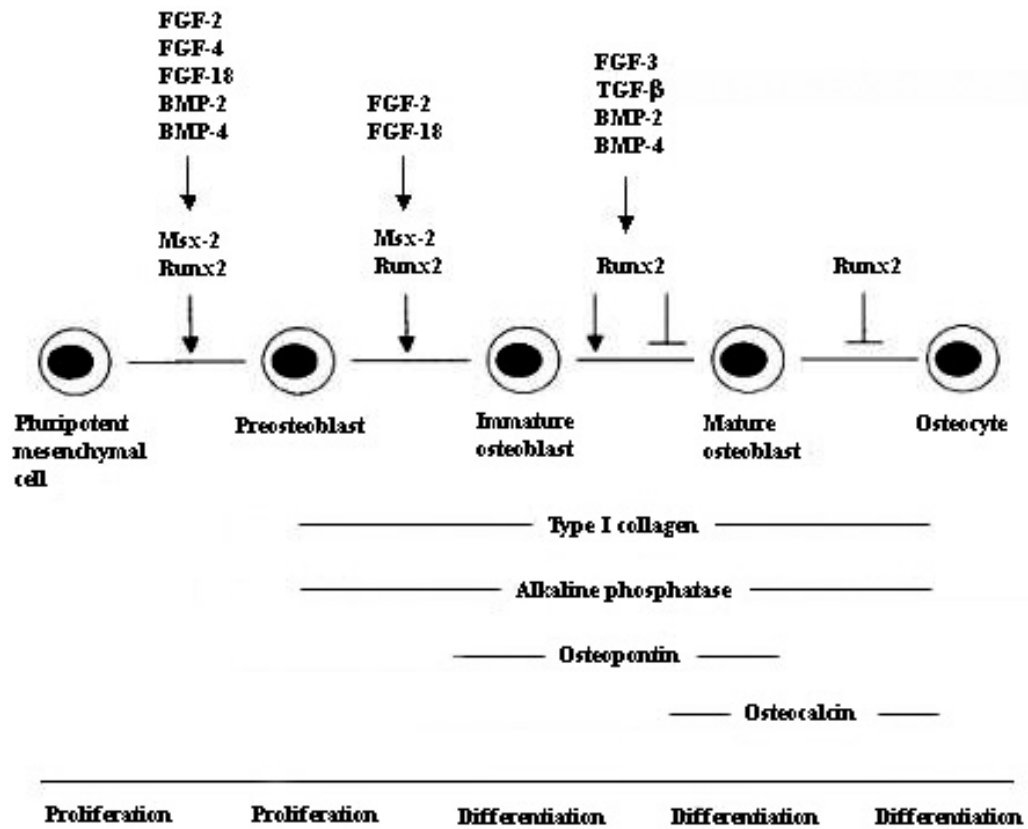


Figure 2.3: Regulation of Osteoblast Proliferation and Differentiation by Growth Factors and Transcription Factors. See text for details. [Modified from (Komori 2002)].

phase of osteoblast phenotype development.

ENDOCHONDRAL OSSIFICATION: Embryonic cartilage can either remain as permanent cartilage such as hyaline cartilage on the articular surfaces of bones, elastic cartilage in the ear, or fibrocartilage in intervertebral discs or it can provide a template for the bones through the process of endochondral ossification. Majority of the bones (axial and appendicular skeleton) in the body except calvarial bones, clavicles and mandible are formed by endochondral ossification in which mesenchymal cells differentiate into chondrocytes and the formation of cartilage models (anlagen) occur first, followed by replacement of the models by bone (see Fig.2.2B). (Komori 2002; Cohen 2006).

It is a multi-step process that involves two successive cell-differentiation processes (Fig. 2.4). Undifferentiated mesenchymal cells from somites and lateral plate mesoderm migrate to the sites of future bones and form chondrogenic condensations, and under the control of SOX family of transcription factors, these mesenchymal cells differentiate first into *COL-2A* producing pre-chondrocytes and then into immature chondrocytes that proliferate until the general shape of the future bone is established. This cartilage template (anlagen) is eventually replaced by bone. The type of skeletal elements that form from the immature chondrocytes depends on several transcription factors. *OSF-2/RUNX2* (and possibly *OSX*) induces the formation of replacement cartilage while continued action of *SOX9* (and possibly *SOX5/SOX6*) produces persistent cartilage. These *COL-2B* producing (chondrocyte specific collagen) immature chondrocytes further proliferate under the influence of FGF-3, mature and then arrest in their cell cycle. The mature chondrocytes undergo morphological and gene expression changes. *COL-1* is turned off and *COL-10* is turned on as cells differentiate further into hypertrophic chondrocytes. The latter express predominantly *COL-10* and synthesize a cartilaginous matrix that eventually calcifies. At the same time these terminally differentiated hypertrophic chondrocytes start expressing a high level of vascular endothelial growth factor (VEGF), a growth factor needed for the invasion of blood vessels into the cartilage and undergo apoptosis. The invading blood vessels bring chondroclasts (which degrade mineralized chondrocyte matrix), osteoblasts and

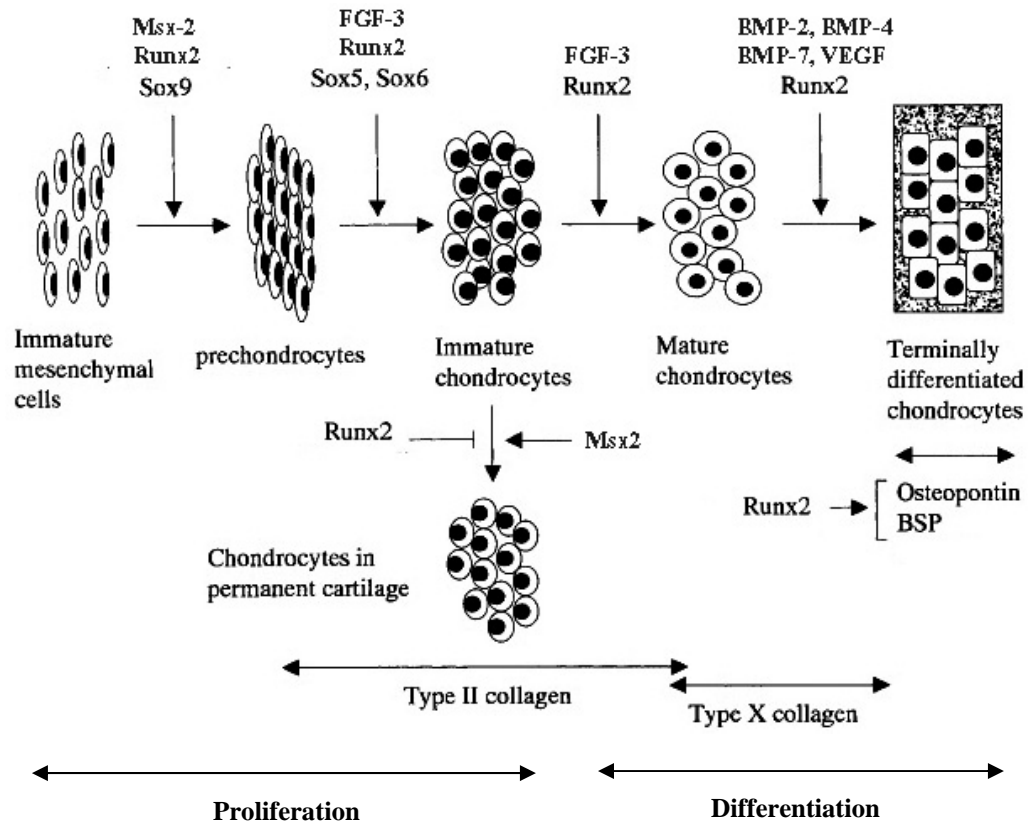


Figure 2.4: Regulation of Chondrocyte Proliferation and Differentiation by Growth Factors and Transcription Factors. See text for details. [Modified from (Komori 2002)].

osteoclasts into the ossification center. The cartilaginous matrix is then degraded and eventually replaced by a bone synthesized by the osteoblasts. In the developing long bones, the primary ossification centers split into opposite growth plates in which the maturation of cartilage and subsequent bone formation continues. The growth plate cartilage is responsible for the longitudinal bone growth during postnatal life and as the bones grow, the increasing space between the growth plates becomes filled with bone marrow (see Fig.2.2B). (Ducy et al. 1998; Shum et al. 2002; Zelzer et al. 2003).

Development of Axial Skeleton: The vertebrate axial skeleton consists of the skull base, vertebral column and ribcage. The vertebral column is the primary and most important component of the axial skeleton that arises via endochondral ossification. This skeletal structure not only supports and stabilizes the vertebrate organism but also permits various types of mobility. The vertebral column is comprised of a series of anatomical structures called the vertebrae, which are arranged in craniocaudal pattern. There are seven cervical, twelve thoracic and five lumbar vertebrae in humans (Sofaer 1985). There are at least twenty-five intervertebral discs between the adjacent vertebrae, which are made up of three integrated tissues: the gelatinous nucleus pulposus, fibrous annulus fibrosus, and the cartilage end plate. Intervertebral discs provide stability and flexibility to the spine and protect it by absorbing and distributing physical and mechanical loads (Humzah et al. 1988).

Axial skeleton morphogenesis requires a coordinated series of cellular and molecular events, which are regulated by transcription factors like *MSX-1* and *-2*, *PAX1*, *3*, and *9* and growth factors like *FGF-8*, *BMP-4* and *-2* (Watanabe et al. 1998; Peters et al. 1999; Pourquie 2003). Vertebral column development starts with the formation of somites from the unsegmented paraxial mesoderm on both sides of the neural tube. The somites then compartmentalize, differentiate and de-epithelialize to generate dermomyotomes and sclerotomes. Dermomyotomes give rise to appendicular and axial musculature while sclerotomes form the skeletal elements of the vertebral column and ribs. The densely packed cells at the anterior sclerotomal region give rise to intervertebral discs while less dense areas between intervertebral disc regions form the cartilage model

(anlage) for vertebral bodies. The sclerotome cells then migrate ventrally and medially, ultimately surrounding the notochord to form the perichondral tube. This tube eventually becomes segmented and gives rise to vertebral bodies and intervertebral discs. During the 6th week of gestation pre-vertebrae are converted to cartilage and the endochondral ossification begins at the 8th week. (Christ et al. 1998; Peters et al. 1999; Giampietro et al. 2003). During the vertebral column development, somitogenesis is regulated by a segmentation clock, a timing mechanism responsible for the periodic production of somites by periodic expression of ‘cyclic’ genes (related to Notch pathway) and FGF signaling wave front, which in turn are regulated by Wnt and Notch signaling (Pourquie, 2003). Abnormalities in the genes controlled by segmentation clock are known to cause severe defects during vertebral column development and are similar to pathological conditions like scoliosis (Giampietro et al. 2003; Sparrow et al. 2006). Currently there is a wealth of information available on early patterning process (embryonic segmentation of vertebral column), in terms of patterning genes, growth factors and transcription factors that are involved in the vertebral column development. However, the events, which occur later during the development of vertebral column like chondrogenesis and osteogenesis and the factors and pathways that regulate these processes, are not clearly understood.

MOLECULAR BASIS FOR BONE AND CARTILAGE FORMATION

Skeletogenesis is a very complex process, which is regulated by a series of molecular events involving many transcription factors, growth factors and ECM proteins. Importance of transcription factors like OSF-2/RUNX2, MSX2 and growth factors like FGFs, BMPs, TGF- β along with ECM proteins like collagens, matrilins, tenascins, thrombospondins and signal transducers like PKC, in both osteogenesis and chondrogenesis has been demonstrated by studies conducted in both human and mouse (Pacifci et al. 1993; Prockop et al. 1995; Jena et al. 1997; Komori et al. 1997; Wilkie 1997; Liu et al. 1999; Chapman et al. 2001; Hay et al. 2001; Komori 2002; Rosado et al. 2002; Marie 2003; Hankenson et al. 2005; Bandyopadhyay 2006; Desai et al. 2006). *NELLI* is a relatively new gene with osteoinductive properties that is rapidly emerging as

a new player in the field of osteogenesis and chondrogenesis. All the proteins mentioned above along with *NELLI* are involved in the signaling pathways that are utilized in osteogenesis/chondrogenesis and *NELLI* is known to be regulated (directly or indirectly) by these transcription and growth factors and it in turn regulates some of these proteins.

TRANSCRIPTION FACTORS: There are several transcription factors (TFs) that play central regulatory roles during bone and cartilage development. The expression of these factors in osteoblasts and chondrocytes coincides with the sequential development of these cells. Proliferation-specific TFs like *MSX-2* and *TWIST* are expressed in pre-osteoblasts; and *MSX-2*, *SOX-5*, *-6*, and *-9* in pre-chondrocytes, while *RUNX-2* and *Osterix (OSX)*, which are associated with terminal differentiation, are expressed in mature osteoblast.

Osteoblast specific factor (Osf-2): *OSF-2*, also known as *AML-3* or core-binding factor-1 (*CBFA-1*) or *RUNX2*, is a transcription factor that belongs to the Runt family of transcription factors that is essential for bone formation during embryogenesis. It is a master transcription factor that is necessary for all stages of bone formation (Ducy 2000). *Osf-2/Runx2* is expressed in mesenchymal condensations (osteochondroprogenitor cells) during the early development on embryonic day 12 (E12). From mid-gestation (E14) *Osf-2/Runx2* expression becomes progressively stronger in the cells of osteoblast lineage (Karsenty 2001). *OSF-2/RUNX2* is crucial for osteoblast development from mesenchymal stem cells and maturation into osteoblasts by regulating the transcription of several target genes. Multiple *OSF-2/RUNX2* binding sites were found in promoter regions of all the major genes expressed by osteoblasts, such as *COL-1* and *2*, *BSP*, *OPN* and *OCN* (Ducy 2000) and also craniosynostosis-associated gene, *NELLI* (Truong et al. 2007). All these bone matrix proteins are sequentially expressed during osteoblast differentiation and bone matrix mineralization.

Although the level and pattern of *OSF-2/RUNX2* transcriptional indicated its involvement in osteoblast differentiation, human genetic and *Osf-2/Runx2* knockout mouse studies confirmed that it is an essential factor for osteoblast differentiation. *Osf-*

2/Runx2^{-/-} mice die at birth and lack both endochondral and intramembranous ossification. These mice completely lack osteoblasts, are devoid of mineralized bone and the entire skeleton consists of only cartilage. The skeletal structures like calvarial bones and clavicles are missing. Additionally, the mice do not express certain ECM proteins like *Bsp*, *Opn*, and *Ocn*, which are known biomarkers for osteoblast differentiation (Komori et al. 1997; Otto et al. 1997). Human mutations in *OSF-2/RUNX2* cause cleidocranial dysplasia (CCD), an autosomal dominant disease characterized by the defects in both endochondral and intramembranous bone formation, such as absence of clavicles, persistent open fontanelles, supernumerary teeth, and short stature (Lee et al. 1997). Mice with heterozygous mutation in *Osf-2/Runx2* showed a phenotype similar to CCD in humans (Mundlos et al. 1996).

As mentioned above *Osf-2/Runx2* is expressed early during the development (E12.5) in osteochondroprogenitor cells in mice. However, from E12 to birth, its expression in cartilage is restricted to prehypertrophic and hypertrophic chondrocytes (Karsenty 2001). This spatio-temporal pattern of *OSF-2/RUNX2* expression along with its transcriptional control of *COL-10* gene (chondrocyte differentiation marker) suggests that it may be involved in chondrocyte terminal differentiation. These findings were further confirmed by the observation that in *Osf-2/Runx2*^{-/-} mice, the entire skeleton is composed of cartilage, chondrocyte differentiation is severely affected in most of the skeleton and no *Col-10* expression and vascular invasion of the cartilage is detected (Inada et al. 1999). Forced expression of *Osf-2/Runx2* driven by *Col-2* or *Col-10* promoter which target chondrocytes in these mice, partially rescued *Osf-2/Runx2* deficient mice by inducing hypertrophic chondrocyte differentiation (Takeda et al. 2001).

OSF-2/RUNX2 also plays a role in postnatal bone formation. It is expressed in mature postnatal osteoblasts and over-expression of dominant negative *Osf-2/Runx2* in these cells results in osteopenia, with decreased expression of *Col-1* and *-2*, *Bsp*, *Opn*, and *Ocn* (Ducy et al. 1999). Furthermore, over-expression of *Osf-2/Runx2* in adult aging mice resulted in severe osteopenia due to impaired osteoblast maturation and increased bone formation as well as bone resorption (Geoffroy et al. 2002). Transcription of *OSF2/RUNX2* is regulated by many growth factors and transcription factors that are

known to play a critical role in skeletogenesis. It is positively regulated by BMPs, FGFs, retinoic acid and down-regulated by 1, 25(OH)₂ D3 and TNF and OSF-2/*RUNX2* itself (Lee et al. 2000; Komori 2002). Depending on the cell type it is positively or negatively regulated by TGF. *RUNX2* forms a heterodimer with transcription cofactor CBF- β (core binding factor β) and interacts with many other transcription factors (Smad, C/EBP and Ets) and cofactors (Rb). Additionally it is positively regulated by the transcription factor, *MSX2*. (Komori 2002).

Msx-2: *MSX-2* is a member of a small family of homeobox containing genes related to the muscle-segment (*msh*) gene in *Drosophila* (Liu et al. 1999). In the developing vertebrate, it is expressed in several tissues and is known to mediate craniofacial and limb morphogenesis (Bendall et al. 2000). In mice, *Msx-2* is expressed during critical stages of neural tube, neural crest, teeth and skull and facial bone development (Foerst-Potts et al. 1997). It is expressed in the developing calvaria and is involved in osteoblast proliferation, differentiation and function. Several studies show that *MSX-2* down-regulates the differentiation in calvarial osteogenic cells and maintains them in a proliferative state. This in turn increases the pool of proliferative osteogenic cells and ultimately increases calvarial bone growth (Dodig et al. 1999). Forced expression or over-expression of *Msx-2* in mouse calvarial osteoblast enhanced calvarial bone growth. (Dodig et al. 1999; Liu et al. 1999). Gain-of-function mutation in the human *MSX-2* gene causes an autosomal dominant disorder, Boston type craniosynostosis. Liu et al (1999) postulated that *MSX-2*-mediated craniosynostosis arose by transient retardation of osteogenic cell differentiation in developing cranial suture. *Msx-2*-deficient mice exhibit a marked delay in the ossification in calvarial bones, calvarial foramen and overall decrease in bone volume (Satokata et al. 2000). This phenotype results from decreased proliferation of osteoprogenitors at the osteogenic front in cranial sutures and closely resembles the phenotype associated with human haploinsufficiency in parietal foramina (Wilkie et al. 2000). Additionally, *Msx-2*^{-/-} mice also have defects in cartilage and endochondral bone formation. Axial and appendicular skeletal lengths were reduced; mutants had reduced number of osteoblasts and chondrocytes at the epiphysis. In mutant

long bones, postnatal expression of bone differentiation marker genes like *Bsp*, *Osf-2/Runx2* and *Ocn* were also reduced (Satokata et al. 2000). These reports demonstrate that MSX-2 is required for both chondrogenesis and osteogenesis and acts upstream of *OSF-2/RUNX-2*.

EXTRACELLULAR MATRIX (ECM) PROTEINS: Most of the cells in multicellular organisms are surrounded by a complex network of macromolecules that make up the extracellular matrix. The ECM provides structural support for the cells, tissues and organs, facilitates cell communication and acts as a physical barrier or selective filter to soluble molecules. In addition, macromolecules in the ECM regulate the behavior of the cells that contact them and thereby influence their development, survival, migration, proliferation, differentiation, shape and size. Although cells in connective tissue are surrounded by ECM, its composition and spatial relationship with cells differ between tissues (Alberts 1994). ECM is a complex network of macromolecules like glycosaminoglycans (hyaluronan, heparin sulfate, keratin sulfate, chondroitin sulfate and dermatan sulfate), proteoglycans (aggrecan, decorin, dyndecans, chad, proteoglycan 4), glycoproteins (thrombospondin, tenascin), fibrous proteins (collagen, elastin, fibronectin and laminin), and non-collagenous proteins and polysaccharides. These macromolecules are mainly produced by fibroblasts in the matrix. However, in certain types of connective tissues, such as cartilage and bone, they are secreted by chondrocytes and osteoblasts. Aggregates of collagen fibers and proteoglycans provide the structural base for ECM architecture. (Alberts 1994).

Collagens: The collagens are a family of fibrous ECM proteins that play a role in maintaining the structural integrity of various tissues. They are the most abundant proteins in animals, consisting of 25% of the total protein mass in these organisms. Collagens also play a role in the early development and organogenesis, chemotaxis, cell attachment and platelet aggregation (Kivirikko 1993). They are secreted by both connective tissue cells and other cell types and are present in most tissues and especially abundant in cartilage, bone, skin, tendons and ligaments. So far, at least 27 genetically

distinct collagen proteins have been identified (Kivirikko 1993; Myllyharju et al. 2004). Collagens can be classified into subgroups on the basis of their particular structural features. These groups are: 1. Fibrillar collagens (fibril forming collagens) such as COL I, II, III, V and XI. These are the main collagens found in connective tissue. COL I is the principal collagen of skin and bone. 2. Collagens that form network-like structures such as COL IV, VIII and X. 3. Fibril-associated collagens with Interrupted Triple-Helices (FACIT) such as COL IX, XII, XIV, XVI and XIX. These collagen types are known to associate with the fibrous collagen. 4. Collagens with transmembrane domains, types XIII and XVII. 5. Collagens that form anchoring fibrils for basement membrane, type VII. 6. Beaded filament forming collagen. Type VI. (Kuivaniemi et al. 1997).

Mutations in collagen genes cause a variety of human diseases such as Osteogenesis imperfecta, some types of Ehlers-Danlos syndrome, Chondrodysplasias, some forms of osteoporosis and osteoarthritis, arterial and intracranial aneurisms and epidermolysis bullosa (Prockop et al. 1995).

Collagen ii (col-2): COL-2 is the major fibrous collagen found in cartilage and constitutes 80-90% of the collagen content of the cartilage matrix. It is also found in related tissues such as the intervertebral disc, vitreous humor of the eye and the inner ear. It is preferentially expressed in the perichondrium, in pre-cartilage limb mesenchyme in chicks and in non-cartilage tissues. It is expressed in spatio-temporal pattern during the development of craniofacial, heart, brain, skin, skeletal muscle and nucleous pulposus of the intervertebral disc. (Thorogood et al. 1986; Nah et al. 1991; Sandell et al. 1991; Helminen et al. 1993). Several studies indicate that mutations in COL-2A cause a number of diseases of joints and skeleton. These include several chondrodysplasias, a heterogeneous group of disorders that are characterized by malformations of cartilaginous structures and degenerative changes of joints. Mutation in human *COL-2A1* gene caused osteochondroplasia in transgenic mice and they exhibited flattened vertebral bodies, dysplastic changes in long bones, osteoarthritis in their joints, degenerated intervertebral discs with altered histological structures, and these changes were more severe in mice with no murine Col-2A1 allele (Sahlman et al. 2004). Thus it is an important component

of the cartilage matrix that is formed during skeletogenesis and it especially plays a critical role in endochondral ossification (Helminen et al. 1993).

Collagen v (col-5): COL-5 is a minor fibrillar collagen, which participates in the formation of fibrillar collagen network and the regulation of fibrillogenesis. It is expressed in a variety of tissues such as bone, cornea, placenta and fetal membranes (Malfait et al. 2005). It occurs as a heterotrimer of three different polypeptide chains, $\alpha 1$ (Col-5A1), $\alpha 2$ (Col-5A2) and $\alpha 3$ (Col-5A3). It can form two forms of heterotrimers $(\alpha 1)_2\alpha 2$ and $\alpha 1\alpha 2\alpha 3$ or as $(\alpha 1)_3$ homotrimers. It regulates fibrillogenesis by co-assembling with COL-1 (Malfait et al. 2005).

Collagen-5a1 (col-5a1): It is expressed in adult skin, tendon and in calvaria and long bones but not in the cartilage of the developing mouse embryo. Mutations in the COL-5A1 and COL-5A2 genes result in classic EDS (type I and II) and in one third of patients, the disease is caused by mutant non-functional COL-5A1 allele (Schwarze et al. 2000; Malfait et al. 2005). Hence the mutation in COL-5A1 leads to classical EDS, which is caused by aberrant fibrillogenesis.

Collagen-5a3 (col-5a3): It is highly expressed in mammary gland, placenta, uterus, fetal, heart and lung, moderately in adult heart and brain. In addition, it is primarily expressed in epimysial (connective tissue) sheaths of developing muscles and within nascent ligaments adjacent to forming bone and joints during the development. Due to its expression in epimysium, it has been speculated that altered expression of COL-5A3 might result in some muscle myopathies. (Imamura et al. 2000). Based on its expression in developing tendons and joints and its ability to form heterotrimers with COL-5A1 and -A2 chains, it has been suggested that altered expression of COL-5A3 may account for at least some cases of classical EDS in which COL-5A1 and -A2 have been excluded (Imamura et al. 2000). Defects in COL-5A3 may also contribute to at least some cases of hypermobility type of EDS, which is characterized by chronic diffuse muscle pain along with classical EDS symptoms (Imamura et al. 2000).

Collagen vi (col-6): COL-6 belongs to a subtype of bead forming collagens and assembles into beaded microfibrils in cartilage and in other tissues such as aorta, placenta, uterus, intervertebral disc, tendon, cornea, muscle, liver and kidney (Thomas et

al. 1994). These microfibrils localize close to cells, nerve, blood vessels, and large collagen fibrils and may be involved in the anchoring process. It is known to bind cells via COL-1, decorin and hyaluronan (which in turn binds to cartilage proteoglycan). This binding activity suggests that COL-6 may be involved in cell migration, differentiation, growth, remodeling process of connective tissue and embryonic development. (Bidanset et al. 1992; Kielty et al. 1992). It is expressed in a spatio-temporal manner during mouse embryogenesis; expression was detected in 10.5 day embryos, in branchial arches, large blood vessels and cephalic mesenchyme. By 16.5 days *Col-6A* expression increased in joints, intervertebral discs, perichondrium, periosteum, dermis skeletal muscle and heart valves (Marvulli et al. 1996).

Increased COL-6 collagen synthesis and disposition has been detected in several fibrotic diseases, osteoarthritis and patients with cutis laxa, which is characterized by loss of elasticity in the skin (van der Rest et al. 1991). A recent study indicates COL-6A1 on chromosome 21 as the locus of ossification of the posterior longitudinal ligament (OPLL). OPLL is a subset of disease, characterized by ectopic ossification in the spinal ligaments, is a common disorder that affects elderly population in eastern Asia and is a leading cause of spinal stenosis in Japan (Tanaka et al. 2003).

Collagen x (col-10): COL-10 belongs to a subtype of network-forming collagens. This homotrimeric, developmentally regulated collagen has a very restricted pattern of distribution. It is expressed only by the hypertrophic chondrocytes transiently during endochondral bone formation, and such as a tissue specific expression makes COL-10 an only known molecular marker specific for chondrocyte differentiation (Thomas et al. 1994). Transcription factor *OSF-2/RUNX-2* is required for differentiation of the mesenchymal stem cells into osteoblast lineage (Komori et al. 1997) and for chondrocyte differentiation during endochondral ossification (Enomoto et al. 2000), and multiple *Osf-2/Runx-2* binding sites have been identified within the promoter region of the human, mouse, and chick *Col-10* (Zheng et al. 2003). Decreased *Col-10* expression and altered chondrocyte hypertrophy was detected in *Osf-2-2/Runx-2* heterozygous mice and no *Col-10* expression was detected in *Osf-2/Runx-2* null mice (Zheng et al. 2003), suggesting *Col-10* is a direct transcriptional target of *Osf-2/Runx-2* during chondrogenesis. Mutation

in human *COL-10* is associated with a cartilage disorder, Schmid metaphyseal chondroplasia (SMCD) (Warman et al. 1993). The *Col-10*-null mice exhibit growth plate compressions partially resembling SMCD (Kwan et al. 1997).

Collagen xii (col-12a1): COL-12A1 belongs to subgroup FACIT collagens. It is expressed in embryonic tendon and skin, periodontal ligament, and perichondrium at the articular surface and around cartilage canals. Its functions are not clear but evidence suggests that COL-12A1 interacts with COL-1 (van der Rest et al. 1991; Thomas et al. 1994).

Collagen xvi (col-15a1) and collagen xviii (col-18a1): COL-15A1 and COL-18A1 together form a distinct not yet named subgroup of non-fibril forming collagens. COL-18A1 is the precursor of endostatin (anti-angiogenic factor) and the corresponding fragment in COL-15A1 has also been shown to have anti-angiogenic activity (Ramchandran et al. 1999; Sasaki et al. 2000). COL-15A1 is expressed in many tissues including kidney, lungs, most capillaries, heart and skeletal muscle (Hagg et al. 1997). COL-18A1 is expressed in several tissues including liver, lung, kidney, and eye (Oh et al. 1994). COL-15A1 provides mechanical stability to skeletal muscle cells and micro vessels (Eklund et al. 2001). COL-18A1 functions as an endogenous inhibitor of angiogenesis and tumor growth and also known to play a critical role in maintenance of the retinal structure and in neural tube closure (Sertie et al. 2000).

Collagen xvii (col-17a1): COL-17A1 belongs to a subclass of collagens with a transmembrane domain, and is a structural component of hemidesmosomes (multiprotein complexes that mediate the adhesion of epidermal keratinocytes to the underlying basement membrane) and is expressed in stratified squamous epithelium (Diaz et al. 1990; Li et al. 1993). Mutations in *COL-17A1* cause generalized atrophic epidermolysis bulbosa, a condition characterized by universal alopecia and atrophy of skin (Gatalica et al. 1997).

Non-Collagenous Extracellular Matrix Proteins: The non-collagenous proteins like glycosaminoglycans and proteoglycans together form hydrated gel-like substance and occupy a large volume of extracellular space. This fibrous protein embedded gel-like

substance not only helps to resist the comprehensive force on the matrix but it also permits the diffusion of nutrients, metabolites and hormones. While fibrous proteins like collagens and elastin provide tensile strength and elasticity to the tissues, non-collagenous proteins help cells in the tissue to carry out many of their biological functions. They facilitate cell adhesion, migration, differentiation and signaling. Several cell surface proteoglycans act as co-receptors for collagens, growth factors and other ECM proteins. (Alberts 1994). Some of the following non-collagenous proteins are associated with bone and cartilage development, cell growth and differentiation, cell adhesion and communication.

Matrilins: Matrilins belong to the superfamily of proteins with von Willebrand factor type A-like (vWF- A) modules. Matrilins are adapter proteins that form both collagen-dependent and collagen-independent filamentous networks (Mates et al. 2004). The matrilin family has four members, each containing one or two vWF-A domains, a variable number of EGF-like domains and a coiled coil c-terminal domain. vWF-A domains are known to mediate interactions with other proteins and are implicated in oligomerization, formation of macromolecular networks, cell adhesion and spreading (Jackson et al. 2004). Matrilins interact with collagens and proteoglycans. *Matn-1* binds to aggrecan (Hauser et al. 1996) as well as to *Col-2 in vivo* (Winterbottom et al. 1992) and is also known to bind integrin $\alpha 1\beta 1$, suggesting its involvement in cell adhesion and spreading (Makihira et al. 1999). Matrilin (MATN) -1 associates with cartilage proteoglycans in addition to being a component of both collagen- dependent and – independent fibrils (Deak et al. 1999). Furthermore, MATN-1, -3, and -4 are associated with COL-6 microfibrils in rat chondrosarcoma tissue and connect these fibrils to aggrecan and COL-2 (Wiberg et al. 2003). While MATN -1, -2, -3, and -4 are expressed in cartilaginous tissue; only MATN-2 and -4 are expressed in a variety of ECMs including non-skeletal tissues (Deak et al. 1999).

MATN-3 is a monomeric protein with only one vWFA domain followed by four EGF-like domains and a C-terminal coiled -coil domain. MATN-3 is known to form homotrimers via coiled-coil domain and mixed trimers and tetramers of MATN-3 and -1

have been detected in humans (Kleemann-Fischer, 2001) but not in mice (Klatt et al. 2000). Mouse *Matn-3* is highly homologous to human and chicken (Klatt et al. 2000). In mouse, earliest expression of *Matn-3* could be detected at E12.5 in cartilage anlagen of developing bones and in newborn mice; it is expressed in developing occipital bones and bones of nasal cavity. At E14.5 it was detected in the cartilage primodium of the vertebral bodies, the ribs, sternum, trachea, as well as the long bones (Klatt et al. 2000; Klatt et al. 2002). In six week-old mice, its expression was restricted to the growth plates of the long bones, sternum and vertebrae (Klatt et al. 2002). In addition to cartilaginous tissues, *Matn-3* is expressed in the osteoid around the osteoblasts attached to bone trabecula in the subchondral bone and around the osteocytes inside the cancellous bone (Klatt et al. 2000). In limbs, *Matn-3* is highly expressed in proliferating chondrocytes, weakly in resting cartilage, while no expression was detected in the hypertrophic zone (Klatt et al. 2000). *Matn-3* is also expressed in and secreted by osteoblasts (Klatt et al. 2000). All four members of the matrilins are expressed during mouse development (Klatt et al. 2000), suggesting that they may play an important role in endochondral bone formation. Although *MATN-1* and *-3* co-localize due to their ability to form heterodimers, they differ in their spatial and temporal expression. Only *MATN-3* but not *MATN-1* is detected in a region adjacent to the resting cartilage of the developing joint. Furthermore, *Matn-3* expression gradually ceases after birth, while *Matn-1* is continuously expressed in cartilage throughout life (Klatt et al. 2002).

Mutation in vWF-A domain of human *MATN-3* gene leads to autosomal dominant skeletal disorder, such as multiple osteochondroplasia (MED), a form of osteochondrodysplasia that is characterized by short stature, delayed and irregular ossification of the epiphyses and early onset of osteoarthritis (Chapman et al. 2001). In addition, *MATN-3* was reported to be highly upregulated in human osteoarthritic cartilage and a missense mutation in *MATN-3* was implicated in hand arthritis in a group of patients in Iceland (Stefansson et al. 2003). Another study by Ko et al (Ko et al. 2004) showed that absence of *Matn-3* had no obvious effects on mouse skeletal development. However, they suggest that other members of the Matrilin family may compensate for *Matn-3*.

Tenascins: Tenascins are a family of large oligomeric glycoproteins primarily found in the ECM of vertebrates. To date, five members of the family have been identified in mammals: tenascin-X (TNX or TNXB), tenascin-C (TNC or cytotactin), tenascin-R (TNR), tenascin-W (TNW), and tenascin-N (TNN) (Hsia et al. 2005). All members of the tenascin family have common motifs and are characterized by N-terminal globular domain and heptad repeats, which facilitate multimerization, followed by one or more EGF-like repeats, several fibronectin (FN) type III domain repeats, and a C-terminal fibrinogen-like globular domain (Weber et al. 1999). All vertebrates express more than one tenascin gene and each member has a distinctive expression pattern, and their expression is regulated during development and throughout the organism's life span. Different connective cells secrete different types of tenascins and they contribute to ECM structure and influence the function and behavior of the cells in contact with them. Several studies suggest that tenascins play an important role in regulating cell-extracellular matrix interaction, thus promoting cell rounding, migration and differentiation (Chiquet et al. 1994; Matsumoto et al. 1994). This protein family plays an important role during embryogenesis as well as during pathological states in adults such as inflammatory disease, tissue injury, tumorigenesis and wound healing (Tucker et al. 2006).

Tenascin-x (Tnx, Tnxb): TNX is the largest known member of the tenascin family. TNX gene lies in the major histocompatibility complex (MHC) class region in both human and mouse and it overlaps the gene encoding 21-hydroxylase and a gene encoding an untranslated adrenal specific RNA on human chromosome 6 (Bristow et al. 1993). Although TNX is capable of forming trimers, it differs from other family members in that it is unable to form hexamers because it lacks the N-terminal cysteine residues that are required for hexamer formation. It has 18.5 EGF-like repeats and 29 (mouse) or 32 (human) FN type III repeats domains. Furthermore, unlike TNC and TNR, TNX is not heavily glycosylated and does not contain the RGD sequence, and hence cannot bind to RGD-dependent receptors (Bristow et al. 1993).

TNX is known to interact with several ECM proteins. C-terminal domains of *TNX* bind to major fibrillar collagens like *COL-1*, -3, -5, -6 and topoelastin (Minamitani et al. 2004; Egging et al. 2007). Bovine and murine *Tnx* bind heparin (Matsumoto et al. 1994; Lethias et al. 2001) and since this heparin-binding site is also involved in the binding of *TNX* to decorin, a proteoglycan, it is suggested that *TNX* interacts with collagen fibrils through decorin and this association contributes greatly to the integrity of ECM (Elefteriou et al. 2001). *TNX* is also involved in cell-matrix and cell-cell adhesion. *TNX*-null fibroblasts exhibit adhesive defect in ECM (Minamitani et al. 2004). *TNX* is also known to modulate fibrillogenesis and expression of *COL-6*. *TNX* increases the rate of collagen deposition while *COL -6* accelerates the rate of collagen formation (Minamitani et al. 2004).

TNX is widely expressed during human fetal development, with high levels of expression in testis, skeletal, cardiac, and smooth muscle. In adults expression is limited to musculoskeletal, dermis, and cardiac tissues (Hsia et al. 2005). *TNX* expression is also detected in adult peripheral nerves. Investigations into the mechanisms of *Tnx* activity in the cardiac and skeletal muscle suggest that the protein exerts functions during morphogenesis and cell migration in connective tissues (Burch et al. 1997). *Tnx* expression is complementary to *Tnc* during mouse heart development, (Elefteriou et al. 2001), but its expression is often reciprocal to *Tnc* in several adult and fetal tissues (Matsumoto et al. 1994; Geffrotin et al. 1995; Imanaka-Yoshida et al. 2003). In pigs, it is significantly expressed in two thirds of the 28 tissues examined while *Tnc* is expressed in 50% of them. *Tnx* is highly expressed in adult and fetal nerves, dermis, skin, heart, uterus, placenta, and aorta, lung, mammary gland, stomach, skeletal and adrenal gland of fetuses. In contrast, *Tnc* is highly expressed in fetal brain and adult spinal cord, ligament, tendon, and colon (Geffrotin et al. 1995). *TNX* is also expressed in human intervertebral discs throughout the annulus (Gruber et al. 2002).

TNX deficiency in humans is associated with a clinically distinct, autosomal recessive form of Ehlers-Danlos Syndrome (EDS), which is characterized, by hyperextensible skin, hypermobile joints, and tissue fragility (Schalkwijk et al. 2001). Even though haploinsufficiency of *TNX* is associated with EDS, it is distinguished from

the classic autosomal dominant EDS by its mode of inheritance, lack of atrophic scars and an etiology due to a mutation in a gene that does not encode a fibrillar collagen or collagen-modifying enzyme (Zweers et al. 2005). *Tnx* null mice were viable and normal at birth. The skin of these mutant mice was histologically normal, but was noticeably hyperextensible. Collagen content was significantly reduced although *Tnx* skin fibroblasts synthesized near normal amount of *Col-1*. This discrepancy was attributed to a significant reduction in collagen deposition thus confirming the hypothesis that *TNX* deficiency causes EDS through regulation of collagen fibril deposition into the matrix and not by interfering with collagen synthesis or processing as observed in other forms of EDS. (Mao et al. 2002; Bristow et al. 2005).

The mechanism by which *TNX* regulates fibrillogenesis is not clear but a recent report suggests that *TNX* can affect the rate of collagen fibril formation either by directly binding to collagen or through regulating the synthesis of *COL-6*, which is known to affect fibril formation (Minamitani et al. 2004). Moreover, Letias et al. (Lethias et al. 2001) reported that *TNX* is capable of binding decorin, which is known to bind collagen and regulate fibrillogenesis (Elefteriou et al. 2001). *TNX* also seems to regulate elastogenesis and matrix remodeling. Patients deficient in *TNX* have abnormal elastic fibers characterized by fragmented clumped elastic fibers (Zweers et al. 2005). Furthermore, fibrilin-2 and stromelysin, a protease and regulator of α -1 proteinase inhibitor that binds and inhibits elastase were significantly upregulated in *Tnx* null mice fibroblasts (Bristow et al. 2005). These studies indicate that *TNX* plays an important role in maturation and/or maintenance of higher order collagen structures in the ECM and the elastic network.

Tenascin c (tnc): TNC (haxabrachion or cytotactin) is a hexameric, multidomain ECM glycoprotein with a spatially and temporally restricted tissue distribution. Each subunit of hexameric protein consists of N-terminal tenascin assembly domain (TA), followed by 14.5 EGF-like repeats, and 8 FN type III repeats (Gulcher et al. 1991). *TNC* is known to interact with cell surface proteoglycans, fibronectin, and various collagens (Hoffman et al. 1988; Chiquet-Ehrismann 1991; Salmivirta et al. 1991). In the developing embryo, *TNC* is expressed in the skeletal and nervous system (Tucker

et al. 1994; Hsia et al. 2005), particularly in myotendinous joints and at insertions of ligaments and tendons (Thesleff et al. 1988; Chiquet et al. 1994). It is selectively expressed in mesenchymal condensation sites prior to intramembranous ossification and chondrogenesis (Mackie et al. 1987). During endochondral ossification it is expressed in periosteal cells and in osteoblasts that are invading the primary center of ossification. Transcript levels diminish during chondrocyte differentiation and expression is undetectable in the matrix surrounding the hypertrophic chondrocytes (Mackie et al. 1987; Mackie et al. 1992). In adult cartilage, it is not expressed or expression becomes restricted (Pacifci et al. 1993). Although *TNC* is secreted by osteoblasts, it remains on the bone surfaces and is rarely incorporated into mineralized matrix (Mackie et al. 1987). *TNC* is detectable in small amounts in normal adult tissues such as smooth muscle cells, endothelial cells, myotendinous tissue, spinal cord, kidney and lung (Soini et al. 1993; Roth-Kleiner et al. 2004). However, its expression is upregulated sharply in the tissues undergoing remodeling process as in wound repair, and neovasularization or in pathological states like tumorigenesis and inflammation (Natali et al. 1991).

Exogenous *TNC* is known to stimulate chondrogenesis in limb-bud mesenchymal cells (Mackie et al. 1987). *TNC* has multiple functions during embryonic development and postnatal growth, and some of its roles include participation in regulation of cell proliferation, migration, differentiation, survival, cell adhesion and epithelial mesenchymal interface formation during organogenesis, tissue repair, and somatic growth regulation (Saga et al. 1991; Roth-Kleiner et al. 2004). Additionally, *TNC* participates in chondrogenesis and cartilage development (Pacifci et al. 1993). Pacifci et al. (Pacifci et al. 1993) showed that *TNC* is involved in the genesis and function of articular chondrocytes. *TNC* not only regulates chondrocyte development at the epiphysis of long bone models, but it also assists in maintaining chondrocyte function throughout postnatal life. The latter involves inhibiting the endochondral ossification process that is undertaken by the chondrocytes at the metaphysis and diaphysis of skeletal models (Pacifci 1995). *Tnc* knockout mice are viable, fertile and phenotypically normal, thus questioning the critical role of *Tnc* in embryonic as well as postnatal development (Saga et al. 1992). However, several reports suggest that lack of phenotype in knockout mice

may be due to redundant mechanisms, namely the ability of other tenascin family members, especially *Tnx* to compensate for *Tnc*. Additionally, although *Tnc* knockout mice were initially reported to be phenotypically normal, several studies have reported abnormal tissue restoration after injury to skin, cornea, or after glomerulonephritis (Nakao et al. 1998; Matsuda et al. 1999) and abnormal behavior due to reduced production of certain neurotransmitters (Tamaoki et al. 2005).

Proteoglycan 4 (Prg4): *PRG4*, also known as Lubricin or Megakaryocyte-stimulating factor (MSF) or superficial zone protein (SZP), is a large multifaceted, cytoprotective proteoglycan. It is a major component of synovial fluid that acts as a major lubricant in articular cartilage; protecting the cartilage surface from friction-induced wear, protein deposition and cell adhesion and also preventing synovial outgrowth. *PRG4* is produced and secreted by synovial cells and superficial zone chondrocytes and is expressed in superficial zone of both adult and fetal articular cartilage, synovial cells, bone, liver, heart, and lung. (Rhee et al. 2005).

PRG4 is a paralog of vitronectin and contains multiple domains that are likely to contribute its diverse biological functions (Rhee et al. 2005). It contains somatomedin B (SMB) and O-linked glycosylated homopenin-like (PEX) and mucin-like domains. In vitronectin, both SMB and PEX domains have been known to mediate extracellular matrix attachment, promote cell attachment and proliferation, and regulate the complement and coagulation system (Deng et al. 2001). The negatively charged sugars in mucin-like domains enable the *PRG4* to act as a lubricant due to strong repulsive hydration forces (Jay 1992). Additionally, diverse biological functions have been attributed to other mucin-containing proteins such as proteins of epithelial surfaces, which control cell growth and regulate cell differentiation (Van Klinken et al. 1995; Simmons et al. 2001). Furthermore, its increased expression during ectopic ossification in mouse also suggests that *Prg4* may be involved in the regulation of ossification (Ikegawa et al. 2000). Loss-of-function mutation in *PRG4* causes the rare, autosomal recessive disease Comtodactyly-arthropathy-coxavara-pericarditis syndrome (CACP), which is characterized by precocious joint failure (Marcelino et al. 1999). *Prg4* knockout mice

exhibit similar defects as CACP patients and have severe joint pathology due to abnormal protein deposits on cartilage surface, articular cartilage destruction and marked synovial cell outgrowth (Rhee et al. 2005). Early loss of *PRG 4* from cartilage surface in association with a decrease in its expression in chondrocytes implicates *PRG 4* in the pathogenesis of osteoarthritis (Young et al. 2006).

Thrombospondin III (Thbs3, Tsp-3): *TSP-3* is a member of a family of modular, multifunctional glycoproteins that mediate interactions between cells and ECM (Adams et al. 1993). The thrombospondin family consists of five structurally related genes designated as *TSP-1*, -2, -3, -4 and COMP (cartilage oligomeric matrix protein). *TSP-3* is an oligomeric heparin binding protein that resembles *TSP-1* and -2 in its C-terminal domain, which includes seven type III (Ca²⁺ binding repeats) and carboxy terminal region. *TSP-3* contains a distinct N terminus and four type II EGF like repeats but it lacks procollagen homology and type I repeats that are found in *TSP-1*, -2 and -4 (Bornstein 1992). TSPs are known to interact and bind to cell surface molecules like heparin sulfate proteoglycans, $\alpha\gamma\beta3$ integrins, glycoprotein IV, sulfated glycolipids and to ECM proteins like *COL-1* and *COLI-5*, fibronectin and laminin (Frazier 1991).

TSP-1, -2 and -3 are expressed in a unique spatio-temporal manner during murine embryogenesis, especially in the nervous system, gut, cartilage and lung. In general *TSP-3* is highly expressed in endocrine, muscle and fetal tissue (Qabar et al. 1994). Several studies show that *TSP-3* is expressed in the early articular cartilage while *TSP-1* is expressed in early or immature chondrocytes (Tucker et al. 1997). On day 19, *Tsp-3* expression was also high in the sternum and vertebral bodies, especially in perichondrium and hypertrophic chondrocytes, and it was expressed in moderate levels in the spinal cord and brain (Qabar et al. 1994). In addition, in postnatal bovine tissues, *Tsp-3* is almost exclusively expressed in chondrocytes (Qabar et al. 1994) and in four week old mice, it is highly expressed in lungs, bone, tail, skin, skeletal muscle and heart (Vos et al. 1992). Gruber et al (Gruber et al. 2006) recently reported the presence of *TSP* in the outer annulus of both human and sand rat intervertebral discs, indicating a role for *TSP* in

maintenance of disc health (maintenance of avascular status) in adult human and sand rats.

In general, TSP family members have been implicated in a large number of cellular processes such as embryonic development, tissue differentiation, blood coagulation, tumor growth and metastasis, angiogenesis, nerve development, wound healing and inflammation (Frazier 1991; Adams et al. 1993; Bornstein et al. 1994). They have been known to regulate cell-matrix interaction (may increase or decrease these interactions), inhibit endothelial cell growth but stimulate neurite outgrowth and smooth muscle cells, stimulate chemotaxis and inhibit angiogenesis (reviewed in (Vos et al. 1992). Even though both human and mouse *TSP-3*'s have been characterized, their functions remain unclear. However, based on several studies mentioned above, it may play a role in chondrogenesis, and in the development of lung and central nervous system during embryogenesis. Since *TSP-3* and other members of TSP family are sometimes expressed in complementary pattern and also due to its structural similarity with other family members, *TSP-3* may have some similar functions or its functions could overlap with other members of the family. *Tsp-3* null mice are viable, fertile and show normal prenatal skeletal development. However, developing postnatal skeleton showed subtle and transient abnormalities. *Tsp*-knockout mice exhibit more mature skeleton and accelerated the rate of endochondral ossification in the cartilage of femoral head (Hankenson et al. 2005). These results along with the presence of *TSP-3* in cartilage and bone suggest that *TSP-3* plays an important role in the regulation of postnatal bone modeling, maturation and endochondral ossification.

Chondroadherin (chad): *CHAD* is a noncollagenous ECM protein and is a unique member of the small leucine rich repeat (LRR) proteoglycan family. Unlike other LRR proteins *CHAD* shows restricted tissue distribution. Under normal conditions its expression is mainly confined to tendons and cartilage (femoral head and rib cartilage), bone marrow and is also expressed during chondrogenic differentiation of mesenchymal stem cells. (Shen et al. 1998; Barry et al. 2001). It is known to bind to *COL-2*. Both *COL-2* and *Chad* bind to chondrocytes partly via $\alpha_2\beta$ integrin but elicit different cellular

responses. It has been suggested that sharing one of the receptors on chondrocytes and by interacting with each other, both *COL-2* and *CHAD* may facilitate cell communication with their surrounding matrix and/or regulate collagen fibril assembly. (Mansson et al. 2001). *CHAD* may mediate attachment and/or cell signaling by interacting with $\alpha_2\beta$ on cells. Temporal expression of *CHAD* during skeletal development suggests that it plays an important role in the regulation of chondrocyte growth and proliferation (Mansson et al. 2001). Additionally, *CHAD* promotes attachment of osteoblasts to solid-state substrates and binds collagen, suggesting that *Chad* is important in maintaining osteoblasts on the collagen matrices of bone (Mizuno et al. 1996).

BONE MORPHOGENETIC PROTEINS (BMP) AND BMP RECEPTORS

(BMPRs): BMPs are members of the Transforming growth factor (TGF- β) superfamily that regulate cell proliferation, differentiation and apoptosis in many cell types including, bone and cartilage cells, monocytes, neural cells, and epithelial cells (Sakou 1998). These proteins were first identified by their ability to promote ectopic cartilage and bone development. BMPs induce differentiation of mesenchymal cells into osteoblast and chondrocyte lineage cells *in vitro* (Ahrens et al. 1993). BMP-2, -4, -7 (osteogenic protein) mediate bone and cartilage formation *in vivo* (Wozney et al. 1988), while GDF-5 (cartilage derived morphogenetic protein 1) and GDF-6 induce formation of cartilage and tendon-like structures *in vivo* (Hotten et al. 1996; Wolfman et al. 1997). Several studies show that induction of mesenchymal cell differentiation toward cells of osteogenic lineage, promotion of osteoblastic maturation and function by BMPs are mediated by Smad1/5 and *OSF-2/RUNX2* (Gori et al. 1999; Lee et al. 2000). *OSF-2/RUNX2* is upregulated by *BMP-2, -4, and -7* via *MSX-2* in multipotential, osteoblastic and chondrogenitor cell lines (Tsuji et al. 1998; Gori et al. 1999). BMPs stimulated chondrocyte maturation and the enhancement of the function of chondrocytes is mediated by *SOX9*, a gene critical for chondrogenesis (Semba et al. 2000). *BMP-2, -4, and -6* induce *SOX9* and over-expression of *BMP-2* and *-4* results in increase in chondrocyte number and cartilage formation (Duprez et al. 1996). Additionally, interaction between

BMPs, Smads and *OSF-2/RUNX2* is required for chondrogenesis and *COL-10* transcription during chondrogenesis (Leboy et al. 2001).

The importance of BMPs in bone development has been demonstrated by mouse gene knockout studies. Mice deficient in *Bmp-2* and *-4* are not viable. In conditional *Bmp-2* and *-4* knockout mice, chondrogenic condensations fail to form and osteogenesis was severely impaired (Bandyopadhyay 2006). The *Bmp-6* null mice are viable and fertile and exhibited a delay in the ossification of the sternum (Solloway et al. 1998). *Bmp-7* mice die after birth because of poor kidney development. In addition, these mice have eye defects and modest defects in skeleton such as fused ribs and skull, hind limb defects and vertebral defects such as lack of fusion of the neural spines of the atlas, twelfth thoracic and first sacral vertebrae, and opening on the sides of the neural arches of the third and fourth thoracic vertebrae and the absence of lumbar vertebrae. Intervertebral discs have unequal thickness and mutants have small or no ossification centers (Jena et al. 1997).

BMPs exert their biological effects by binding to heterotrimeric complexes of type I (BMPR-1A) and type II (BMPR-1B) serine/threonine kinase receptors. Upon BMP binding, constitutively active *BMPR-1B* transphosphorylates *BMPR-1A*. Activated BMPR-1A then phosphorylates/activates intracellular Smads, which then translocate to nucleus and regulate the transcription of target genes (ten Dijke et al. 1994). Both receptors can bind to *BMP-2*, *-4*, *-7* and *GDF-5*. In the chick, *Bmpr-1a* is expressed in joint interzones, perichondrium, periarticular cartilage, and hypertrophic chondrocytes while *Bmpr-1b* is expressed primarily in condensing precartilaginous mesenchymal cells, perichondrium and periarticular cartilage (Dewulf et al. 1995; Yoon et al. 2005). In mice, both of these receptors are expressed in pre-cartilaginous mesenchymal cells (Yoon et al. 2005). Several reports show that BMP signaling via *Bmpr-1a* and *-1b* are essential for multiple aspects of early chondrogenesis and both BMP receptors have some overlapping functions (Yoon et al. 2005). The constitutively active forms of *Bmpr-1a* or *Bmpr-1b* promote chondrogenesis. A null mutation in the *Bmpr-1b* gene produce viable mice with defects confined to phalangeal elements while *Bmpr-1a* deficient mice die during gastrulation (Mishina et al. 1995; Baur et al. 2000). *Bmpr-1a* conditional knockout mice

(*Bmpr-1a^{cko}*) have similar and few skeletal defects like *Bmpr-1b* null mice, and both *Bmpr-1a^{cko}* and *Bmpr-1b^{-/-}* double mutants develop severe and generalized chondroplasia (Yoon et al. 2005). Additionally, over-expression of *Bmpr-1a* rescued the differentiation defect of pre-chondrogenic cells in *Bmpr-1b* null mice (Kobayashi et al. 2005). These reports show that *Bmpr-1a* and *-1b* have overlapping functions in chondrogenesis. In *Bmpr-1a^{cko}* mice, ossification of long bones is delayed, bone sizes are reduced and ribcage is smaller and flattened, leading to respiratory distress and subsequent death. In both *Bmpr-1a* and *-1b* double conditional null mice, majority of skeletal elements that form through endochondral ossification are absent or malformed presumably due to impaired differentiation of prechondrocytes into chondrocytes. Moreover, the expression of cartilage specific ECM proteins (*Col-2*, *Col-10* and aggrecan) is severely reduced in mutants. In contrast, development of clavicles and craniofacial bones, which form through intramembranous ossification, is not affected in these mutant mice. (Yoon et al. 2005).

NELLI: A NOVEL CELL DIFFERENTIATION SIGNALING PROTEIN IN BONE AND CARTILAGE DEVELOPMENT

Several specific growth factors and transcription factors are known to regulate both osteoblast and chondrocyte proliferation and differentiation. As discussed in the previous section, many growth factors like FGF-3, TGF- β , BMPs and transcription factor like OSF-2/RUNX2 are already known to regulate osteoblast/chondrocyte differentiation. In the past decade, increasing evidence from several studies, including the work presented in this dissertation, have identified a novel signaling protein, designated as *Nelli/NELLI* that controls cell differentiation in bone, cartilage and muscle (Kuroda et al. 1999; Zhang et al. 2002; Desai et al. 2006).

GENE AND PROTEIN STRUCTURE: In 1995, Matsushashi et al. (Matsushashi et al. 1995) cloned the gene encoding a novel protein from a chicken embryonic cDNA and designated this protein as nel (neural epidermal growth factor-like) because it was

strongly expressed in neural tissues and contained six EGF-like domains. In the following year, Watanabe et al. (Watanabe et al. 1996) cloned two novel genes from a human fetal brain cDNA library that were homologues of nel like type 1 (NELL1) and nel like type 2 (NELL2). Kuroda et al. (Kuroda et al. 1999) then used a yeast two-hybrid system to clone closely related genes coding for *Nelli* proteins from a rat brain cDNA library, which were mapped to human chromosomal bands 11p15.1-p15.2 and 11q13.11-q13.12 respectively. Human *NELL1* is highly homologous to rat (87%) and mouse (87%) at the nucleotide level. *NELL1* is a large gene, ~ 1mb (907311 bp) in length, with a transcript of 3245 bp, which encodes an 810 amino acid protein. Mouse *Nelli* is 889138 bp long with a transcript of 2812 bp, which encodes an 810 amino acid protein. Both human and mouse *NELL1/Nelli* have 20 exons while rat has 24 exons. [<http://www.ensembl.org>, (Desai et al. 2006)].

The *NELL1* gene encodes a 90 Kda polypeptide that is glycosylated and then processed into a 130 Kda cytoplasmic protein and is secreted as a 400 Kda trimeric form (Kuroda et al. 1999). *NELL1* is a complex multidomain protein. Human *NELL1* has a thrombospondin (TSP)-like domain, Laminin G (LAM G)-like domain, five von Willbrand factor C (vWC)-like domains and six epidermal growth factor (EGF)-like domains, while mouse *Nelli* has one TSP like domain overlapping the LAM G domain, one EGF like domain and two vWC like domains (Desai et al. 2006). It is known to bind to specific forms of PKC (PKC- β 1, - δ , - τ) through EGF-like domains and heparin through its TSP-1 like domain and its vWC domains are involved in oligomerization of the protein (Kuroda, 1999). Human *NELL1* protein shares high homology with mouse (93%) and rat (92%) *Nelli* proteins (Kuroda et al. 1999; Desai et al. 2006).

EXPRESSION PROFILE IN HUMANS AND MOUSE: In mouse, *Nelli* expression was detected as early as embryonic days 11-14 (Ting et al. 1999) and is preferentially expressed in the craniofacial region (calvarial bones and mandible), during both embryogenesis and after birth (Zhang et al. 2002). In rat, *Nelli* is expressed in neuronal cell (Kuroda et al. 1999) and calvarial osteoprogenitor cells, but it was largely absent in rat long bones (Ting et al. 1999). It is expressed in human fetal brain but not in other fetal

organs like kidney, liver and lung (Ting et al. 1999). In humans, *NELL1* is specifically expressed in osteoblasts and mesenchymal cells around the newly formed bones along the parasutural bone margins and within the abnormally fusing and recently fused sutures. Additionally, it was markedly upregulated in prematurely fusing and fused coronal sutures. Conversely, it was absent or down regulated in patent normal sutures (Zhang et al. 2002). *NELL1* is also expressed in several embryonal neuroepithelial tumors (neuroblastoma, neurocytoma, and meduloblastoma) (Maeda et al. 2001), leukemic cell lines (Luce et al. 1999), and Burkitt's lymphoma Raji cells (Kuroda et al. 1999).

GENE REGULATION AND ASSOCIATED PATHWAY(S): *NELL1* is regulated by several growth factors and transcription factors. Osteoinductive growth factors like *FGF-2* and *TGF- β 1* stimulate *NELL1* expression while *BMP-2* had no direct effect on it (Aghaloo et al. 2006). *Nell1* seems to operate downstream of these growth factors because there is no change in the expression of *Tgf- β 1*, *- β 2*, *- β 3* or *Tgf- β /Bmp* receptor and *Fgfr/Fgfr2* in *Nell1* infected MC3T3 cells (mouse calvarial osteoblast cell line) (Zhang et al. 2002). Furthermore, *NELL1* expression is also modulated by transcription factors such as *MSX-2* and *OSF-2/RUNX2*. *NELL1* promoter contains multiple conserved *MSX-2* and *OSF-2/RUNX2* binding sites. Fetal rat calvarial cells (FRCCs) transfected with *Osf-2/Runx2* upregulated *NELL1* expression, while *Nell1* did not upregulate *Osf-2/Runx2* expression (Lu et al. 2007; Truong et al. 2007). This shows that *Nell1* functions downstream of *Osf-2/Runx2* and is directly regulated by it. In contrast, *Msx-2* transfection and *Osf-2/Runx2/Msx-2* co-transfection of FRCCs downregulated *Nell1* expression (Zhang, 2002). *MSX-2* functions upstream of *OSF-2/RUNX2* and suppresses its transcription (Shirakabe et al. 2001; Yoshizawa et al. 2004).

NELL1 is known to regulate the expression of several genes, which are involved in bone development. It is known to upregulate osteoblastic differentiation marker genes like *OPN*, *OCN*, *BSP* and chondrocyte differentiation marker *COL-10* (Zhang et al. 2002; Cowan et al. 2006).

FUNCTIONS: *NELLI* is a newly characterized gene and its functions in the mammalian system are just beginning to be elucidated. After the identification of the human gene sequence, the *NELLI* protein was predicted to facilitate cell growth and differentiation based on the presence of EGF-like domains. The capability to bind heparin through TSP-like domains, further suggested that it signals osteogenic differentiation. (Kuroda et al. 1999). Several recent studies using *in vitro* systems and *in vivo* mutant mouse models (including the work described herein) have revealed significant insights into the nature and mechanisms of *NELLI/Nell1* function.

Overexpression of human *NELLI* in the cranial sutures is associated with unilateral coronal craniosynostosis (UCS), the premature closure of cranial sutures in newborns (Ting et al. 1999). Zhang et al (Zhang et al. 2002) further characterized the role of *Nell1* in suture fusion by creating an overexpressing transgenic mouse model. Since the complete gene sequence of the mouse *Nell1* was not available unlike the rat and human genes at the time of this study, the rat gene was used to create transgenic mice overexpressing *Nell1* protein. Despite generalized, non tissue-specific overexpression of *Nell1*, the skeletal defects in these mice were restricted to the calvarial bones. The transgenic mice exhibited CS and no apparent defects in other organs. As in human CS, transgenic mice exhibited prematurely closing/closed sutures and the osteogenic fronts of these abnormally closing/closed sutures exhibited calvarial outgrowth and overlap along with reduced proliferation and increased osteoblast differentiation. *In vitro* studies were consistent with the transgenic mouse data since *Nell1* overexpression in FRCCs and MC3T3 accelerated osteoblast differentiation and mineralization along with upregulation of late osteoblast differentiation markers like *Opn*, *Ocn* and *Bmp-7*. Conversely, downregulation of *Nell1 in vitro*, reduced *Ocn* and *Opn* expression and delayed osteoblast differentiation (Zhang et al. 2002).

Several reports show that *Nell1* also has a profound effect on osteoblast and chondrocyte apoptosis. A study by Zhang et al (Zhang et al. 2003) indicated that *Nell1* modulates calvarial osteoblast differentiation and apoptosis pathways during intramembranous ossification in the developing skull. The *Nell1* overexpression transgenic mouse model exhibited various degrees of CS and showed increased apoptosis

in calvarial osteoblast. Also, overexpression of *Nell1* in FRCCs and MC3T3 cells induced apoptosis. These studies suggest that dysregulation of proliferation, differentiation and apoptosis along with imbalance between osteogenic inducers and inhibitors at osteogenic fronts in calvarial bones leads to premature suture closure. They further suggested that the overexpression of *NELL1* disrupts the delicate balance between proliferation, differentiation and apoptotic pathways and this in turn leads to craniofacial anomalies such as CS.

A recent study by Zhang et al (Zhang et al. 2006) shows that overexpression of *Nell1* induces acrania-like cranioskeletal deformities. Acrania is a craniofacial developmental deformity characterized by partial or complete absence of flat bones of skull with complete, but abnormal development of the brain. Overexpression of *Nell1* induced acrania at E15.5 day in mouse embryos, through massive Fas-mediated apoptosis in osteoblast and neural cells. In the previous *Nell1* transgenic model, apoptosis was induced in differentiated osteoblast but not in undifferentiated mesenchymal cells. In this new mouse model *Nell1* was discovered to regulate cranial neural crest cell migration/differentiation (Zhang et al. 2006) and to induce apoptosis in these cells with subsequent acrania. This study further suggests that moderate upregulation of *Nell1* leads to increased osteoblast differentiation and CS, while exaggerated overexpression of *Nell1* like in *Nell1* transgenic mice model induces massive apoptosis in osteoblast and cranial neural crest cells and subsequently neural tube defect like acrania (Zhang et al. 2002; Zhang et al. 2006).

The earlier reports have demonstrated unequivocally that *Nell1* plays a critical role during intramembranous bone formation. The focus of these studies was on the effect of *Nell1* on calvarial osteoblast biology and craniofacial development. However, several recent studies show that *Nell1* regulates intramembranous as well as endochondral bone development. The work described here represents the first report on the involvement of *Nell1* in chondrogenesis and endochondral ossification (Desai et al. 2006). Recently, Cowan et al (Cowan et al. 2006) reported that *Nell1* accelerates chondrocyte hypertrophy and endochondral bone formation within the distracted maxillary suture. When overexpressed, it also induced premature hypertrophy and increased apoptosis of

chondrocytes, which in turn leads to distortion of chondrocranium and subsequent acrania-like cranial deformity during mouse development (Zhang et al. 2006).

Furthermore, several recent reports show that *NELLI* frequently undergoes loss of heterozygosity (LOH) in human cancers (Dolan et al. 1998; Jin et al. 2007). LOH and promoter hypermethylation are few of the mechanisms that lead to gene inactivation (Knudson 2001). *NELLI* promoter is hypermethylated in esophageal adenocarcinoma and squamous cell carcinoma (Jin et al. 2007), colon cancer (Mori et al. 2006), and lung carcinoma (Shiraishi et al. 2002). The promoter hypermethylation has been shown to be involved in silencing of tumor suppressor genes (Herman et al. 2003). All these studies suggest that *NELLI* may function as a tumor suppressor gene in certain human cancers.

PROTEIN KINASE C SIGNALING PATHWAYS AND ITS RELATIONSHIP TO

NELLI: Several previously published reports show that PKC and *NELLI* are involved in the signal transduction pathways that are utilized in osteogenesis and chondrogenesis. Additionally, *NELLI* is known to bind and become phosphorylated by specific isoforms of PKC (Kuroda et al. 1999; Hay et al. 2001; Rosado et al. 2002; Marie 2003).

Protein kinase C (PKC): PKC comprises a family of serine/threonine kinases that control a vast variety of cellular functions in various cell types. The PKC family consists of at least twelve isoforms with different tissue expressions, subcellular localization, and substrate specificity. These PKC isoforms are involved in signal transduction pathways that regulate cell proliferation, differentiation, development and apoptosis (Nishizuka 1988). Based on their structure and cofactor requirements, PKC family members are classified into the following categories: a) classical PKCs (PKC- α , PKC- β II and PKC- γ) which bind phorbol esters and are Ca^{2+} dependent, b) novel PKCs (PKC- δ , PKC- ϵ , PKC- η and PKC- θ) that bind phorbol esters but are not Ca^{2+} dependent, and c) atypical PKCs (PKC- ι , PKC- ζ , PKC- λ and PKC- μ) which do not bind to either phorbol or Ca^{2+} . (Hug et al. 1993). Different isoenzymes may have unique or sometimes similar or even opposite effects on cell growth (Svensson et al. 2000). Most cell types contain more than one subspecies of PKC.

The PKC isoenzymes are expressed in a tissue-specific manner (Table. 2.1), and the amount and number of PKC isoenzymes varies within a given tissue depending on its developmental stage. PKC- α , - β , - ϵ and - δ are expressed in osteoblasts (Yang et al. 2002)). Differential expression of PKC isoenzymes was detected during the development of human fetal vertebral column. PKC- α and - β I were highly expressed and PKC- δ , - β II and - ζ in moderate amounts in chondrocytes of vertebral bodies, whereas PKC- α , - ζ and - θ were expressed more in intervertebral space (Bareggi et al. 1995). PKC was expressed highly in mature cells that are close to ossification centers as well as near vertebral discs and especially PKC- β and - ϵ were highly expressed in proliferating chondrocytes and hypertrophic chondrocytes. The presence and differential expression of PKC isoforms was detected during the 8th week of developmental age in human fetal vertebral column when most of the chondrogenic and osteogenic events occur (Bareggi et al. 1995).

PKC is regulated by several growth factors including FGFs, BMPs and TGFs and parathyroid hormone (Opperman et al. 2000; Marie 2003). These growth factors along with the transcription factor OSF-2/RUNX2 and *NELLI* play a major role in bone and cartilage development. Members of the FGF family are known to play important roles in skeletal development and postnatal development and activating mutations of human *FGFR-1*, -2, and -3 genes cause craniosynostosis and other skeletal defects (Wilkie 1997). FGFs controls bone formation by regulating the expression of various genes involved in osteoprogenitor cell proliferation, osteoblast differentiation and apoptosis via PKC and MAP kinases (ERK and p38 MAP kinases) which in turn regulate transcription factor like OSF-2/RunX2 and regulate the expression of target genes like COL-1, IL-6, OCN, OPN, VEGF, alkaline phosphatase and *NELLI* (Marie 2003; Aghaloo et al. 2006). BMPs play a critical role in bone and cartilage development and postnatal bone formation. They are known to regulate the genes involved in the differentiation of osteoprogenitor cells, endochondral ossification, chondrogenesis and apoptosis (Hay et al. 2001; Marie et al. 2002). BMPs are known to mediate their action through PKC and OSF-2/RUNX2 development pathways (Hay et al. 2001; Lee et al. 2002). TGF- β is a potent regulator of osteo-chondroprogenitor cell migration and proliferation and differentiation of osteoblasts and chondrocytes (Mehrrara et al. 2002; Rosado et al. 2002).

Table. 2.1: Tissue Specific Expression of Protein Kinase C (PKC) Isoforms.

PKC Isoforms	Expression
PKC- α , - β I/II, - δ , - ϵ and - ζ	brain, lung, spleen, thymus, skin and liver (Hug, 1993)
PKC- θ	skeletal muscle (+ +), lung, spleen, skin, and brain (+) (Hug, 1993)
PKC- η	skin and lung (+ +), brain and spleen (+) (Hug, 1993)
PKC- ϵ	hematopoietic cells and skeletal muscles (Hug, 1993)
PKC- α , - β , - ϵ and - δ	osteoblasts
PKC- α , - β I, - δ , - β II and - ζ	chondrocytes and vertebral bodies
PKC- α , - ζ and - θ	intervertebral space

+ + Indicates predominant/ strong expression, + indicates moderate expression.

TGF- β is known to upregulate PKC and OSF-2/RUNX2 in both osteoblast and chondrocytes and mediates some of its biological functions through activating MAP kinases via PKC and thereby regulates OSF-2/RUNX2 and transcription of target genes (Lee et al. 2002; Mehrara et al. 2002; Rosado et al. 2002).

As mentioned previously, osteogenic protein *NELL1* plays an important role in bone development. Its overexpression is associated with human craniosynostosis and regulates osteoblast differentiation and apoptosis during craniofacial development (Zhang et al. 2002; Zhang et al. 2003). Loss of function mutations in *Nell1* results in cranial and vertebral defects in mouse (Desai et al. 2006). *NELL1* interacts and is phosphorylated by specific isoforms of PKC such as PKC- β I, δ , and - ζ (Kuroda et al. 1999).

Based on findings that FGFs, TGF- β , and BMP upregulate PKC and signal through PKC via OSF-2/RUNX2 and regulate the genes involved in osteogenesis and chondrogenesis and the association of *NELL1* with certain PKC isoforms and its regulation by OSF-2/RUNX2, it is very clear that PKC plays a major role in both intramembranous and endochondral ossification.

BONE AND CARTILAGE DISORDERS ASSOCIATED WITH *NELL1*- MEDIATED PATHWAYS

Osteogenesis and chondrogenesis are complex processes involving a series of several coordinated cellular events. Normal bone formation involves a delicate balance between proliferation, differentiation and apoptosis in osteoblasts and chondrocytes. Disruption of this balance causes many serious human birth defects and diseases like craniosynostosis, osteochondrodysplasias, epiphyseal dysplasia, arthritis, and osteoarthritis etc. Additionally, several osteoblast and chondrocyte ECM proteins like collagens and number of non-collagenous proteins have crucial roles in both osteogenesis and chondrogenesis. Mutations or aberrant expression of collagen genes underlie human diseases such as Osteogenesis imperfecta, some types of Ehlers-Danlos syndrome, Chondrodysplasias, some forms of osteoporosis and osteoarthritis, arterial and intracranial aneurisms and epidermolysis bullosa (Prockop et al. 1995).

As previously noted, overexpression of *Nell1* is associated with both human and mouse craniosynostosis and acrania-like cranial defects (Ting et al. 1999; Zhang et al. 2002; Zhang et al. 2006) while reduced expression leads to both craniofacial as well as vertebral column defects. The specific ECM proteins (*Col-10*), transcription factors (*Osf-2/Runx2*), BMP receptor etc. that are downregulated by aberrant expression of *Nell1* are known to play important roles in both intramembranous and endochondral bone formation and are also associated with certain form of Ehlers -Danlos syndrome (finding of the current study) (Desai et al. 2006).

CRANIOSYNOSTOSIS (CS): The mammalian cranial vault consists of five bones: the pair of frontal and parietal, and the unpaired interparietal bones (Fig.2.5). Interactions between the developing brain, the growing calvarial bones and the sutures (fibrous joints) are essential for the coordinated growth of brain and skull (Wilkie 1997). Most calvarial bones are formed by intramembranous ossification in which mesenchymal cells differentiate into osteoblast that deposit mineralized bone matrix. Growth of the calvarial bones occurs in two phases: 1) outward growth from the centers of ossification, eventually

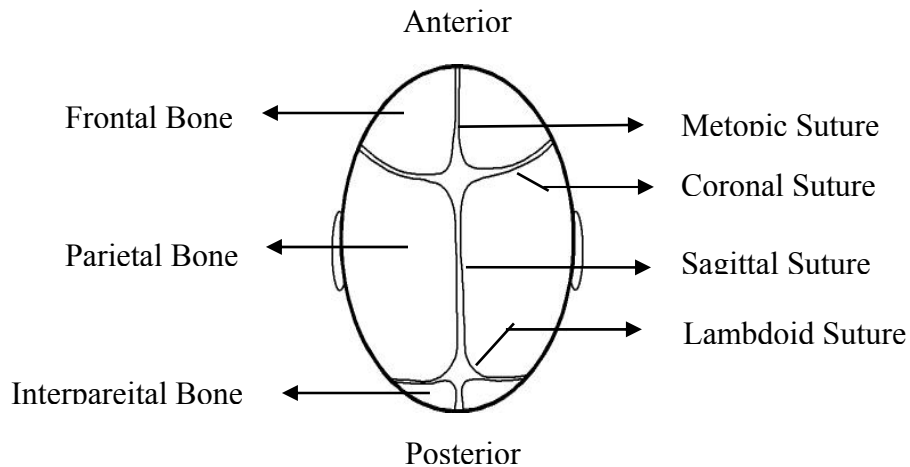


Figure. 2.5: Calvarial Bones and Sutures. (Top View of the Skull)

uniting in fibrous sutures; and 2) growth at the sutures in concert with the expanding calvarium and brain. These cranial sutures serve as the growth centers of the skull and allow the skull to enlarge by the appositional growth in concert with the brain. The sutures also allow calvarial bones to expand without fusing. Continued growth of the skull vault depends on maintenance of a balance between recruitment of the osteogenic stem cells, proliferation, differentiation and apoptosis and disruption of this balance leads to premature or delayed fusion of the sutures and formation of abnormal calvarial bones. (Cohen 1993; Jiang et al. 2002).

Craniofacial abnormalities are very common birth defects in humans caused by genetic mutations, exposure to environmental agents and physical stresses (De Pollack et al. 1996). Craniosynostosis is a heterogeneous disorder characterized by the premature fusion of one or multiple cranial sutures in newborns. CS affects 1 in 3000 infants and is one of the most common human congenital craniofacial deformities (Cohen 1993; Wilkie 1997). In CS, constrained brain growth due to cessation of skull growth leads to a severe cranial dysmorphism, often leading to increased intracranial pressure, impaired cerebral flow, airway obstruction, impaired vision and hearing, and mental retardation requiring series of major cranial surgeries in infants or young children (Fig.2.6).



Pre-surgery

Post-surgery

<http://www.erlanger.org>

Figure. 2.6: Human Craniosynostosis. An infant with a unilateral coronal synostosis. Arrow indicates prematurely fused left coronal suture resulting in a disproportionate growth of the brain into the right side of the cranium.

(Wilkie 1997; Carver et al. 2002). Additionally, certain types of CS are associated with defects in the limb and spine development (Anderson et al. 1996; Anderson et al. 1997) suggesting craniofacial, rib and spine development utilize common molecular pathways. Mutations in several genes are known to cause CS. Gain of function mutations in *FGFR-1*, *-2*, and *-3* are linked to several syndromes involving CS, such as Apert Syndrome, Pfeiffer Syndrome, and Jackson-Weiss Syndrome (Reardon et al. 1994; Lajeunie et al. 1995; Muenke et al. 1997). Furthermore, mutations in transcription factors that regulate osteoblast proliferation and differentiation have been implicated in CS. Gain-of-function mutations in *MSX-2* results in Boston-type CS while, loss-of-function mutations in *Twist* are associated with Saethere-Chotzen CS (Howard et al. 1997; Liu et al. 1999).

EHLERS- DANLOS SYNDROME (EDS): EDS is a heterogeneous group of heritable connective disorders that affect one in five thousand individuals (Mao et al. 2001). There are six major subtypes of EDS, each with slightly different symptoms and causes. Complexity of symptoms and lack of specific genetic tests makes diagnosis of EDS often difficult. The main characteristics of EDS are skin hyperextensibility, tissue fragility, and joint hypermobility. Additionally, EDS patients also exhibit easy bruising, prolonged bleeding, delayed wound healing, mitral valve prolapse, and chronic joint pain (Beighton et al. 1998).

The six major types of EDS are: **1.** Classical type (EDS type I and II). It is an autosomal dominant disorder caused by mutations in *COL-5A1* and *COL-5A2*. **2.** Hypermobility type (EDS type III). It is an autosomal dominant disorder with unknown genetic defect. **3.** Vascular type (EDS IV). It is an autosomal dominant disorder due to mutation in *COL-3A1*. **4.** Arthrochalasia type (EDS type VII A and B). This autosomal dominant disorder is due to mutation in *COL-A1* and *-A2*. **5.** Dermatosparaxis (EDS type VII C). Autosomal dominant EDS VII C is due to mutation in Procollagen N-peptidase. **6.** Kyphoscoliosis type (EDS VI). This autosomal recessive disorder is due to mutation in *Lysyl hydroxylase 1* (procollagen posttranscriptional modifying enzyme) gene and is characterized by neonatal onset of kyphoscoliosis, ocular fragility, and joint laxity,

muscle hypotonia, skin fragility and hyperextensibility. (Beighton et al. 1998; Yeowell et al. 2000).

Most types of EDS have been attributed to mutations in collagens and collagen-modifying enzymes. However, identification of clinically distinct, recessive type of EDS caused by mutation in *TNX* shows that EDS is not solely a disease of collagens. Unlike other forms of EDS, which are due to aberrant collagen synthesis or processing, *TNX* deficiency causes EDS through regulation of collagen fibril deposition and which in turn leads to a reduction in the amount of collagen and due to elastic fiber abnormalities. (Bristow et al. 2005; Zweers et al. 2005).

N-ETHYL- N- NITROSOUREA (ENU) MUTAGENESIS

The *Nell^{6R}* mutant mouse that was characterized in this work was recovered as part of a large series of recessive lethal mutations in the *17R6* locus generated from a large-scale ENU mutagenesis experiments conducted at ORNL (Rinchik et al. 1999; Rinchik 2000; Rinchik et al. 2002). ENU is the most potent germline mutagen of the mouse genome. In spermatogonial stem cells, ENU induces mutations at a frequency of $\sim 6-1.5 \times 10^{-3}$ i.e. one mutation /gene/175-655 gametes screened (Justice et al. 1999). It is an alkylating agent that induces random point mutations by transferring its ethyl groups to oxygen or nitrogen radicals in nucleic acids causing inaccurate DNA replication. Subsequent mispairing leads to single base-pair substitution preferentially in AT base pairs. In mouse, it predominantly modifies A/T base pairs (44% A/T \rightarrow T/A/ transversions) and also induces A/T \rightarrow G/C transitions (38%). These changes result in 64% missense mutation, 26% abnormal splicing, and 10% nonsense mutations. (Justice et al. 1999; Noveroske et al. 2000). Large scale phenotype-driven ENU mutagenesis experiments can be used to identify dominant as well as recessive traits and is useful for creating a series of mutant alleles for a single gene to uncover multiple gene functions. This mutagenesis strategy does not require any prior knowledge of specific gene or its function (Herron et al. 2002). ENU can be used to generate a large number of mutants with specific phenotypes of interest and obtain mutants that display a various degree of

mutation, from complete to partial loss of function, as well as exaggerated function (Justice et al. 1999).

CHAPTER 3

MATERIALS AND METHODS

MOUSE BREEDING AND MAINTENANCE

All the animals were bred at the Mammalian Genetic Research Facility at ORNL. Large-scale N-ethyl- N- nitrosourea (ENU) mouse mutagenesis experiments conducted at ORNL have yielded several recessive lethal mutant alleles for the *l7R6* locus on mouse chromosome 7 (Chr 7) proximal to *p* (Pink-eyed dilution) gene. The identification and fine structure mapping of the *l7R6* locus in mouse Chr 7 was conducted by Rinchik et al. (Rinchik et al. 2002). One of the mutated alleles of *l7R6* locus, 102DSJ (*Nell1*^{6R}) was induced in the *p* chromosome from non-inbred, closed-colony 21A strain.

GENERATION OF MUTANT HEMIZYGOTES AND HOMOZYGOTES FOR DSJ LINE: The ENU mutagenesis strategy used by Rinchik et al. (Rinchik et al. 2002) to generate the DSJ line was conducted by treating non-inbred Go males 21A (*a/a; p/p*) mice with four weekly intraperitoneal injections (85mg/kg each) of ENU. Treated males were mated with wild-type females [F₁ (C57BL/10R1 X C3H/R1) or F₁ (C57BL/6JRn X C3H/R1) or C3H/R1]. All the G₁ animals from this cross that carry a mutation (*m*) induced in parental genome in Chr 7 were recovered by linkage to the pink-eyed dilution locus (*p*). The *p* gene is tightly linked to *l7R6* locus/mutation. The *p* locus is one of the coat color mutations in mouse chromosome 7. It is one of the loci used as markers for experimental mutagenesis at ORNL. Animals carrying wild-type allele exhibit intense pigmentation in both skin and eye while animals with recessive alleles (*p/p*) exhibit reduced or no pigmentation (Lyon et al. 1992; Johnson et al. 1995). The *p*^x is an intermediate allele of *p*. Animals homozygous for *p*^x have a darker eye/coat color and lighter eye/coat color when heterozygous with most null *p* mutations (Rinchik 2000). The G₁ females were then crossed with *a/a; p^x/ Del (ru2p)^{46DfioD}* males. In G₂ progeny ENU-induced recessive mutations closely linked to *p* and included within the deleted segment in *Del (ru2p)^{46DfioD}* were recovered in the pink-eyed dilute class (*m p/ Del (ru2p)^{46DfioD}*).

In G₂ progeny, three different eye pigment phenotypes were generated to correspond with the genotype at the mutant locus: wild-type (dark pigment, $+/p^x$ or $+/\text{Del}(ru2p)^{46DfioD}$), Heterozygote (light pigment, $m p/+ p^x$), and hemizygote (no pigment, $m p/\text{Del}(ru2p)^{46DfioD}$) (Fig. 3.1A). [(Rinchik 2000) <http://bio.lsd.ornl.gov/mgd/index.html>].

To generate fetuses hemizygous for 102DSJ, progeny-tested males $+ p^x / l7R6^{6R}$ were mated with $+ p^x / \text{Del}(Hps5^{ru2} p)^{46DFiOD}$ females. The 102DSJ lethal mutation was recognized when G₁ female #102 failed to yield any pink-eyed-dilute G₂ progeny when she was crossed to a $+ p^x / \text{Del}(Hps5^{ru2} p)$ G₁ male. The deletion mapping was done as described in Rinchik et al (2002), which also revealed that the 102DSJ lethal allele mapped to the same deletion interval as the other *l7R6* alleles. To confirm the allelism, 88SJ ($Hps5^{ru2} l7R6^{1R} p/Hps5^{ru2} +$) and 102DSJ ($+ 102DSJ p/++p^x$) were crossed. It was confirmed that *l7R6*^{6R} (102DSJ) was a new allele of *l7R6* locus, when the cross failed to produce more than 30 pink-eyed dilute heterozygote progeny, when 25% were expected ($p < 0.001$) (Desai et al. 2006)

To generate homozygous *l7R6*^{6R} (102DSJ) mutant mice, the heterozygote carriers ($l7R6^{6R} p/+ p^x \times l7R6^{6R} p/+ p^x$) were crossed, which produced pink-eyed homozygotes ($l7R6^{6R} p/l7R6^{6R} p$, no eye pigment), dark-eyed wild-type mice ($+ p^x/+ p^x$), and medium pigmented heterozygote carriers ($l7R6^{6R} p/+ p^x$ or $p^x/l7R6^{6R}$) (Fig.3.1 B).

COLLECTION OF MOUSE EMBRYOS

Mouse matings were done for 1 hour early in the morning, and the females were examined for the presence of vaginal plugs (gestation day 0). The embryos/fetuses were collected at 10, 12, 14, 16, 18.5/19 days of gestation. The pregnant females were euthanized by cervical dislocation and embryos were collected by caesarean section. The embryos were then examined for eye-pigmentation and associated gross morphological abnormalities (head shape and size, body length, overall pallor, positioning of appendages, reflexes and breathing). About 2-3 mm tail tips were snipped for genotyping by microsatellite analysis. The embryos were sorted based on their eye pigmentation: Non-pigmented (*Nell1*^{6R} homozygote or hemizygote mutants), light pigmented (*Nell1*^{6R}

A.

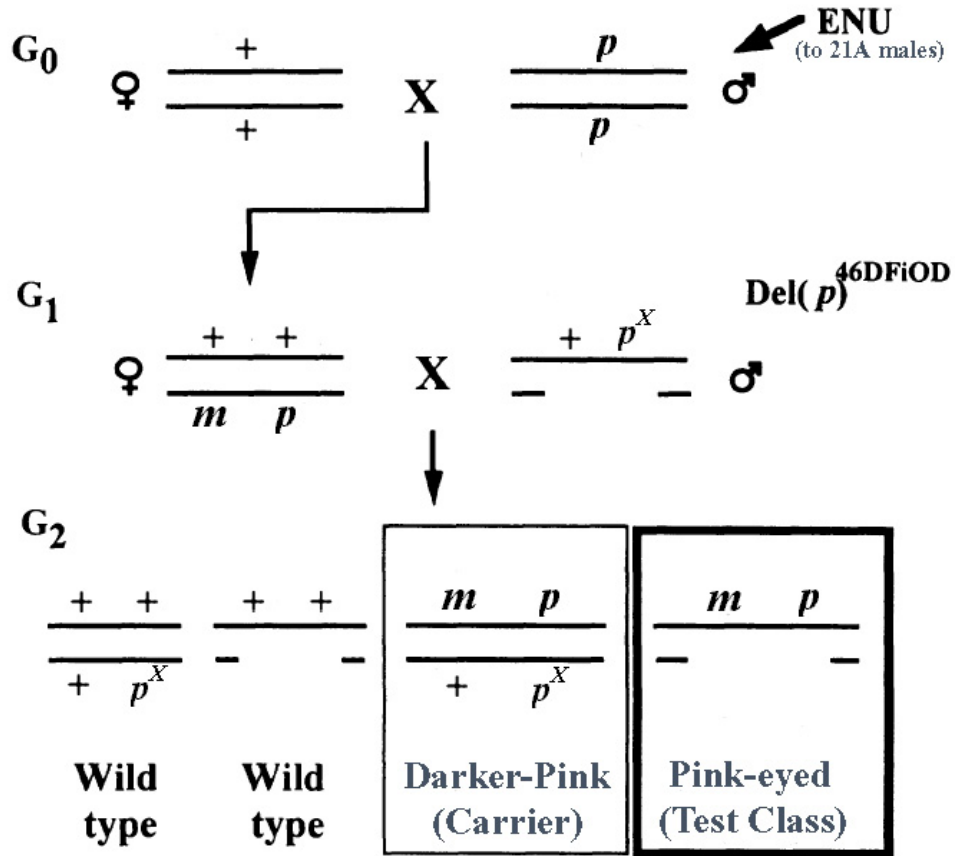


Figure. 3.1: Breeding Protocol Used to Generate Hemizygous and Homozygous *I7R6^{6R}* (102DSJ) Mice. See text for details. (A). The hemizygous pink-eyed dilute test class (heavily out lined box) G₂ progeny carries the mutant *I7R6^{6R}* allele. Darker “pink” G₂ progeny (lightly boxed) carry mutation, from which mutations can be propagated. (B). Homozygous *I7R6^{6R}* (102DSJ) mutant animals were obtained from mating darker “pink” carriers (heterozygous for mutation) from G₂ generation. Pink-eyed (heavily outlined box) G₃ progeny are homozygous for mutation and medium pink-eyed (lightly outlined box) animals are heterozygous for mutation. The “wild-type” animals are wild-type for *I7R6^{6R}*, but not for eye pigmentation. *m* is the mutation induced by ENU; *p* pink-eyed dilution; *p^x* another allele (intermediate allele) of *p* gene. [Modified from (<http://bio.lsd.ornl.gov/mgd/index.html>)].

B.

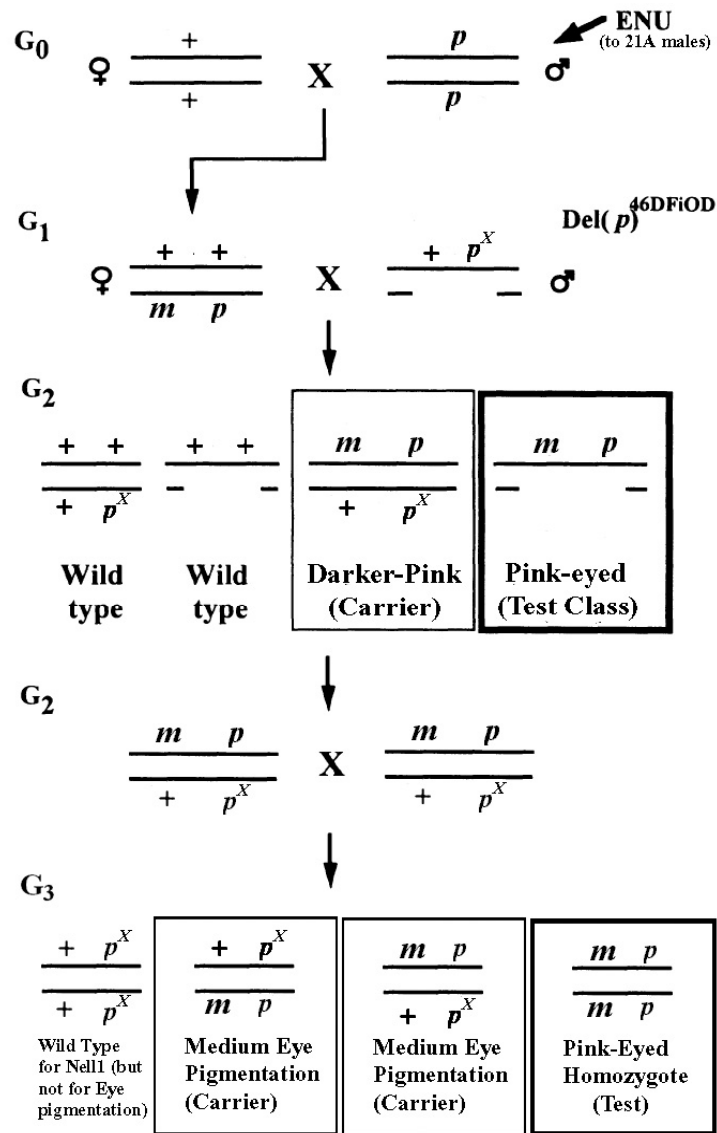


Figure. 3.1: Breeding Protocol Used to Generate Hemizygous and Homozygous *17R6^{6R}* (102DSJ) Mice. Continued.

heterozygote), and dark pigmented (*Nelli* wild-type). Mutants were also easily distinguished by their slightly enlarged heads, curled position, and weak responses to touching. Embryos or parts of the embryos (head, body, dissected vertebral column etc) were collected and fixed as necessary: Frozen in liquid nitrogen for RNA and DNA extraction or fixed in 10% Formalin for histology.

GENOTYPING OF WILD-TYPE AND *l7R^{6R}* MUTANTS

Mutant fetuses were distinguished from wild-type by molecular genotyping for size polymorphisms using *D7Mit315* microsatellite, which is tightly linked to *p* gene, which in turn is tightly linked to *l7R6* locus. The snipped tails were digested in digestion buffer [200 µl of 1X PCR buffer (Invitrogen) and 20 µl of 10mg/ml Proteinase K] for 2 hours or overnight at 60°C. Proteinase K was deactivated by incubating digests at 95°C for 20 minutes. Digested DNA from tail snips was amplified by PCR using standard techniques using 3 µl of DNA from tail snips and primers for microsatellite markers, *D7Mit 315* for DSJ lines (*D7Mit315* F: TGATAACAAAACAGFCAGTAATGAAGC and *D7Mit315* R: CTGATCCATC TGT ATGATGTTACTTG). PCR products were resolved on 3.5% metaphor gel with 0.5 X TBE buffer (Tris, boric acid and EDTA). *Nelli^{6R}* homozygotes were distinguished by a single 146 bp band, wild-type animals by a single 166 bp band and heterozygotes, which have two bands, 146 bp and 166 bp.

ISOLATION OF TOTAL AND mRNA

Total RNA was extracted from E10 embryos, head and bodies of E12-E19 fetuses, and adult tissues such as liver, spleen, kidney, thymus, heart, lung and muscle and also from the heads of E15 *l7R6* fetuses using standard guanidine isothiocyanate procedure based on and modified protocol from 5'- 3' Rapid Total RNA Isolation Kit (5' Prime → 3' Prime, Inc, Boulder, CO). RNA was isolated from subsequent phenol-chloroform extractions using Phase Lock Gels™ (Eppendorf, Hamburg, Germany) and precipitated with isopropanol followed by centrifugation and re-suspension of the pellets

in RNase-free water. The total RNA was further purified by using RNeasy Mini Kit (Qiagen, Valencia, CA) including DNase I treatment step according to the manufacturer's protocol to eliminate the contaminating genomic DNA. RNA quality was assessed by visualization in denaturing agarose gel electrophoresis and spectrophotometrically by the 260nm/280nm ratio of absorbance. For some experiments, mRNA was isolated from the total RNA using QIAGEN Oligotex mRNA isolation kit (Qiagen) according to manufacturer's protocol. 500 µg to 1mg of total RNA per sample was used to isolate the mRNA by Oligotex mRNA spin-columns.

The cDNA probe for *Nell1* was generated from the mouse brain mRNA by RT-PCR using primers designed from the mouse EST sequences matching 5' and 3' ends of human *NELL1* (Primers: ctc55: TGCAGCAGAAGCCTCCA; ctc59: CAAACTAGGGCAAGCTAGAG). The First-Strand cDNA templates were generated from mRNA extracted from wild-type E18.5 fetal brain using RETROscript (Ambion, Austin, TX). A 1920 bp cDNA probe was generated by Long Range PCR using ExpandTM Long Template PCR System kit (Roche Diagnostics, Switzerland) according to manufacturer's instructions and using primers ctc55 and ctc59. The PCR products were gel purified by using QIAquick Gel Extraction Kit (Qiagen). The cDNA probe spans the last half of the exon 3 (~55 bp) to first 20 bases of exon 19 of the *Nell1* transcript.

***Nell1* GENE PROFILING BY NORTHERN BLOT AND RT-PCR**

One to three µg of mRNA in a volume of 4.5µl was mixed with 15.5µl of RNA loading buffer [Formamide 720 µl, Formaldehyde 260 µl, 10X MOPS (3-N-Morpholino-propane-sulfonic acid) 160 µl, 80% Glycerol 100 µl and RNase-free water 80 µl]. The 10X MOPS buffer contains 200 mM MOPS, 50 mM NaOAC, 5 mM EDTA, and was adjusted to pH 7.0. Samples were denatured at 65°C for 10 minutes, chilled on ice and loaded onto an RNA gel (1% agarose, 1X MOPS, 24.6% Formaldehyde, 1ng/ml Ethidium bromide), electrophoresed at 80 volts for 4-5 hours and photographed under UV light. The gel was incubated in NaOH solution (5ml 10 N NaOH/liter of double distilled water) for 10 minutes. Nylon membrane (Duralon-UVTM, Stratagene, La Jolla,

CA) and Whatman filter paper that were cut according to the gel size were equilibrated in 20X SSC buffer (3 M NaCl, 0.3 M sodium citrate). The gel was then transferred to the Nylon membrane overnight according to the Northern Blot set-up in Sambrook et al. (Sambrook 1989). The nylon membrane was rinsed in 2X SSC, baked at 80°C in vacuum oven for 2.5 hours and immediately cross-linked at 250 LED in UV cross-linker. The blot was then prehybridized by incubating in 1X prehybridization buffer (20X SSC, 0.5 M NaPO₄, pH 7.0, 50X Denhardt's solution, 10% SDS and 10 mg/ml sonicated salmon sperm DNA) for at least 2-3 hours at 42°C. Denhardt's solution contains 1% Ficoll (type 400), 1% polyvinylpyrrolidone (PVP-360), and 1% BSA (bovine serum albumin). 20-40 ng of cDNA probe was labeled with [α -³²P]-CTP overnight and precipitated [in ethanol, 3M NaOAc pH 5.2, 10mg/ml yeast tRNA and TE buffer (10 mM Tris, 1 mM EDTA)] and re-suspended in TE buffer, boiled for 5min at 100°C and hybridized to the blot in hybridization buffer (50% 2X-prehybridization buffer, 50% formaldehyde) overnight at 42°C. The membrane was washed in 2X SSC containing 0.1% SDS for 30 minutes twice, in 1X SSC containing 0.1% SDS for 30 minutes at room temperature and then in 0.2X SSC containing 0.1% SDS for 30-45 minutes at 68°C and exposed to X-ray film at – 80°C.

Expression of *Nell1* was further confirmed by RT-PCR analysis. About 500ng of mRNA from wild-type and mutant fetal heads was reverse transcribed using RETROscript Kit (Ambion). The two fragments of cDNA were amplified by standard and long range PCR. The smaller fragment (~ 557 bp) at the 5' end was generated by standard PCR techniques using primers ctc138: CTGAAGCATTGGTTTCTTGC and ctc149: TCGACATGGAGTAGGAGGTGAGAGG and the longer fragment (1465 bp) spanning the middle and 3' end of the gene was generated by Long Range PCR (Expand™ Long Template PCR System kit, Roche Diagnostics) using primers ctc150: GCAGAGACGAGACTTGGTCAACTGG and ctc59: CAAACTAGGGCAAGCTAGAG. The PCR products were resolved on 1% agarose gel and stained with ethidium bromide and visualized under UV light. The 5' end of the *Nell1* amplicon (~557 bp) covers the exons 1 to most of the exon 8 while the amplicon

spanning the mid and 3' end of the *Nell1* transcript covers the exons 13 to the first ~ 42 bp of exon 19.

GENERATION AND SEQUENCING OF *Nell1* cDNA

To generate a full-length mouse *Nell1* cDNA sequence, direct sequencing was performed with the PCR products amplified from cDNA template. Total RNA was extracted from BJR E18.5 fetuses and then mRNA was isolated from the total RNA. The cDNA was obtained by generating short 300-400 bp overlapping PCR fragments. To synthesize the *Nell1* cDNA, 500ng of mRNA was reverse transcribed using the RETROscript kit (Ambion). Eleven overlapping segments covering the entire coding region plus 5' and 3' untranslated regions were generated using the eleven sets of primers (listed in Table. 3.1) by standard PCR techniques. Primers to produce overlapping amplicons were designed (based on mouse EST sequences matching human *NELLI* cDNA) using Primer3 database (Rozen et al. 2000). The PCR products were electrophoresed on 1% agarose gel to confirm amplicon size and checked for non-specific products. The PCR products were purified using QIAquick PCR purification kit (Qiagen) and the purified amplicons were sequenced (using the primers that generated the products) bi-directionally using Big Dye version 3.1 dye terminator kit (ABI, Foster City, CA) and analyzer on an ABI 3100 Genetic Analyzer. The sequenced overlapping cDNA segments were edited to remove overlaps and assembled into one contiguous segment of 2862 bp. This 2862 bp mouse *Nell1* cDNA covers the entire coding region (20 exons) plus the 58 bp of 5' end and 250 bp of untranslated regions.

To determine the identity and homology of the new mouse sequence to other mammalian species BLAST analysis was conducted against human, rat and existing partial sequences from the mouse Celera database [(Altschul et al. 1990); (<http://www.ncbi.nlm.nih.gov/BLAST>)]. The coding region for the full-length *Nell1* cDNA as well as translated protein sequences was obtained by using NCBI's ORF finder (<http://www.ncbi.nlm.nih.gov/gorf/gorf.html>). Additionally, *Nell1* protein domains were predicted using NCBI's Conserved Domain database

Table. 3.1: Primers Used to Synthesize and Sequence Mouse *Nell1* cDNA.

Primer Pairs	Sequence of Forward Primers	Sequence of Reverse Primers	Fragment Size
ctc138/Jaya1R	CTGAAGCATTGGTTTCTTGC	TGGATGGTTTCTGCTGCA	356 bp
Jaya 2F/2R	GATGTACAGAGAGAGATCCA	TGCTTCCTGGAGGAAGGTG	355 bp
Jaya 3F/3R	GGCAGACGGACAATGGCACA	AGTTGACCAAGTCTCGTCTC	375 bp
Jaya 4F/4R	CCAACATGCAGTGAATTCTT	AGACTCCACCTCGACATTCC	400 bp
Jaya 5F/5R	CACTTCCTGTGCACATTTCC	GGTGTGGCATGACAATAGTG	394 bp
Jaya 6F/6R	ACCTGTGAGTGCAAGAATGG	CAGACACACTTGTTAGGAGC	367 bp
Jaya 7F/7R	CATCTGTACCAACACAGTCC	GATGCAGGCAGAGTCATTCC	370 bp
Jaya 8F/8R	ACCACTGTGAGTGCAGAAGC	CTAAACATTGGCTGGTGACC	369 bp
Jaya 9F/9R	CAGTCTGTTCTGCAAG	CAGCCTCGAAACACCAAAGC	368 bp
Jaya 10F/10R	GCTGTGAATACACAGCCATG	GCAATCCAAACGCCTTCTC	370 bp
Jaya 11F/ctc174	CTCGTCACGTGAGAAAATGG	GGTGCCAAGTCTCTATTATGTCAG	326 bp

(<http://www.ncbi.nlm.nih.gov/Structure/cdd/wrpsb.cgi>). The 2862 bp full-length mouse *Nell1* cDNA sequence with open reading frame of 2433 bp, which encodes 810 amino acid protein, was submitted to the NCBI's Gene Bank as accession number (AY622226).

IDENTIFICATION OF MUTATION IN *Nell1*^{6R}

For identifying the *Nell1*^{6R} mutation, direct sequencing was performed with the PCR products amplified from the genomic DNA templates. DNA was extracted from *Nell1*^{6R} hemizygous mutant mice and control strains (BJR and 21A). Briefly, tails of mutant and wild type E18.5 fetuses were snipped and digested in a buffer containing 1M Tris pH 7.6, 5M NaCl, 0.5M EDTA pH 8.0, 10% SDS and 10mg/ml Proteinase K in SST tubes (serum separation tubes, Becton Dickinson) overnight at 45°C. DNA was extracted

by phenol and precipitated with 95% ethanol. Precipitated DNA was collected by a glass loop and solubilized in TE pH 7.6 buffer. Twenty primer sets were designed to amplify each exon of *Nell1* from flanking intron sequences and two additional primer sets to amplify conserved upstream elements (listed in Table.3.2). Each amplicon was amplified from the genomic DNA by standard PCR techniques. The corresponding wild-type and mutant PCR products were mixed in equal volumes in 96-well plates, heteroduplexed and scanned for point mutations using Temperature Gradient Capillary Electrophoresis (Li et al. 2002). Three overlapping temperature gradients were used: 50-60°C, 55-62°C and 60-68°C. The heteroduplex formed by the mismatch of the ENU-induced point mutation and the wild-type segment was detected in exon 14. The 421 bp amplicon containing the mutation in the *l7R6^{6R}* allele was PCR-amplified using the primer pairs designed from the intron sequences flanking the 131 bp exon 14 of *Nell1*: Nell E14 (F): ATAGACCAGGGGCAGAAACC and Nell E14(R): TTGCTCAACCTCAATATCC. The PCR products were purified using QIAquick PCR Purification Kit (Qiagen) and directly sequenced using the same primer set as above.

BODY AND HEAD MEASUREMENTS

E18.5 fetuses were recovered by caesarean section from nine pregnant females. A total of 16 wild-type and 19 homozygous mutant fetuses were measured for body length, head height, head length, and head width. These morphometric measurements were obtained using a Fisher Scientific Digital Caliper. Two-tailed Student T-test with a P-value cutoff of 0.005 was used to analyze the data and determine statistically significant differences between mutant and wild-type fetuses.

SKELETAL ANALYSIS

Skeletal defects in *Nell1^{6R}* homozygotes were evaluated using standard protocols for Alizarin Red-Alcian blue staining of intact fetuses (Hogan 1994). Briefly, 13 wild-type and 13 homozygous mutant fetuses were recovered by caesarean section at E18.5

Table. 3.2: Primers Used to Amplify Mouse *Nell1* Genomic DNA.

Primer Pairs	Sequence of Right Primer	Sequence of Right Primer	Fragment Size
Nell E1AF/ E1AR	GCCCGTCAGAGATA	CTGCCGCCCCGTAG	575 bp
Nell E2AF/ E2AR	TAACTGCCTGGCTGAATCC	GCCTCTGCTCACTCTCAGAAC	519 bp
Nell E3AF/ E3AR	GGCAATCTGGGCTCTTAAATG	GAACAGAAGGCAAAGGCAAG	415 bp
Nell E4AF/ E4AR	GAGTCACGGAAGGTCAAAGC	TCCATGTCAGAAGCTCAAGG	403 bp
Nell E4BF/ E4BR	GCCAAACATACCTATTGCAGTC	TAGTGGGTTTTCCCTCATCG	436 bp
Nell E5AF/ E5AR	GGCTGCTATGAACATAGTGGAG	ATGTGGGAGAGGCTGAAGAG	410 bp
Nell E6AF/ E6AR	TTGTCTGACACTAGGAACAAGT CAC	GAATGCAGATATCCCCTACTGC	385 bp
Nell E6BF/ E6BR	TTTTGTCTGACACTAGGAACAA GTC	TTATTTCCCCCTCCAAAAGC	504 bp
Nell E7AF/ E7AR	ACGGGCAGTCTCATTTCAAG	TGAGGGAAACAGTGTTAGGAAC	392 bp
Nell E8AF/ E8AR	GGCTTACTTTGCATGTG	CACACGCTGTCATGGATACC	449 bp
Nell E8BF/ E8BR	ATGTGCAGTTCCTGCAGTTG	CACACGCTGTCATGGATACC	438 bp
Nell E9AF/ E9AF	CAGGTGGATGAAGCCAGTG	TTAGTTGGGTCCCGAACAG	399 bp
Nell E9BF/ E9BF	CAGGTGGATGAAGCCAGTG	GATCACTGTGACCCTTGGTG	449 bp
NellE11AF / E11AR	CTTTGCATGCTCCTCTTTCC	CTCCAGCCGATTA ACTCTGC	349 bp
NellE12AF / E12AR	CCTGATTTCTCTCCCTGGAC	GATGGAGTGAGCAAGACAAGC	399 bp
NellE13AF / E13AR	GCACATCAGGAAACATGCTC	GACAGTGGGGAGACGGTATG	492 bp
NellE14AF / E14AR	AGCAGGCAAAGAATGCTAGGG	AGTGCACCAACTGGCTTTG	404 bp
NellE15AF / E15AR	ATAGACCAGGGGCAGAAACC	TTGCCTCAACCTCAATATCC	421 bp

Table. 3.2: Continued.

Primer Pairs	Sequence of Right Primer	Sequence of Right Primer	Fragment Size
Nelle16AF / E16AR	ATTCTGTGTCCAGAAAAGAAAAG G	TCCCTGGGATGGATACACAC	434 bp
Nelle17AF / E17AR	ATTTGAAGGGCAGAGTCACG	ATGAGGATGTGGGGCTAATG	278 bp
Nelle17BF / E17BR	TTCCTCGGTTTCAAGGTTTG	GCCCACATCTTTGGTCTCC	409 bp
Nelle18AF / E18AR	GCACTGGGCACTTACACTCC	CCAGTCAGCTTACCTTACAGGAA C	406 bp
Nelle18BF / E18BR	ACTGGGCACTTAACCTCC	TCAGCTTACCTTACAGGAACAGA C	402 bp
Nelle19AF / E19AR	GGTCCAGTTGTCTCCAC	ACAAGGCAGCACAGTTAGGG	464 bp
Nelle19BF / E19AR	TGTCTCCACTTCGATAGAGCTT C	ACACTGGCAACCGAGTCAG	470 bp
Nelle20AF / E20AR	TGGATCATAACACATTAGGGTTC C	TGTCCTCCTGTGAGAACATACAC	464 bp
Nelle21AF / E21AR	GGAGCTGACCCCTGTGTTC	GTGTGCAGCGGATGAGATAG	507 bp
Nelle21BF / E21BR	CTGGAATTAAAGGCGTGTGC	CACATCTCCATCAACACGTC	687 bp
Nell CONB F / CONBR	AGCTCGGTACCGCTGGTG	AGCTTGGTACAAGGCCAATC	450 bp
Nell CONC F / CONCR	CACCCTCAACTCTCCCTCAG	TCCACTGGGCCTATTCTCTG	419 bp
NellCOND F / CONDR	ACCATGTCCCACCCTCAAC	CTGGACCAACAGGTCTACCG	408 bp

days of gestation from seven pregnant females. The fetuses were soaked in tap water for 2-5 hours, and then briefly in 70°C water and the skin and the internal organs were removed. The fetuses were fixed in 95% ethanol, stained in Alcian blue (in 95% ethanol and glacial acetic acid (Sigma-Aldrich, St Louis, MO) for 1-2 days and rinsed in 95% ethanol. They were then cleaned in 1% KOH for 2-6 hours, counterstained subsequently in Alizarin Red solution (Sigma-Aldrich) for 2-3 hours and cleared further by placing in 2% KOH overnight. To complete the clearing of the fetuses in order to visualize the internally stained skeleton, fetuses were incubated further for at least a day in each of the following series of solutions: 2% KOH/glycerol: Solution I (80:20), Solution II (60:40), Solution III (40:60), and Solution IV (20:80). Skeletal preps were then stored indefinitely in the final solution. Skeletal defects of fetuses were further analyzed by using the small animal Micro Cat system developed at ORNL in collaboration with Dr. Mike Paulus.

HISTOLOGICAL ANALYSIS

Histological analysis was done on 10% Formalin-fixed, paraffin-embedded sections of E18.5 fetuses (6 mutants and 6 wild-type specimens) recovered by caesarean section. Haematoxylin and Eosin (H and E), Masson, Periodic Acid Schiff (PAS) was done according to standard protocol (Carson 1990). Haematoxylin stains nucleic acids blue while Eosin stains basic proteins in the cytoplasm red. Masson stains cytoplasm, keratin and muscle fibers red and collagen and mucins blue while PAS stains glycogen, mucopolysaccharides, glycolipids, and glycoproteins purple. The van Kossa staining was used to assess the extent of mineralization of vertebral and calvarial bones. Briefly, sections were dewaxed, rinsed in alcohol and distilled water and treated with 5% silver nitrate and exposed to a bright lamp for 1-2 hours. Sections were first rinsed in distilled water and then in 5% sodium thiosulphate for 2-3 minutes and counterstained with eosin for 1-2 minutes. Sections were then rinsed in distilled water, dehydrated and mounted. The van Kossa staining stains calcium salts black. Sectioning of the embryos and paraffin embedding of the sections was done by a commercial histology service, Ridge Microtome.

IMMUNOHISTOCHEMISTRY

Expression of *Nell1* and *Col-10* was detected by a standard avidin-biotin complex/immunoperoxidase protocol using VECTASTAIN[®] *Elite* ABC kit (Vector laboratories Inc, Burlingame, Ca) according to manufacturer's protocol with a few modifications. Briefly, paraffin-embedded sections were incubated at 60°C for few minutes, dewaxed in xylenes and rehydrated in graded ethanol baths. Sections were rinsed in tap water for 5 minutes and enzyme-treated for antigen retrieval with 20 µg/ml Proteinase K (Roche Diagnostics) at 37°C for 10 min, washed in 1X PBS (phosphate buffered saline, Sigma-Aldrich) and blocked for 20-30 minutes in Blocking buffer (1.5-5% rabbit serum (Vectastain kit) in 1X PBS). The sections were incubated with anti-*Nell1* (1:100, a kind gift from Dr. Kang Ting, UCLA, California) or anti-type X collagen (1:30-1:60, Fitzgerald industries, Concord, MA) primary antibodies for 30 minutes at room temperature or overnight at 4°C and then incubated with biotinylated anti-rabbit secondary antibody (Vectastain kit) for 30 –60 minutes at room temperature. The sections were washed in PBS buffer and positive immunoreactivity was detected using Vectastain ABC reagents and AEC (3-amino-9-ethylcarbazole) substrate (both from Vector Laboratories) according to manufacturer's instructions. The sections were then washed in PBS buffer, rinsed in water and counterstained with hematoxylin QS (Vector laboratories) for 5-45 seconds. The sections were again rinsed in tap water and mounted in aqueous mounting medium (Vectamount, Vector laboratories). The *Nell1* antibody was raised against the specific COOH-terminal region of rat *Nell1* protein (Kuroda et al. 1999).

HIGH-THROUGHPUT REAL-TIME qRT-PCR ASSAYS

These assays were done in collaboration with Dr. Mark Shannon at Applied Biosystems as described in Desai et al (Desai et al. 2006). Total RNA from the heads and bodies of four *Nell*^{6R} mutant and four wild-type E18.5 fetuses were extracted individually

(16 RNA samples). DNase1-treated RNA was ethanol precipitated and resuspended in nuclease-free water. 2.5µg of total RNA was reverse transcribed to cDNA using the random-priming High-Capacity cDNA Archive Kit (Applied Biosystems, Foster City, CA).

MULTIPLEX PRE-AMPLIFICATION OF cDNA TARGETS: To enable maximum sensitivity and detection of hundreds of gene expression targets from a small amount of cDNA, a novel multiplex PCR pre-amplification strategy was used prior to conventional quantitative PCR. 225 (219 experimental and 6 endogenous control genes) TaqMan[®] Gene Expression Assays (PCR primer/FAM-probe stock solutions) were pooled together and used in a single PCR to amplify all targets equally from the same cDNA template. The FAM-probe is a component of the final configuration of the manufactured TaqMan[®] Gene Expression Assays and does not interfere with the preamplification process. To prepare the multiplex pre-amplification primer pool, equal volumes of the 225 TaqMan[®] Gene Expression Assays were mixed together, dried under vacuum, and resuspended with water to generate a multiplex-pooled primer set with a concentration of 180 nM for each primer. The pre-amplification reaction was set up as follows: A 250 µl volume of 500 ng of cDNA was combined with 250 µl of the multiplex-pooled primers. Then, 500 µl of 2X Multiplex Pre-amplification Master Mix was added to generate the final 1000 µl of reaction volume (Applied Biosystems). The reaction mix was divided into 50 µl aliquots in a 96-well PCR tray and cycled on an ABI 9700 thermalcycler under the following conditions: 95° C for 10 minutes; then 10 cycles at 95° C for 15 seconds; and 60° C anneal/extension for 4 minutes.

REAL-TIME PCR REACTIONS: Pre-amplification products were recombined into one tube and diluted 1:5 with water. Individual singleplex TaqMan[®] Gene Expression Assays for each of the 225 pre-amplified markers, along with 18S rRNA (which was not included in the pre-amplification reaction due to its high level of expression) were prepared as follows: 5.0 µl of 2X TaqMan[®] Universal PCR Master Mix, 0.5 µl of TaqMan[®] Gene Expression Assay 20X primer/FAM-probe solution and 2.0 µl of water,

and 2.5 μ l of preamplified cDNA product. For all samples, each assay was carried out in quadruplicate wells of 384-well plates and run in the ABI PRISM[®] 7900HT Sequence Detection System under two-temperature cycling: 95° C for 10 minutes, then 40 cycles of 95° C for 15 seconds and 60° C for 1 minute. C_T (threshold cycle) values, the cycle number at which the PCR amplification fluorescence signal crosses a fluorescence threshold, were generated using the FAM dye layer setting at a threshold of 0.2 and a baseline of 3-13.

DATA ANALYSIS: The relative levels of transcripts for each gene in wild-type and mutant samples were compared following normalization to endogenous control targets. GeNORM software (Vandesompele et al. 2002) was used to select the two best targets with the least variation across samples from a collection of 6 potential endogenous controls (Hprt, Tfrc, Tbp, Gus, Pgk1 and 18s rRNA). Gus and Hprt were selected for heads, while Gus and Pgk1 were selected for bodies. The geometric mean of the selected targets was then used as the reference for determining ΔC_T values. For each sample, $\Delta \Delta C_T$ values were determined by the following equation: $\Delta C_T \text{ Marker} = C_T \text{ Marker} - C_T \text{ Reference}$. Statistically significant differences between ΔC_T values of wild-type and mutant groups were determined by a two-tailed t test without assuming equal variances and with a p value cutoff of 0.005. $\Delta \Delta C_T$ s were also calculated between wild-type and mutant groups based upon average ΔC_T values for each group, and relative fold differences between them were determined by $2^{-\Delta \Delta C_T}$ (Applied 2001).

CHAPTER 4

RESULTS

CHARACTERIZATION OF MOLECULAR BASIS OF THE *Nell1*^{6R} MUTATION

To accomplish this task, the following experiments were conducted: a) identification of the *Nell1* mutation in 102DSJ, b) expression profiling of the *Nell1* gene during mouse development, c) investigation of the impact of the mutation on the expression of *Nell1* gene. Since the mouse *Nell1* sequence was not available during the start of this project, sequencing of the complete coding region of the gene was necessary to accomplish this task. Characterizing the molecular basis of the 102DSJ was essential in understanding the gross morphological aberrations and cellular phenotypes that were observed in the latter part of this study.

In the past two decades ORNL has pioneered and conducted large-scale ENU mutagenesis experiments to recover ENU-induced mutations at specific segments of mouse chromosome 7 (Rinchik et al. 1999; Rinchik et al. 2002). One of these experiment generated mutations mapping to a small segment of mouse chromosome 7 proximal to *p* gene and homologous to human chromosome 11p15. One of the loci mutated in this experiment was *l7R6* and it yielded eight recessive neonatal lethal alleles: 88SJ, 335SJ, 2038SJ, 102DSJ, 45DSJ, 11DSJ, 244DSJ, and 141SJ. Trans complementation analysis with a number of *p* deletions mapped *l7R6*^{6R} to the same <1 cM segment of chromosome 7 (Fig. 4.1 and materials and Methods) as other *l7R6* alleles, with homology to a region of human 11p15.

EXPRESSION ANALYSIS OF MOUSE *Nell1* GENE: Gene content analysis of the human chromosomal region suggested at least six candidate genes for *l7R6* (<http://genome.ucsc.edu>), including *NELLI*, which was particularly provocative because of its overexpression in the prematurely fused sutures of patients manifesting unilateral coronal synostosis. The pronounced enlarged head phenotype (see fig.4.5), high mutation

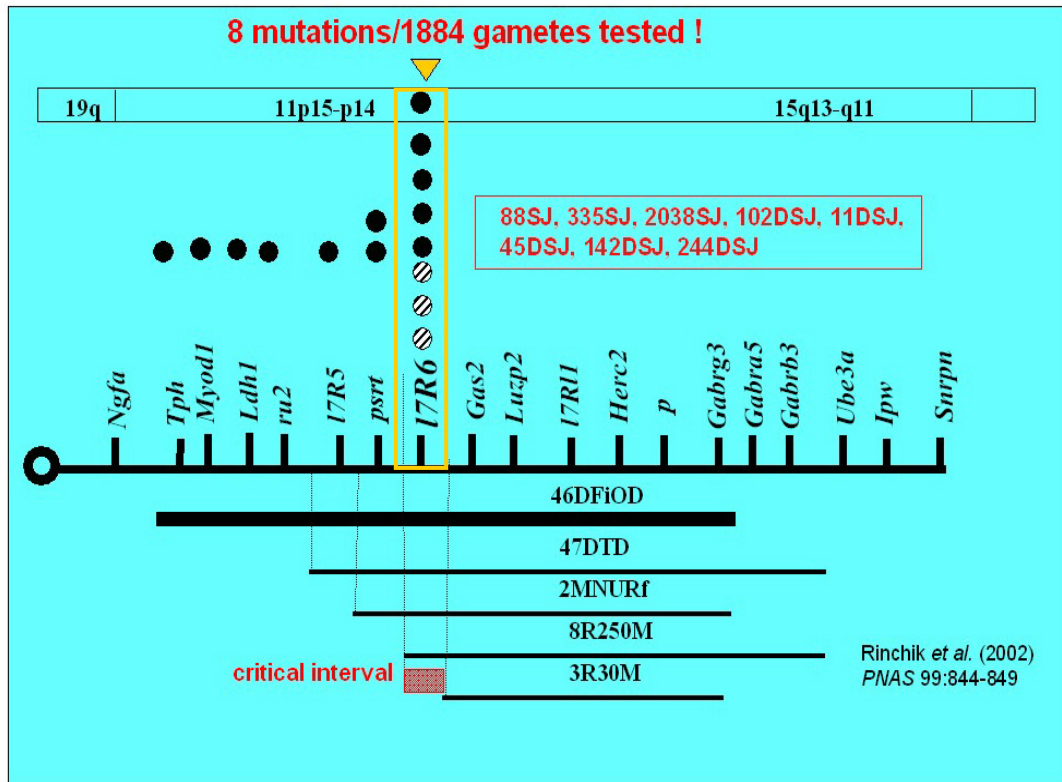


Figure 4.1: Complementation Analysis. Showing the mapping of the *I7R6* locus into an interval in mouse chromosome 7 (red box) that is homologous to a segment of human chromosome 11p15 where the *Nell1* gene is located. Mouse chromosome 7 is represented by the line with a filled circle at the left (indicating the centromere) and relative positions of genes and markers are indicated above the line. The 3 crossed circles (88SJ, 335SJ, and 2038SJ) and the 5 filled circles (102DSJ, 11DSJ, 45DSJ, 142DSJ, and 244DSJ) represent 8 alleles of *I7R6* including *I7R6^{6R}*. Five mutant mouse lines carrying deletions of varying lengths and surrounding the pink-eyed dilution gene (*p*) are shown as 46DFiOD, 47DTD, 2MNURF, 8R20 M and 3R30M. Among these mutations, only the 3R30M deletion can complement the ENU-induced mutations at *I7R6* indicating that this deletion does not extend to the position where the *I7R6* gene is located. The interval is therefore defined by the proximal deletion breakpoints of the 8R250M and 3R30M mutant mouse lines.

rate, along with the high-resolution deletion-map position, suggested that recessive *l7R6^{6R}* mutation might be a loss-of-function allele in the *Nell1* gene. To test this hypothesis, *Nell1* gene expression in wild-type and mutant embryos and in wild-type adult tissues was assayed by Northern blot analysis. The cDNA probe detected a 3.5 kb transcript in wild-type embryos from E10-18 days of gestation (Fig. 4.2). During gestation, expression was first detected as early as E10 and from E 14-18 it steadily increased in the head region and slightly decreased in the body. In adult tissues, normal expression was observed primarily in adult brain (Fig.4.2). In contrast to wild-type embryos, the *Nell1* expression was barely detectable in 102DSJ mutant embryos (Fig. 4.3A).

The expression analysis of wild-type and mutant alleles were also confirmed by RT-PCR analysis (Fig. 4.3B). The two cDNA fragments, one short fragment (~ 557 bp) covering the 5' end and one long fragment (1465 bp) covering the middle and 3' end of the gene were generated by standard PCR (short fragment) and Long Range PCR (bigger fragment). The expression analysis revealed that only the 5' end (~ 557 bp) of *Nell^{6R}* (102DSJ) was expressed and rest of the gene segment looked degraded (~ 1465 bp) i.e. drastically reduced band representing the middle and 3' end of the gene was detected, while in wild-type and other mutant animals carrying other alleles of *Nell1*, both of the bands representing the whole gene were detected. This finding is consistent with the mutation scanning data (see Fig. 4.4). The point mutation in *Nell1* at 1547th bp introduces a premature stop codon that truncates the protein and the products of such nonsense mutations are detected and degraded by the cell via a pathway known as nonsense-mediated mRNA decay (NMD) (Nagy et al. 1998; Hillman et al. 2004). The degradation of the nonsense mutation induced transcripts is known to occur from both the 5' and 3' end of the transcript. The degradation from 5' end occurs through decapping and 5' → 3' exonucleolytic decay while the degradation from 3' end occurs through accelerated deadenylation and exosome-mediated 3' → 5' decay. (Chen et al. 2003; Lejeune et al. 2003; Gatfield et al. 2004). In case of nonsense mutation in *Nell^{6R}* mice, the degradation of the *Nell1* transcript seems to occur from the 3' end because, 3' end of the transcript looks completely degraded (lane 12) while 5' end of the *Nell1* transcripts looks slightly

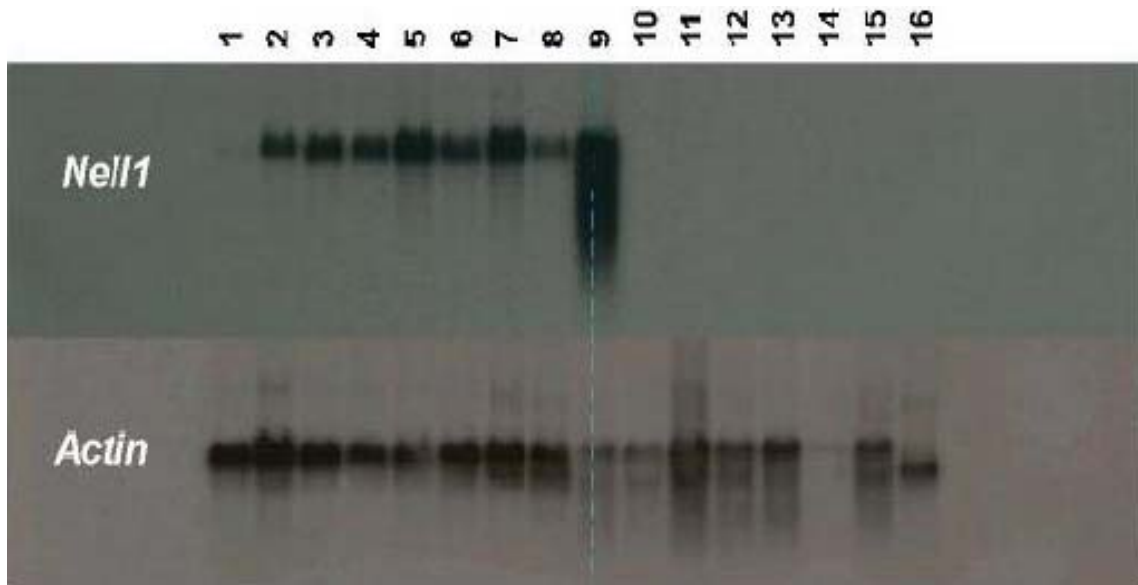
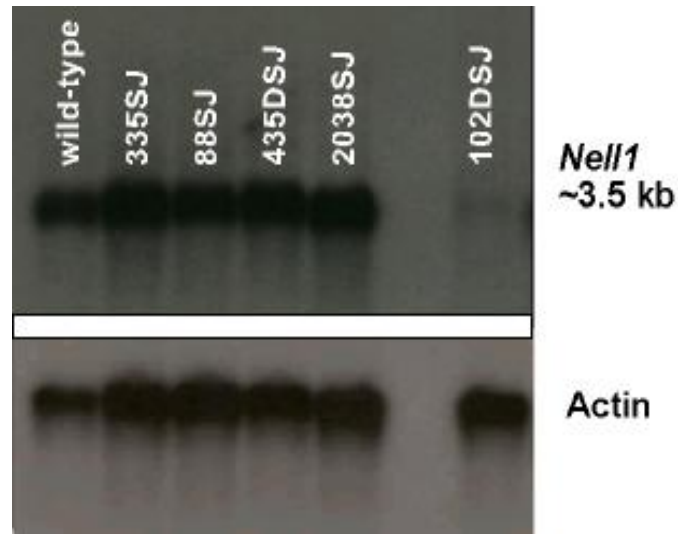


Figure. 4.2: Expression of the Mouse *Nell1* Gene. Northern blot showing expression profiles in heads (H) and bodies (B) of wild-type embryos/fetuses (samples 1-8) and adult mouse tissues (samples 9-16). The lane positions, developmental stages and adult tissues are as follows: 1, E10; 2, E12; 3, E14 H; 4, E14 B; 5, E16 H; 6, E16 B; 7, E18 H; 8, E18 B; 9, brain; 10, liver; 11, spleen; 12, kidney; 13, thymus; 14, heart; 15, lung; 16, muscle. The *Nell1* cDNA probe detects a 3.5-kb transcript as early as E10 days. From E14-E18 days, the *Nell1* message is abundant in both fetal heads and bodies, increasing dramatically in the head as development proceeds. Hybridization of the blot with an actin probe serves as control to compare levels of samples loaded in each lane.

A.



B.

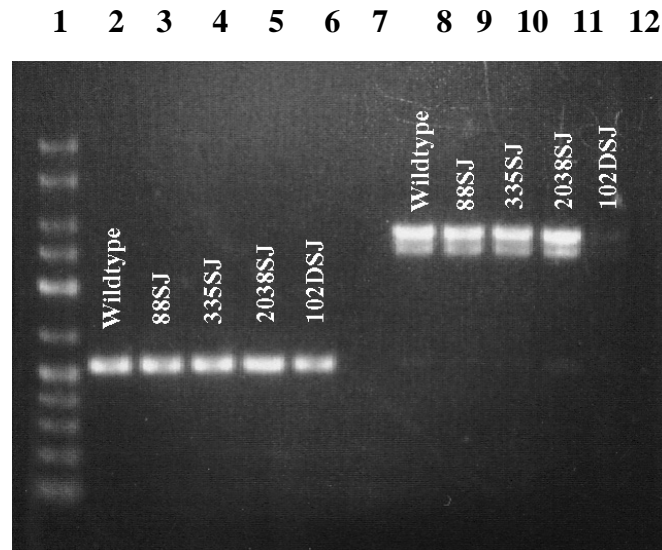


Figure. 4.3: Aberrant Expression of *Nell1* in *l7R6* Mutants. (A). Northern blot showing expression of *Nell1* profiles in heads of E15 *l7R6* embryos/fetuses. There is severe reduction in the expression of *Nell1* gene in the *l7R6*^{R6} (102DSJ) allele compared to normal levels of expression detected in wild-type and other three mutant alleles [88SJ (*Nell1*^{1R}), 335SJ (*Nell1*^{2R}), 2038SJ (*Nell1*^{3R})] at the *l7R6* locus. (B). RT-PCR showing expression of *Nell1* in E18.5 wild-type and mutant embryos/fetuses. Lane1, 2.5 Kb ladder, lanes 2-6 represent 5' end (~ 557 bp) and lanes 8-12 represent middle and 3' end (~ 1465 bp) of *Nell1* gene. The slightly reduced expression of the 5' end of the *Nell1* was detected in 102DSJ (lane 6) compared to wild-type and other mutants while the expression of rest of the gene (middle and 3' end) was drastically reduced (lane 12). See text for details.

reduced (lane 6).

SEQUENCING OF MOUSE *Nell1* cDNA: Even though *Nell1* functions are not clearly understood, the human and rat *Nell1* genes have been well characterized in terms of gene location and sequence analysis. However, at the start of this study there was no mouse full-length cDNA available. Therefore mouse *Nell1* cDNA was generated and sequenced from BJR strain. Eleven sets of primers were designed based on mouse EST's homologous to human *Nell1*. The full-length cDNA covering the entire coding region plus 5' and 3' untranslated regions was obtained by generating short 300-350 bp overlapping PCR fragments. A full-length 2862 bp cDNA was generated (GeneBank Accession #. AY62226) (Fig. 4.4A) with an open reading frame of 2433 bp, which encodes an 810 amino acid protein. Determination of opening reading frame and sequence of translated protein was obtained by using NCBI's ORF finder. The domain prediction for *Nell1* protein was also done by using NCBI's Conserved Domain database. The mouse *Nell1* is a multi-domain protein with one thrombospondin (TSP)-like domain, one Laminin G (LamG)-like domain, one EGF-like domain and two van Willbrand factor C (vWC)-like domains (Fig. 4.4A). The mouse full-length *Nell1* cDNA is highly homologous to human (87% at nucleotide level and 93% at protein level) and rat (98% at nucleotide level and 97% at protein level) *NELL1*.

IDENTIFICATION OF *Nell1* MUTATION IN *Nell1*^{6R} MICE: To identify the mutation in *Nell1*^{6R} (*17R6*^{6R} or 102DSJ) allele, each exon along with the flanking intron sequences was amplified from genomic DNA and analyzed for point mutation by heteroduplex analysis using temperature gradient capillary electrophoresis (Li et al, 2002). Heteroduplexes were detected in exon 14. Sequencing of exon 14 for both wild-type and mutants was done directly from PCR products. The sequence analysis showed that single base pair substitution of T → A that converts a codon for cysteine in to a premature stop codon (TGT → TGA i.e. Cys → Stop) (Fig. 4.4B). This point mutation at Cys truncates the 810 amino acid protein at 502nd amino acid and eliminates EGF like

Figure. 4.4: Identification of the *Nell1*^{6R} Mutation. (A). Mouse *Nell1* cDNA sequence (GenBank Accession No. AY622226) and position of predicted protein domains. Thrombospondin-like (yellow); Laminin G-like (underlined); van Willbrand factor type C like (blue); calcium binding EGF-like (grey). The location of the ENU-induced mutation at bp #1546 in the cysteine codon (amino acid #502) are both highlighted in red text. The premature termination codon introduced at this site will truncate the protein and remove the EGF-like domains that are essential for the binding to PKC β 1. One van Will brand factor type C like domain will also be missing from the putative mutant protein product. (B). Sequence electropherograms showing the T to A base change (red arrows) in the wild-type (left) and the mutant sequence (right) of the *Nell1* gene.

B.

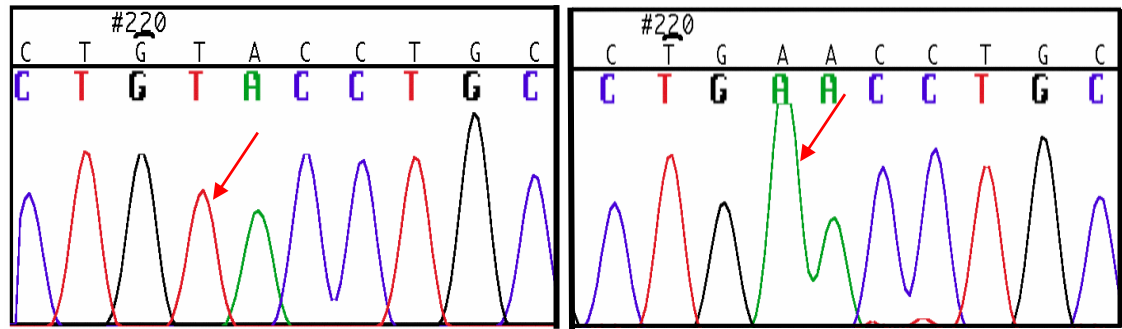


Figure 4.4: Identification of the *Nell1*^{6R} Mutation. Continued.

domains that bind PKC- β 1 protein. One von Willbrand factor type C like domain will also be missing from the mutant protein product and this may interfere with trimerization of *Nell1* protein. In eukaryotes, nonsense mutations like the one observed in *Nell1* 102DSJ allele are detected and degraded by the cell via a pathway known as nonsense-mediated mRNA decay (NMD) (Nagy et al. 1998; Hillman et al. 2004). Therefore mutation-scanning data is consistent with the observation of severely decreased *Nell1* mRNA levels in the mutants. This observation was further confirmed by RT-PCR (see fig. 4.3B).

DETERMINATION OF THE GROSS MORPHOLOGICAL AND SKELETAL DEFECTS IN *Nell1*^{6R} MUTANT MICE

Since several previous studies indicate that *Nell1* plays a role in cranial development and osteoblast differentiation, the impact of *Nell1*^{6R} mutation was evaluated for skull as well as other skeletal defects by comparing wild-type and mutant mice. Morphometric analysis was conducted on the head and overall body. Detailed skeletal analysis was also performed using standard chemical stains specific for bone and cartilage.

GROSS PHENOTYPES: All of the eight *17R6* alleles were recessive lethal mutations. All mutant mice including *17R6*^{6R} hemi- and homozygotes develop till late gestation but do not survive the physical trauma of birth. Observations on females during delivery showed that all the hemi- and homozygous *17R6*^{6R} mutant neonates were born dead, while remaining mutant fetuses that were retrieved by caesarian section were alive. However, the mutant mice rescued by caesarian section quickly died because they were unable to breathe and foster mothers usually cannibalized them. Moreover, additional defects in the heart and vasculature may also contribute to the death of these mutants (Liu and Culiati, unpublished data). Mutant hemi- or homozygote fetuses are easily distinguished from wild-type littermates by their pronounced curled position, enlarged head region (Fig. 4.5), inability to open their mouth and weak reflexes in extremities. All the hemi and homozygote mutant *17R6* mice were phenotypically identical and exhibited enlarged head region and pronounced curled position (data not shown). Heterozygotes survive to adulthood and breed normally, with no readily visible phenotypic differences when compared to wild-type mice.

MORPHOMETRIC ANALYSIS: Of all the ENU-induced mutant *17R6* alleles, *17R6*^{6R} (102DSJ) is the most severe in terms of abnormal head and body morphology. A total of 16 wild-type and 19 homozygote *17R6*^{6r} mutant mice were measured for body length, head height, head length, and head width. Gross anatomical measurements indicated that compared to their wild-type littermates, homozygous mutant fetuses manifested a decreased body length due to the pronounced altered curvature of the spine and an enlarged altered head shape brought about by increased head length (Table. 4.1). No significant changes in head height and width were detected.

***Nell1*^{6R} MUTANT MICE HAVE SKELETAL DEFECTS IN THE SKULL AND VERTEBRAL COLUMN:** The skeletal phenotype of *Nell1* mutants were examined by Alizarin red - Alcian blue staining of fetuses at E 18.5 days of gestation. Alizarin Red stains bone while Alcian blue stains cartilage. The skeletal phenotype of *17R6*^{6R} was compared with skeletal phenotypes other mutant alleles. All mutants show changes in



Figure 4.5: Phenotypes of *I76R* Mutants. Phenotype of *I7R6^{6R}* homozygote mutants at 18.5 days of gestation. On the right is a fetus homozygous for the *I7R6^{6R}* allele (from stock 102DSJ) showing a very curled position, enlarged head size and a more spherical head shape, compared to the control littermate (left). *I7R6^{6R}* mouse fetuses were recovered alive by caesarean rescue because they do not survive delivery through the birth canal perhaps due to the physical trauma in the neck and spine region brought about by the abnormal spinal curvature. The phenotypes of the other alleles of *I7R6* not shown; they are similar to *I7R6^{6R}*

Table. 4.1: Quantitative analysis of changes in body length and head size of *Nell1*^{6R} homozygous mutants compared to wild-type littermates, measured (in mm) at E18 days of gestation.

Litter No.	Genotype	No. Embryos per litter	Body Length	± SEM	Head Length	± SEM	Head Height	± SEM	Head Width	± SEM
1	Wild Type	2	21.49	± 0.28	10.23	± 0.17	5.95	± 0.01	6.37	± 0.35
	Mutant	2	19.28	± 0.05	11.5	± 0.70	6.96	± 0.41	6.88	± 0.54
2	Wild Type	2	17.15	± 0.06	9.72	± 0.20	9.06	± 0.69	6.42	± 0.78
	Mutant	4	16.90	± 0.50	10.37	± 0.75	8.50	± 0.54	6.14	± 0.33
3	Wild Type	1	21.3	± 0.0	10.1	± 0.0	8.0	± 0.0	6.4	± 0.0
	Mutant	1	18.5	± 0.0	11.0	± 0.0	8.7	± 0.0	6.8	± 0.0
4	Wild Type	1	19.9	± 0.0	11.0	± 0.0	8.1	± 0.0	6.5	± 0.0
	Mutant	2	17.8	± 0.4	11.2	± 0.4	8.65	± 0.3	6.95	± 0.5
5	Wild Type	1	23.24	± 0.0	9.77	± 0.0	6.01	± 0.0	6.49	± 0.0
	Mutant	1	20.30	± 0.0	11.15	± 0.0	5.53	± 0.0	6.19	± 0.0
6	Wild Type	4	22.69	± 1.64	10.32	± 0.93	5.17	± 0.41	6.42	± 0.37
	Mutant	2	18.50	± 0.37	11.44	± 0.32	4.55	± 0.14	6.75	± 0.21
7	Wild Type	2	23.86	± 0.37	10.71	± 0.43	5.44	± 0.52	6.66	± 0.61
	Mutant	3	19.11	± 0.63	11.2	± 1.45	5.39	± 0.68	6.67	± 0.06
8	Wild Type	1	22.77	± 0.0	9.47	± 0.0	5.31	± 0.0	6.53	± 0.0
	Mutant	2	18.33	± 0.65	9.94	± 0.88	6.28	± 0.39	6.85	± 0.3
9	Wild Type	2	22.32	± 1.4	10.22	± 0.88	5.66	± 0.46	6.86	± 0.6
	Mutant	2	17.98	± 0.55	10.45	± 1.32	7.19	± 0.41	6.91	± 0.14
TOTAL	Wild Type	16	21.72		10.21		6.27		6.51	
	Mutant	19	*18.25		*10.86		*6.98		6.64	

The body length of mutant fetuses were significantly decreased and the head length increased in comparison with wild-type mice.

head shape, spinal curvature and morphology of the ribcage area. Skeletal defects were very severe in both *l7R6^{6R}* (102DSJ) (Fig. 4.6A) and *l7R6^{1R}* (88SJ) (Fig. 4.6B), while they were relatively milder in *l7R6^{2R}* (335SJ) (Fig. 4.6C) and *l7R6^{3R}* (2038SJ) (Fig. 4.6D). In the spines of mutants from *l7R6^{6R}* and *l7R6^{1R}*, there is a sharp bend between the cervical and thoracic vertebrae (arrows). The spinal phenotype is visible as early as E16 (data not shown) and remarkably consistent in severity among mutants of the same line. The severe phenotype associated with *l7R6^{6R}* fetuses is due to drastically reduced expression of *Nell1* as a result of nonsense mutation and degradation of the *Nell1* transcript (see Figure. 4.3). Figure. 4.7 shows skeletal phenotype of *l7R6^{6R}* fetus in detail. The skeletal analysis clearly showed larger rounder heads, compression of intervertebral spaces and alteration of spinal curvature, and anomalies in the shape and volume of the ribcage (Fig. 4.7A and B). The cervical region of the vertebral column displayed the most dramatic reduction in the intervertebral disc matrix and a pronounced change in spinal curvature was observed at the juncture of the cervical and thoracic vertebral bones (Fig. 4.7A and B). The enlargement and thinning of the parietal, frontal and interparietal bones in the skull were readily apparent (Fig. 4.8A-D). The nasal bones were also enlarged but thinning was not clearly observed in these structures. The consistently decreased staining by Alizarin Red in the *Nell1^{6R}* calvarial bones indicated decreased ossification in the mutant. These *Nell1^{6R}* skeletal defects were confirmed by microcomputerized tomography scanning (Fig. 4.9 and B). The radiographs showed the sharp curvature change between the cervical thoracic vertebrae (Fig. 4.9A). Moreover, the MicroCat scanning data suggested lesser bone density (Fig. 4.9A) and areas of ossification (Fig. 4.9B) in the *Nell1^{6R}* mutant homozygotes. Although the effect of *Nell1^{6R}* mutation in the head region was expected, its profound impact on the development of the vertebral and thoracic skeleton was not anticipated since the deleterious effects of *Nell1* overexpression were confined to the growth and differentiation of the calvarial bones (Zhang et al. 2002).

The gene expression profile resulting from the *Nell1^{6R}* mutation (see Fig. 4.15) is further supported by standard histological analysis. Histological analysis was done on both wild-type and mutant E18.5 embryos. The Formalin fixed embryo sections of

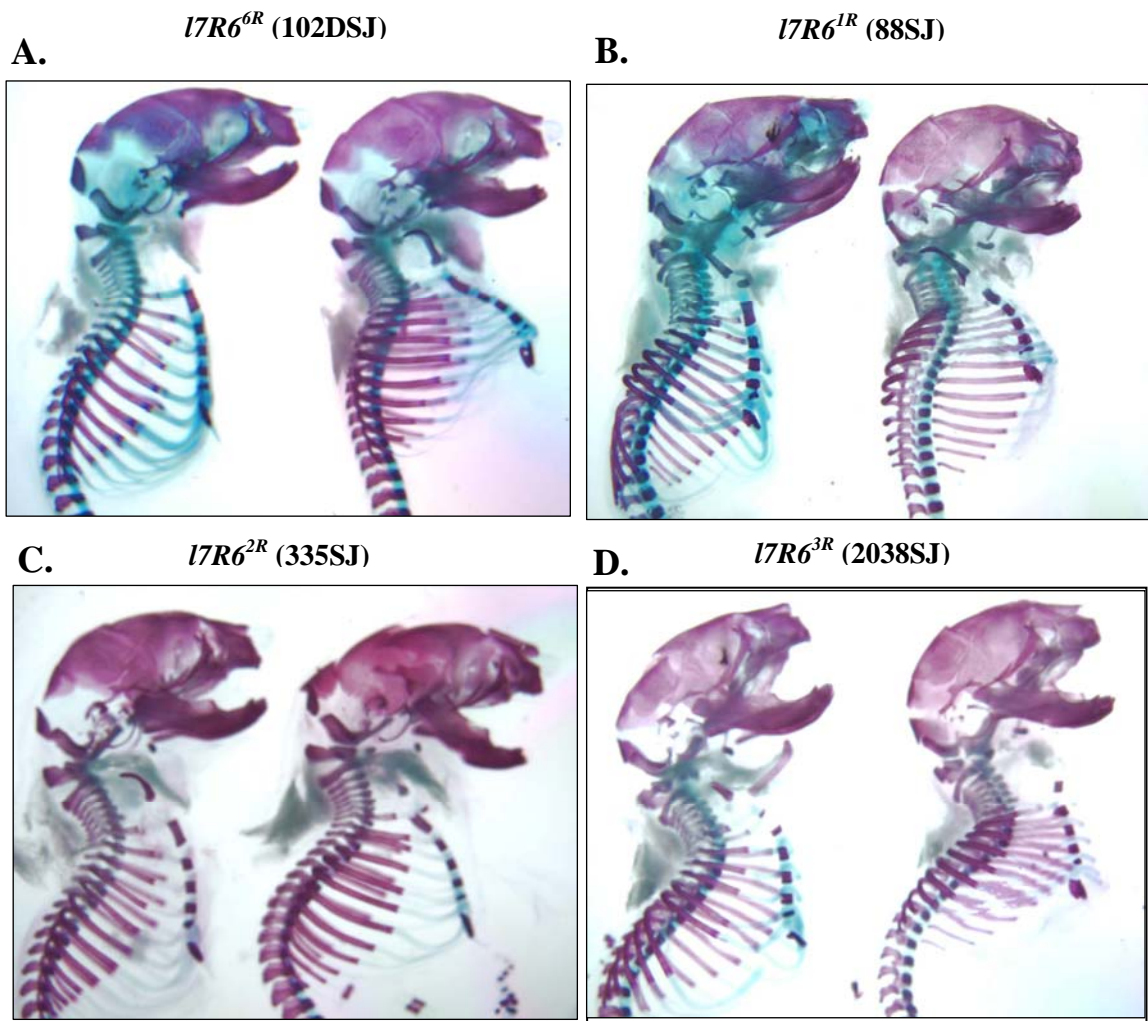


Figure. 4.6: Skeletal Analysis of *I7R6* Neonates. *I7R6^{6R}* (102DSJ) (A), *I7R6^{1R}* (88SJ) (B), *I7R6^{2R}* (335SJ) (C) and *I7R6^{3R}* (2038SJ) (D). Mutants manifest changes in head shape, spinal curvature and morphology of the ribcage area. Both *I7R6^{6R}* and *I7R6^{1R}* show very severe defects in all these three categories of defects, while *I7R6^{2R}* and *I7R6^{3R}* are relatively milder. In the spines of mutants from *I7R6^{6R}* and *I7R6^{1R}*, there is a sharp bend between the cervical and thoracic vertebrae (arrows).

A.



B.

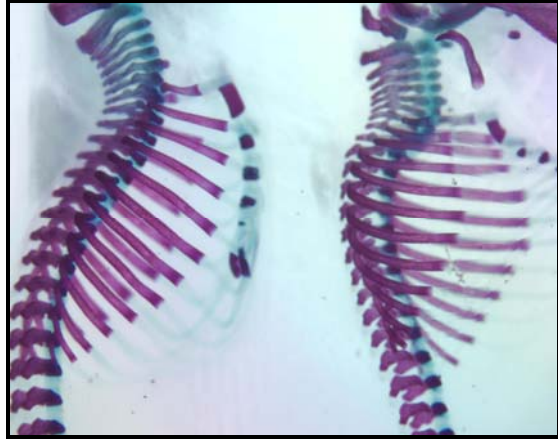
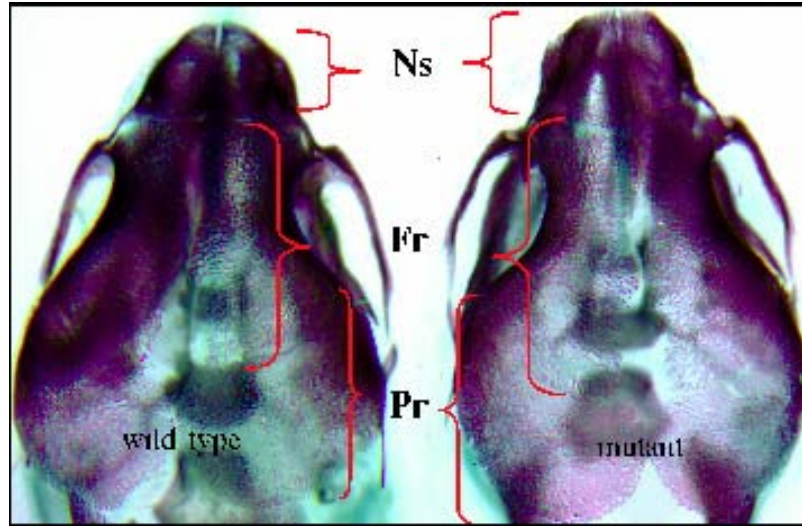


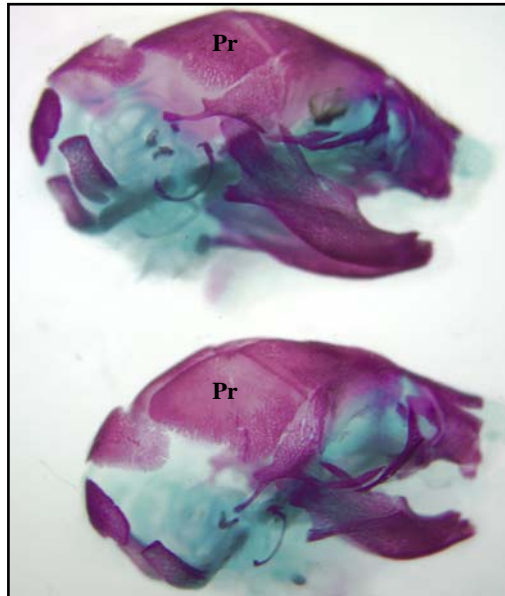
Figure. 4.7: Skeletal Phenotype of *Nell1*^{6R} Homozygote Mutant Mouse. At 18.5 days of gestation. **(A).** There is alteration of spinal curvature, decrease in intervertebral disc spaces, reduced thoracic volume, protruding sternum and a slight enlargement of the skull. **(B).** Close-up of the cervical region where the most pronounced vertebral compression is located.

Figure. 4.8: Cranial Defects in *Nell1*^{6R} Homozygote Mutant Mouse. (A) Top view of the skull showing the increased size of the nasal (Ns), frontal (Fr), and parietal (Pr) bones in *Nell1*^{6R} mutant mice. (B) Side view of the skull showing enlargement of parietal bones (Pr) in mutant fetal heads. (C). Enlargement of the interparietal and (D) Frontal bones. (A-D) The calvarial bones of *Nell1*^{6R} mutant mice are thinner than those of the wild-type and consistently have less Alizarin Red staining, suggesting a lesser degree of ossification.

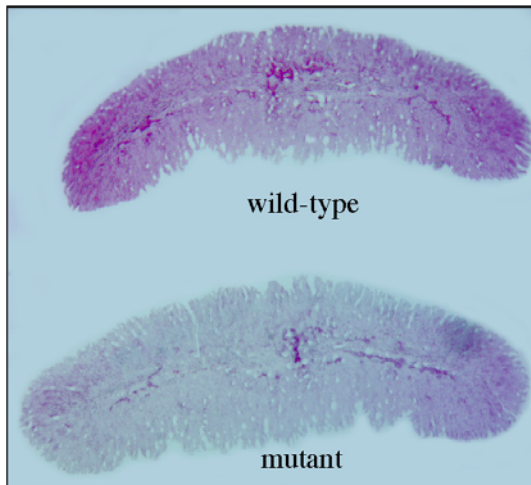
A.



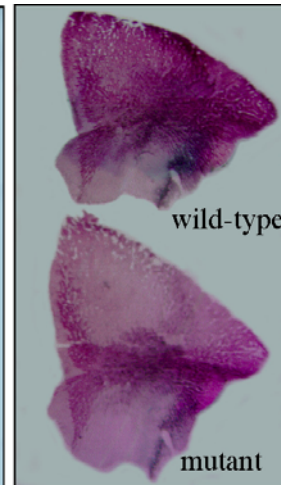
B.



C.



D.



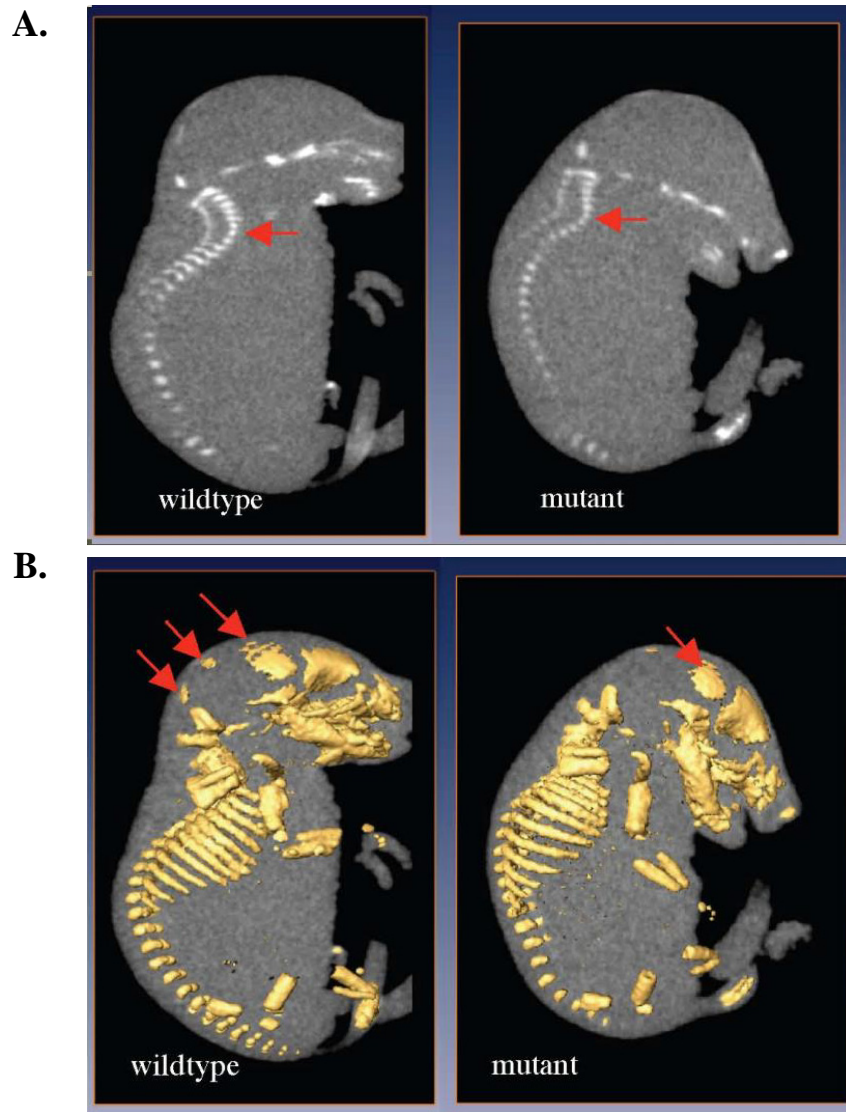


Figure. 4.9: Skeletal Defects in *Nell1^{6R}* Homozygote Mutant Mouse. (A) Radiographs of a wild-type fetus compared to *Nell1^{6R}* mutant littermate. A pronounced alteration in the spinal curvature occurs at the cervical vertebrae in the mutant fetuses (arrow). The lesser intensity of signals in the craniofacial and vertebral skeleton of the mutant suggests lesser bone density. (B) Images of 3D re-construction of MicroCat scans for wild-type and mutant fetuses show lesser areas of ossification in the mutant fetal head (arrow). The observation in earlier skeletal analysis that the mutant calvarial bones are thinner is consistent with MicroCat scan data showing larger areas of dense bone in the wild-type fetus. These MicroCat scans again confirm the alteration of spinal curvature and compression of cervical vertebrae observed in *Nell1^{6R}* mutants.

vertebral columns were stained with Haematoxylin and Eosin (H and E), Masson and Periodic acid Schiff (PAS) stains. In the mutant (Fig. 4.10B) vertebral columns, intervertebral spaces were markedly decreased compared to their wild-type controls (Fig. 4.10A). This observed reduction in intervertebral spaces in mutants may be due to the decreased ECM production due to mutation in *Nelli*, which downregulates expression of specific collagens and non-collagenous proteins due decreased chondrocyte differentiation (see Real-time qRT-PCR results, page 92 and Fig.4.15). H and E staining of vertebral bodies shows that in wild-type, cells look well defined and more differentiated (Fig. 4.10C) while in mutants, cells look less organized and developed (Fig.4.10D). Compared to their wild-type littermates (Fig. 4.10C), *Nelli*^{6R} homozygous mice displayed considerable reduction in the amount of extracellular material surrounding the cells in the developing vertebral body and intervertebral discs (Fig. 4.10D).

EXAMINATION OF THE ROLE OF *NELLI* IN OSTEOBLAST AND CHONDROCYTE DIFFERENTIATION IN THE VERTEBRAL COLUMN

To test the hypothesis that the reduced expression of *Nelli* in *Nelli*^{6R} mutant impairs chondrogenesis and endochondral ossification by decreasing differentiation in both osteoblast and chondrocytes in the vertebral column, expression of specific differentiation markers for both osteoblast and chondrocytes was investigated.

LOCALIZATION OF *NELLI* EXPRESSION IN WILD-TYPE AND MUTANT

***Nelli*^{6R} FETAL VERTEBRAL COLUMNS:** The cell-specific expression of *Nelli* in both wild-type and mutant E18.5 fetal vertebral columns was determined by immunohistochemistry using anti-rabbit *Nelli* antibody. This *Nelli* antibody has been successfully used for immunohistochemistry studies (Zhang et al. 2002). Vertebral column develops by endochondral ossification. Formation of vertebrae is initiated at the center of the vertebral bodies and the growth occurs in a radial fashion with chondrocyte proliferation and differentiation occurring at the central area of vertebrae and the mature

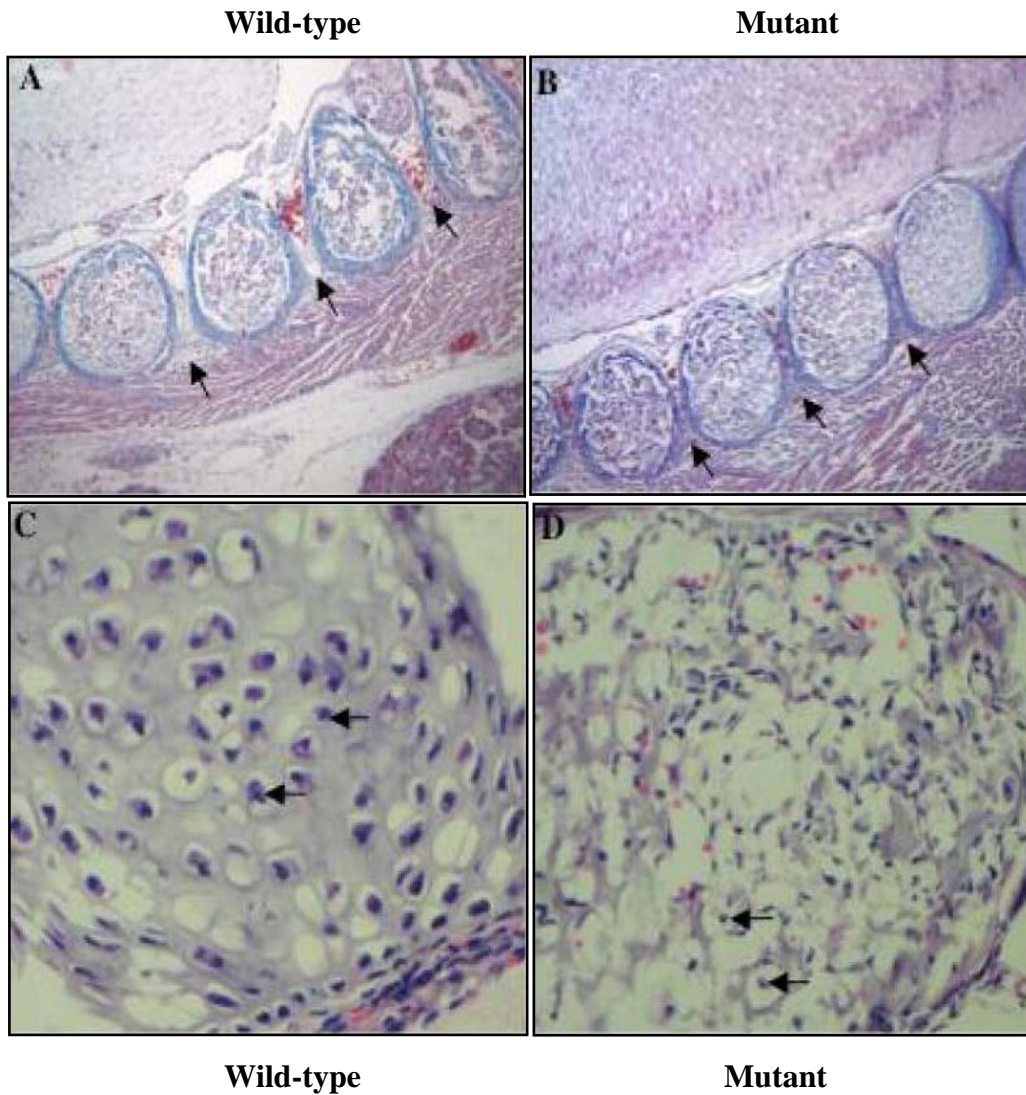


Figure. 4.10: Histological Analysis of Fetal Vertebral Column. (A) The normal architecture of the cervical vertebral column in wild-type E18.5 fetus (sagittal section, Masson staining) compared with the mutant *Nell1^{OR}* homozygote, (B), showing the reduction of intervertebral spaces between the vertebral bodies (arrows). See text for details. (C) and (D). Haematoxylin and Eosin staining of sagittal sections of vertebral bodies (higher magnification) of wild-type (C) and mutant (D) showing lesser amount of ECM and cellular development of chondrocytes in the mutants.

bone formation by osteoblasts at the periphery. Decreased expression of *Nell1* was detected in mutant (*Nell1^{6R}*) vertebral columns (Fig. 4.11C and D) compared to wild-type fetuses (Fig. 4.11A and B). In wild-type vertebral bodies, the expression was restricted to osteoblasts, which are present at the surface of the vertebral body away from center of ossification and there was no staining detected in chondrocytes, which are present at the center of the vertebral bodies, near the site of initial ossification (Fig. 4.11A and B). There was no staining detected in the intervertebral discs (Fig. 4.11A and B) again suggesting, expression of *Nell1* is restricted to osteoblasts at this stage in fetal development. In mutants *Nell1* expression was restricted to osteoblasts at the surface of the vertebral bodies and no staining was observed in intervertebral discs. The dark lines observed in the mutant intervertebral spaces do not represent the staining for *Nell1* protein. They are the artifacts introduced during the sectioning and paraffin embedding of the vertebral column sections. It is possible that chondrocytes in the vertebrae and intervertebral discs do express *Nell1* but at lower levels and is beyond the detection limit of this assay. Alternatively, chondrocytes may express *Nell1* at earlier stages of ossification i.e. earlier in the development when there is more active cartilage and bone formation in the embryo. Even though here (Fig. 4.11) the expression of *Nell1* in the spinal cord is not conclusive, the EST data shows that it is expressed in the mouse spinal cord. The initial phase of chondrocyte proliferation and differentiation in vertebral bodies and chondrocyte proliferation in intervertebral discs may be regulated by *Nell1* secreted by cells in the spinal cord and in later stages by *Nell1* secreted by osteoblasts in the vertebral bodies.

The *Nell1* expression was also detected in wild-type fetal skin. The staining for *Nell1* protein was intense in the epidermal layer of wild-type skin but there was no staining detected in the dermal or hypodermal layer (subcutaneous layer)(Fig. 4.12A and B). The staining looks uniform throughout all the five layers of epidermis. In addition to the epidermis *Nell1* expression was also detected in the wild-type skeletal muscle beneath the skin. In contrast to wild-type fetal skin, *Nell1* expression was markedly decreased in mutant (*Nell1^{6R}*) skin (Fig. 4.12C and D). The staining for *Nell1* was barely detectable in the epidermal layer of mutant skin while no staining was detected in other layers of the

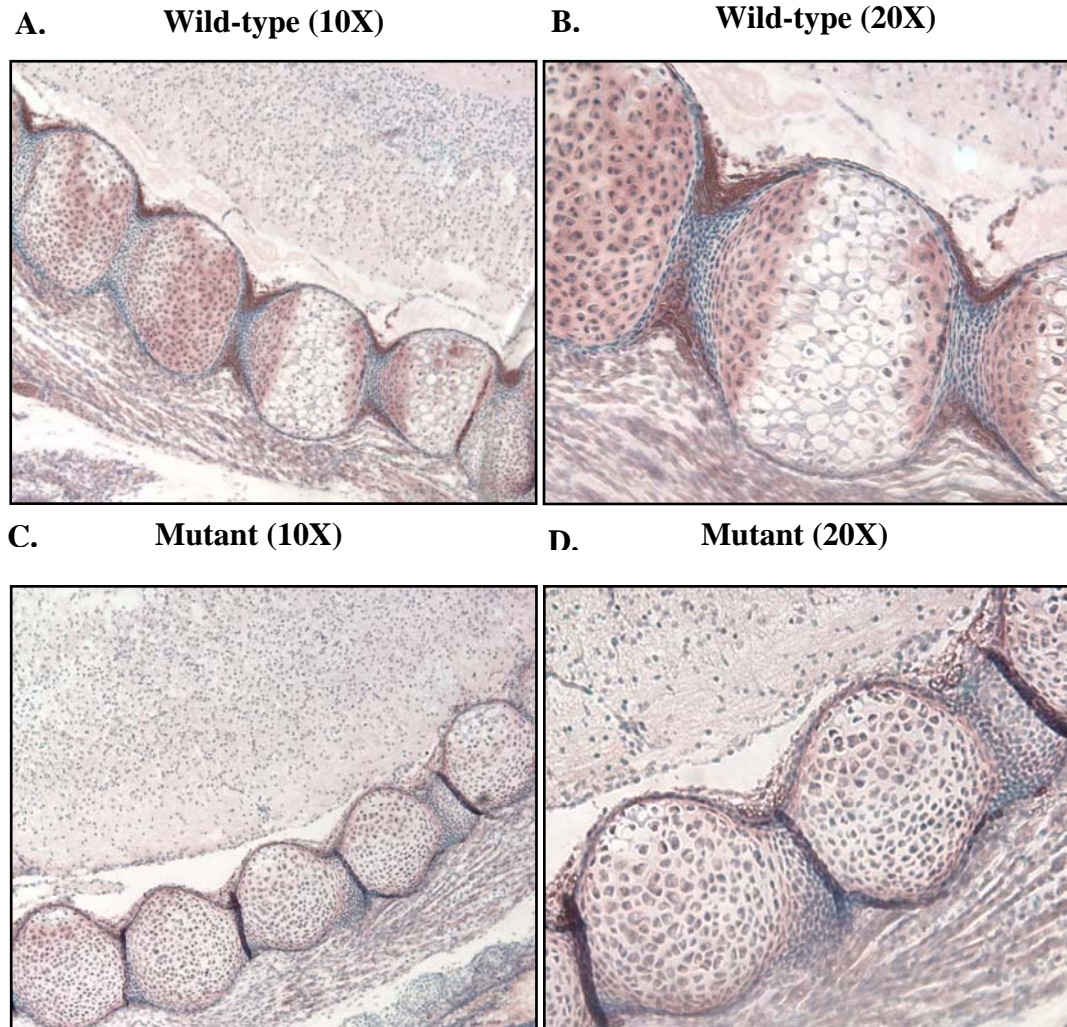


Figure. 4.11: Expression of *Nell1* in Fetal Vertebral Column. Immunohistochemical staining of sagittal sections through the vertebral columns of wild-type (**A**) and (**B**) and mutant (*Nell1*^{6R}) (**C**) and (**D**) E18.5 fetuses showing expression of *Nell1*. Positive immunoreactivity (coppery brown staining) for *Nell1* was detected in wild-type fetal vertebral bodies, (**A**) and (**B**) (higher magnification) but not in intervertebral discs and its expression was restricted to osteoblasts at the surface of the vertebral bodies. There is less or no staining detected in the chondrocytes at the center of the vertebral bodies and chondrocytes in the intervertebral discs. Expression of *Nell1* was less in mutant vertebral columns (**C**) and (**D**) [higher magnification]).

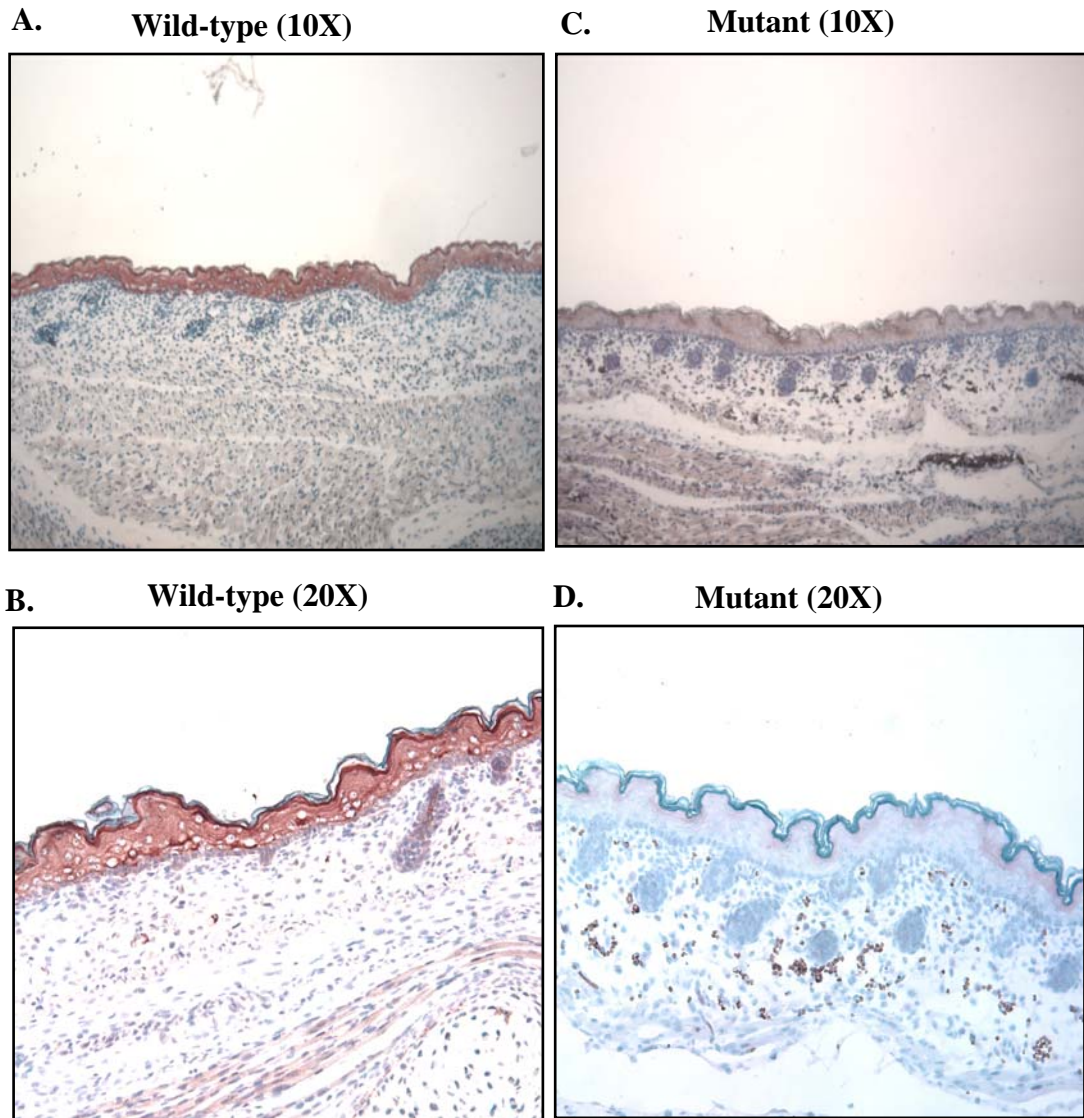


Figure 4.12: Expression of *Nell1* in Fetal Skin. Immunohistochemical staining of sections through the skins of wild-type (A) and (B) and mutant (*Nell1*^{6R}) (C) and (D) E18.5 fetuses showing expression of *Nell1*. Intense positive immunoreactivity (coppery brown staining) was detected in the epidermal layer of the wild type fetal skin and in the skeletal muscle beneath the skin, (A) and (B) (higher magnification) while *Nell1* expression was markedly decreased in mutant skin, (C) and (D) (higher magnification).

skin including the muscle beneath the skin. This was an unexpected finding but rather an important one because mutation in *Nell1* affects specific collagens and ECM proteins (revived in chapter 2) that are also affected in Ehlers-Danlos syndrome, which is also associated with cartilage and skin defects. These results suggest that the hyper-elastic skin observed in the patients with certain type (s) EDS with unknown etiology/genetic defect may be partially due to the mutation in *Nell1* gene.

EFFECT OF *Nell1*^{6R} MUTATION ON DIFFERENTIATION OF OSTEOBLASTS AND CHONDROCYTES IN THE DEVELOPING VERTEBRAL COLUMN:

The skeletal, histological and expression analysis of mutant *Nell1* alleles revealed alterations of head shape and deformities in the vertebral column and suggested dysregulation of cell proliferation, differentiation and apoptosis. The previous *in vitro* studies have demonstrated (Zhang et al. 2002) that downregulation of *Nell1* results in reduced osteoblast differentiation. Both osteoblasts and chondrocytes produce specific collagens and ECM proteins during the differentiation process. The Real-Time qRT-PCR analysis (see Fig. 4.15) showed that ECM proteins like tenascins, matrilins, *Osf-2*, *Col X* and *Chad* are downregulated in *Nell1*^{6R} mutant mice. Therefore, the status of chondrocyte and osteoblast differentiation in *Nell1*^{6R} homozygotes was investigated for expression of known markers of osteoblast and chondrocyte (*Col X*) differentiation and assessed for the extent of bone mineralization, a measure of differentiation status of osteoblasts. The expression of *Col X* in both wild-type and mutant (*Nell1*^{6R}) fetal vertebral column was examined by immunohistochemistry using anti-*Col X* antibody (Fig. 4.13). Reduced *Col X* staining was detected in mutant vertebral bodies (Fig. 4.13 A and B) compared to wild-type (Fig. 4.13C and D), suggesting decreased differentiation of chondrocyte. The *Col X* staining was restricted to chondrocytes in both wild-type and mutant vertebral bodies. The light blue areas around the rim of the vertebral bodies represent the developing bone, which contain osteoblast, do not show any staining for *Col X*. The *Col X* staining was observed more in vertebral bodies than in intervertebral discs. The staining observed in the intervertebral discs may not be due to *Col X* immunoreactivity, but may be due to *Col II* because this particular anti-rabbit *Col X* antibody is known to exhibit slight cross-

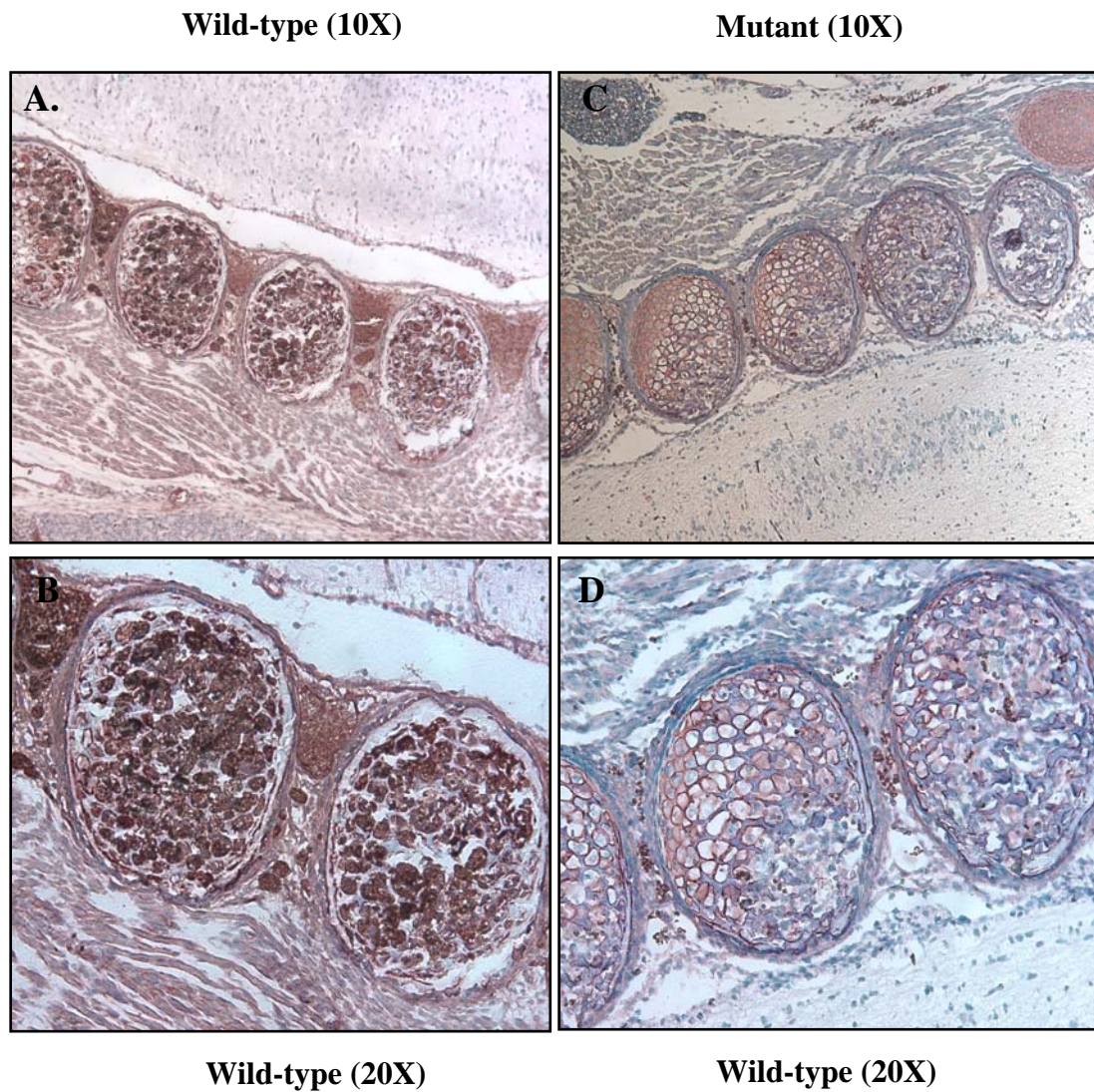


Figure. 4.13: Expression of *Col X* in Fetal Vertebral Column. Immunohistochemical staining of sagittal sections through the vertebral columns of wild-type (**A**) and (**B**) and mutant (*Nell1^{6R}*) (**C**) and (**D**) E18.5 fetuses showing expression of *Col X*. Intense positive immunoreactivity (Dark coppery brown staining) was detected in wild type fetal vertebral bodies as well as intervertebral discs, (**A**) and (**B**) (higher magnification). Staining for *Col X* was less in both mutant (*Nell1^{6R}*) vertebral bodies and intervertebral discs, suggesting decreased differentiation of chondrocytes.

reactivity to *Col II*.

The degree of bone mineralization (extent of osteoblast differentiation) was measured by von Kossa staining of both wild-type and mutant (*Nell1*^{6R}) E18.5 fetal parietal bones and vertebral columns. The results from von Kossa staining of sagittal sections through the vertebral column and parietal bones (Fig. 4.14A-D) showed decreased bone mineralization in *Nell1*^{6R}. The cranial (Fig. 4.14 B and D) and vertebral bones of mutant homozygotes have a lesser number of mineralized areas and exhibit a highly irregular pattern when compared to wild-type bones (Fig. 4.14 A and C) The frontal bones display the same defects in bone mineralization as the parietal bones (data not shown).

DETERMINATION OF THE BIOLOGICAL PATHWAY (S) PERTURBED BY THE *Nell1*^{6R} MUTATION

A large number of genes and pathways have already been defined in osteogenesis and chondrogenesis in the skull and vertebral column. The information acquired from these experiments will aid in placing *Nell1* in a particular biological pathway(s) and relating this to the phenotyping and immunohistochemistry data.

HIGH-THROUGHPUT qRT-PCR: In order to define the genes and pathways that were perturbed by the *Nell1*^{6R} mutation, qRT-PCR analysis of 219 experimental and 6 control genes was carried out in RNA samples extracted from individual heads and bodies of four *Nell1*^{6R} mutants and four wild-type E18.5 fetuses. The 219 genes were carefully selected based on the observed mutant phenotype and the putative domains and functions of the *Nell1* gene. Genes associated with CS (e.g. *Runx2*, *Msx2*, *Fgfr3*), bone and cartilage development, cell growth and differentiation, neural development and signal transduction pathways were also included.

This expression analysis showed an association between the loss of *Nell1* function and reduced expression of genes for extracellular matrix proteins critical for chondrogenesis and osteogenesis. The Real-Time qRT-PCR analysis revealed reduced

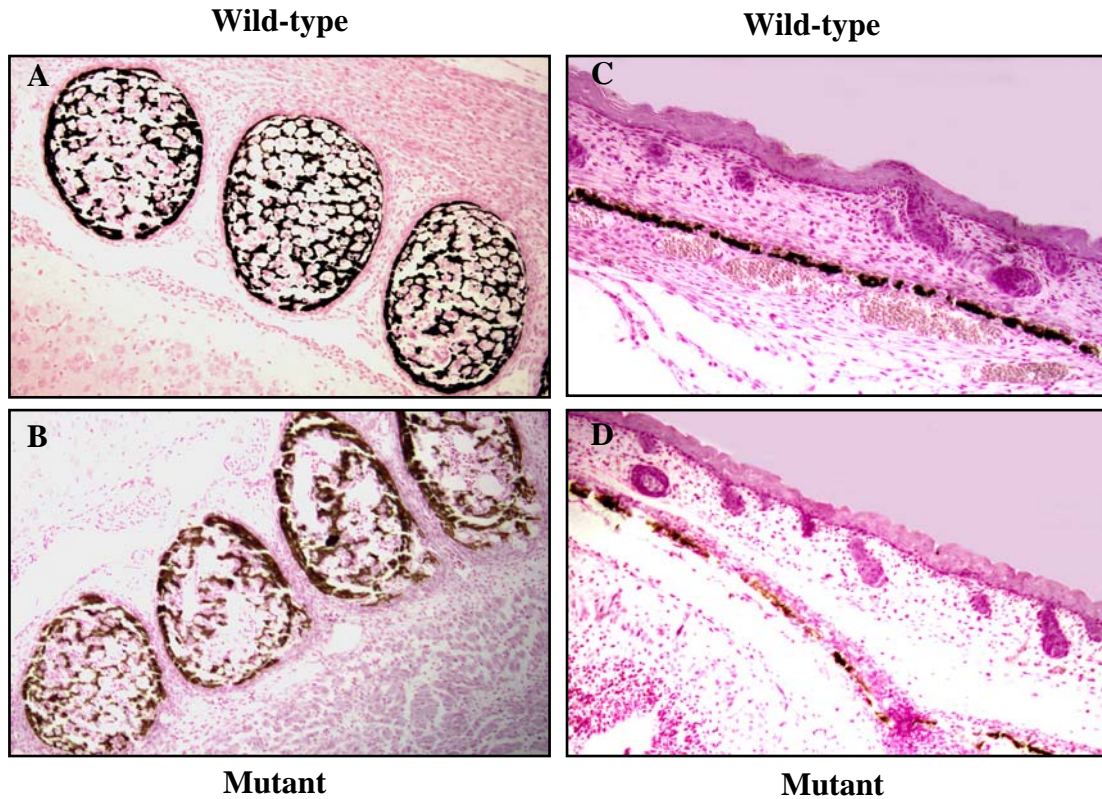


Figure. 4.14: van Kossa Staining of Vertebral Column and Parietal Bone. van Kossa staining of sagittal sections through the vertebral columns of wild-type (**A**) and mutant (**B**) E18.5 fetuses showing decreased bone mineralization in the vertebral bodies of (*Nell1*^{6R}) homozygotes. The intensity and distribution of stained areas (black) are lesser and exhibit an irregular pattern in the mutant fetuses. van Kossa analysis of sagittal sections through the parietal bones of wild-type (**C**) and mutant (**D**) fetuses also revealed decreased mineralization. In mutant parietal bone (**D**), the intensity of van Kossa staining is less and in contrast to the wild-type *Nell1*^{6R} calvarial bones have thinner and more ‘patchy’ pattern of mineralization. There are larger and more frequent gaps between mineralized regions, similar to the pattern seen in vertebral bodies (**B**).

expression of 13 genes in the head and 28 genes in the body due to *Nell1*^{6R} mutation (Fig. 4.15). Expression of the following 9 genes were affected in both heads and bodies: *Col5a3*, *Col5a1*, *Col15a1*, *Tnxb*, *Matn2*, *Osf-2*, *Chad*, and *Tnfrsf11b*. These affected proteins are involved in cell adhesion, communication and provide strength and flexibility to tissues. The most severely affected genes in the head were *Tnxb* and *Col5a3*; in body were *Tnxb*, *Prg4*, *Thbs3* and *Col5a3*. The other genes in the body that are affected by *Nell1*^{6R} mutation such as *Tnc*, *Tnx*, *Matn3*, *Chad*, *Tnfrsf11b* and *Bmpr1a* are known to play a critical role in the development of vertebral column on both human and mouse (Mansson et al. 2001; Cundy et al. 2002; Gruber et al. 2002; Jackson et al. 2004; Yoon et al. 2005). The eight out of 21 collagen genes assayed showed significant changes in expression indicating that the loss of *Nell1* influences only a specific set of collagen subunits. Several affected genes are involved in Ehlers-Danlos Syndrome and other disorders associated with vertebral column defects. It is rather important to note that severely affected genes like *Tnxb* and *Col5a3* cause EDS, a severe cartilage defect (Beighton et al. 1998; Mao et al. 2001). The EDS patients have genetic defects that result in defective fibrillar collagen synthesis and deposition. Additionally, it has been suggested that mutation in *Col5a3*, another gene, which was affected by the *Nell1* mutation may account for at least some types EDS in which COL-5A1 and -A2 have been excluded (Imamura, 2000). Furthermore, one of the six major EDS syndromes, an autosomal recessive EDS-type VI is characterized by abnormal curvature of the spine, hypotonia, joint laxity and ocular fragility (Beighton et al. 1998; Mao et al. 2001).

E18 HEADS

Gene Symbol	Gene Name	NM Number	GI Number	qRTPCR Data Summary							Annotation			
				p-value	AVG (wt)	SD (wt)	AVG(mt)	SD(mt)	DDct	FOLD	ECM	Cell Adh	Cell Comm	others
<i>Tnxb</i>	tenascin	NM031176	13928671	0.0000007	1.76	0.15	3.34	0.39	-1.59	2.99				
<i>Col5a3</i>	collagen 5 alpha 3 subunit	NM016919	8393172	0.0000006	0.59	0.16	1.61	0.22	-1.03	2.04				
<i>Thbs4</i>	thrombospondin 4	NM011592	6755780	0.0046330	1.37	0.16	1.93	0.36	-0.55	1.47				
<i>Col15a1</i>	procollagen type XV, alpha 1	NM009929	24475606	0.0003000	0.09	0.16	0.63	0.23	-0.54	1.46				
<i>Chad</i>	chondroadherin	NM007669	31992462	0.0049249	1.32	0.26	1.8	0.26	-0.49	1.4		?		
<i>Adamsl8</i>	metalloprotease	NM013906	7304656	0.0014971	3.99	0.28	4.45	0.15	-0.47	1.39				
<i>Col5a1</i>	procollagen type V, alpha 1	NM015734	7656396	0.0006699	-2.25	0.11	-1.79	0.22	-0.47	1.39				
<i>Tnfrsf11b</i>	tumor necrosis factor (ligand)	NM008764	31543981	0.0020684	4.3	0.12	4.75	0.26	-0.45	1.37				
<i>Col1a1</i>	procollagen type X, alpha 1	NM009925	6753479	0.0030285	0.25	0.22	0.71	0.24	-0.45	1.37				
<i>Thbs3</i>	thrombospondin 3	NM013691	8567413	0.0008943	1.55	0.13	1.99	0.21	-0.43	1.35				
<i>Osf2-pending</i>	osteoblast specific factor 2	NM015784	7657428	0.0023714	-3.96	0.2	-3.61	0.14	-0.34	1.27				
<i>Col18a1</i>	procollagen type XVIII, alpha 1	NM009929	40789281	0.0039774	-0.65	0.09	-0.51	0.22	-0.34	1.27				
<i>Matn2</i>	matrin 2, cartilage matrix protein 2	NM016762	7949075	0.0029529	0.14	0.1	0.45	0.17	-0.31	1.24				
										No. of Genes	10	8	9	1
										Percentage	77%	62%	70%	8%

E18 BODIES

Gene Symbol	Gene Name	NM Number	GI Number	qRTPCR Data Summary							Annotation			
				p-value	AVG (wt)	SD (wt)	AVG(mt)	SD(mt)	DDct	FOLD	ECM	Cell Adh	Cell Comm	others
<i>Tnxb</i>	tenascin	NM031176	13928671	0.000000002	0.52004	0.16	2.24	0.17	-1.71	3.28				
<i>Pig4</i>	proteoglycan 4	NM021400	7209718	0.000000686	3.5	0.12	4.74	0.25	-1.24	2.36				
<i>Thbs3</i>	thrombospondin 3	NM013691	8567413	0.000261732	1.3	0.18	2.31	0.4	-1.01	2.02				
<i>Col5a3</i>	collagen 5 alpha 3 subunit	NM016919	8393172	0.000001796	-0.05	0.14	0.92	0.21	-0.98	1.97				
<i>Neurog2</i>	neurogenin 2	NM009718	34328159	0.002524664	9.34	0.47	10.2996	0.41	-0.96	1.94				
<i>Col5a1</i>	procollagen type V, alpha 1	NM015734	7656396	0.000348035	-2.49	0.27	-1.78	0.23	-0.71	1.63				
<i>Col6a1</i>	procollagen type VI, alpha 1	NM009933	6753483	0.000073349	-3.54	0.23	-2.69	0.16	-0.65	1.57				
<i>Col15a1</i>	procollagen type XV, alpha 1	NM009929	24475606	0.001447092	-0.78	0.16	-0.17	0.29	-0.61	1.53				
<i>Pacsin3</i>	PKC and casein kinase substrate in neurons 3	NM030890	1365951	0.000000251	0.03	0.16	0.63	0.18	-0.6	1.51				
<i>Tnc</i>	tenascin c	NM011607	7106434	0.000894612	-1.2	0.3	-0.62	0.17	-0.59	1.5				
<i>Col12a1</i>	procollagen type XII, alpha 1	NM007730	6680959	0.000107290	-2.25	0.12	-1.69	0.19	-0.57	1.48				
<i>Chad</i>	chondroadherin	NM007669	31992462	0.002787124	0.09	0.13	0.66	0.31	-0.56	1.48		?		
<i>Osf2-pending</i>	osteoblast specific factor 2	NM015784	7657428	0.000123764	-4.46	0.14	-3.9	0.18	-0.55	1.47				
<i>Col17a1</i>	procollagen type XVII alpha 1	NM007732	6680963	0.001828273	0.65	0.09	1.37	0.27	-0.52	1.43				
<i>Ptkcc</i>	protein kinase C	NM011102	31982442	0.000930095	5.49	0.14	5.95	0.2	-0.46	1.39				
<i>Ptkch</i>	protein kinase C, eta symbol	NM008956	31543510	0.000020964	1.02	0.05	1.47	0.13	-0.45	1.36				
<i>Bk-pending</i>	brain and kidney protein	NM139649	20149721	0.000117374	4.92	0.09	5.35	0.15	-0.44	1.35				
<i>Ptk9l</i>	PTK9L, protein tyrosine kinase 9-like	NM011876	31981351	0.004420696	1.4	0.09	1.82	0.25	-0.42	1.34				
<i>Npdc1</i>	neural proliferation, differentiation and control gene	NM008721	31982835	0.000036599	0.05	0.07	0.46	0.12	-0.41	1.33				
<i>Bmpr1a</i>	bone morphogenetic protein receptor type 1a	NM009758	46519167	0.003942146	0.1	0.13	0.52	0.22	-0.42	1.33				
<i>Pkd1</i>	polycystic kidney disease 1 homolog	NM013630	7305398	0.000077257	0.19	0.09	0.58	0.12	-0.39	1.31				
<i>Tnfrsf11b</i>	tumor necrosis factor (ligand)	NM008764	31543981	0.000525056	3.65	0.15	4.03	0.13	-0.39	1.3				
<i>Mifge8</i>	milk fat globule-EGF factor 8 protein	NM008594	6678669	0.001210953	-1.69	0.14	-1.35	0.14	-0.35	1.27				
<i>Matn3</i>	matrin 3, cartilage matrix protein	NM010770	48976068	0.003725834	0.62	0.13	0.97	0.18	-0.35	1.27				
<i>Bmp7</i>	bone morphogenetic protein type 7	NM007557	31982486	0.004147469	1.58	0.15	1.93	0.18	-0.35	1.27				
<i>Matn2</i>	matrin 2, cartilage matrix protein 2	NM016762	7949075	0.000021505	-0.29	0.06	0.03	0.09	-0.32	1.25				
<i>Ptger4</i>	prostaglandin E receptor 4	NM008965	6679530	0.000059644	3.6	0.11	3.91	0.06	-0.3	1.23				
<i>Notch3</i>	notch gene homolog 3	NM008716	6679095	0.000765094	0.25	0.09	0.54	0.12	-0.28	1.22				
										No. of Genes	11	10	19	5
										Percentage	39%	36%	68%	18%

Figure. 4.15: Gene Expression Profile of *Nell1^{GR}* Mutants Compared with Wild-type Fetuses (E18.5). Genes with significantly reduced expression in mutant mice are listed from highest to lowest fold change. Nine genes (in red text) are affected in both heads and bodies. Majority of the genes that affected by *Nell1^{GR}* mutations encode proteins for the ECM, cell adhesion (Adhn) and cell communication (Comm) during bone and cartilage development.

CHAPTER: 5
CONCLUSION AND FUTURE DIRECTIONS FOR ELUCIDATING
THE ROLE OF *NELL1* IN CRANIOFACIAL AND VERTEBRAL
COLUMN DEVELOPMENT

SUMMARY OF RESULTS AND CONCLUSIONS

A unique neonatal lethal allelic series of mutations for *l7R6* locus in mouse chromosome 7 was recovered from large-scale ENU mutagenesis experiments conducted at Oak Ridge National Laboratory. Transcomplementation analysis with a number of *p* deletions initially mapped *l7R6* to a < 1 cM segment homologous to a region of human chromosome 11p15 (Rinchik et al. 2002). Based on high-resolution mapping, estimation of mutation rate, phenotyping and molecular analysis done in this study, and also based on previously published reports, *Nell1* was tested as a candidate gene for *l7R6* locus. High-throughput mutation scanning and sequencing identified a single base change mutation in the coding region of the *Nell1* gene in the 102DSJ allele (now designated as *Nell1*^{6R}). This ENU-induced nonsense mutation in the *Nell1* gene truncates an 810 amino-acid polypeptide at residue # 510. This is the first *Nell1* loss-of-function mutation reported to date and thus provided for the first time an *in vivo* system to study the consequences of loss-of-function of *Nell1*. The severe reduction of *Nell1* transcripts in *Nell1*^{6R} homozygotes (presumably due to nonsense-mediated decay) results in neonatal lethality, an enlarged skull with thinning at the calvarial bone edges, reduced intervertebral disc spaces, alteration in the vertebral column curvature, abnormal shape and size of the ribcage. The aberrant expression of *Nell1* also leads to decreased expression of specific extracellular matrix proteins that are known to play crucial roles in osteogenesis/chondrogenesis and vertebral column development. The range of skeletal anomalies manifested by *Nell1*^{6R} mutants indicate that the *Nell1* gene plays a key role in both intramembranous and endochondral ossification during early mammalian development. This study demonstrated that *Nell1* is involved in both intramembranous

and endochondral ossification and regulates both osteoblast and chondrocyte differentiation in calvarial bones and vertebral column.

***Nell1* GENE STRUCTURE, WILD-TYPE Vs *Nell1*^{6R}:** Even though the human and rat *NELL1* genes have been well characterized in terms of location and sequence analysis, there was no full-length mouse *Nell1* cDNA available. The only available source was the Celera database but it contained only a partial sequence. Therefore a full-length (2862 bp) cDNA (coding region plus both 5' and 3' untranslated regions) was synthesized and sequenced. The mouse *Nell1* has an open reading frame of 2433 bp, which encodes an 810 amino acid protein, which is highly homologous to human (92%) and rat (97%) *Nell1* protein. The mutation scanning of genomic DNA of *Nell1*^{6R} and sequencing revealed a point mutation in the gene that converts a cysteine codon to a premature termination codon, thereby truncating an 810 amino acid protein at 502nd residue. The mutation at this residue eliminates EGF-like and vWC-like domains. A loss of EGF-like domain may have a profound effect on *Nell1* function. *Nell1* is known to interact and become phosphorylated by specific isoforms of PKC such as PKC- β 1, - δ , and - ζ through EGF-like domains (Kuroda et al. 1999). PKC- β 1 is known to be a key component of cell proliferation and differentiation pathways in many cells including osteoblasts and chondrocytes (Nishizuka 1988; Marie et al. 2002; Rosado et al. 2002; Marie 2003). Additionally, differential expression of PKC isoforms was detected during the 8th week of developmental age in human fetal vertebral column when most of the chondrogenic events are occurring. Thus, mutation in exon 14 may disrupt *Nell1* interaction with PKC- β 1 and interfere with its functions and undermine its role in osteogenesis and chondrogenesis. Furthermore, loss of one of the vWC-like domains due to a mutation may also interfere with trimerization of *Nell1* protein and hence its function.

***Nell1* RNA And Protein Expression:** Expression of the gene in wild-type embryo/fetuses and various adult tissues was assayed by Northern blot. The *Nell1* expression was detected as early as embryonic day 10 and from E14-E18 *Nell1* expression steadily increased in the head and slightly decreased in the bodies of the

fetuses. The increasing expression of *Nell1* coincides with the time when both intramembranous and endochondral ossification occur during mouse embryogenesis. In the skull, the primary ossification centers appear around E13.5 and ossification continues until birth while the endochondral ossification in vertebral column begins around E14.5 and continues till E18 (Kaufman 1999). In contrast to wild-type, due to point mutation in the gene, *Nell1* expression was barely detectable in *Nell1*^{6R} mutant embryos. The severe reduction in the *Nell1* transcript in *Nell1*^{6R} fetuses may be due to nonsense-mediated decay (NMD) of the transcript. In eukaryotes, nonsense mutations like the one observed in *Nell1*^{6R} mice are detected and degraded by the cell via a pathway known as NMD (Nagy et al. 1998; Hillman et al. 2004).

The cell-specific expression of *Nell1* protein was analyzed by immunohistochemistry. The expression of *Nell1* was reduced in mutant fetal vertebral columns compared to wild-type fetuses. In wild-type, *Nell1* was expressed in vertebral bodies but its expression was restricted to the osteoblasts at the surface of the bone. There was no expression detected in the chondrocytes in the vertebral bodies or in the chondrocytes of intervertebral discs. However, one cannot rule out the possibility that it may be expressed by chondrocytes in both vertebral bodies and intervertebral discs but it may be below the detection limit of the assay or it may be expressed during the earlier stages of the development when there is more active cartilage and bone formation taking place in the embryo. The severe reduction in the *Nell1* transcript in *Nell1*^{6R} homozygotes results in neonatal lethality.

PHENOTYPIC CONSEQUENCES OF *Nell1* LOSS OF FUNCTION: The gross morphological analysis revealed decreased body length and enlarged heads in mutants. The skeletal analysis along with MicroCat scans showed overall reduction in the density of the bones, particularly thinning at the edges of the calvarial bones, reduced intervertebral spaces, alteration in the vertebral column curvature and abnormal shape and size of the rib cage in the mutant fetuses. The range of the skeletal anomalies manifested by *Nell1*^{6R} mutation indicate that *Nell1* gene plays a key role in both intramembranous and endochondral ossification during early mammalian development.

In contrast, overexpression of *Nell1* in both human and mouse leads to craniosynostosis (Ting et al. 1999; Zhang et al. 2002). Certain types of CS are associated with limb and spinal defects (Anderson et al. 1996; Anderson et al. 1997). The transgenic mouse overexpressing *Nell1* exhibits CS but no vertebral defects (Zhang et al. 2002). However, reduced expression of *Nell1* in *Nell1*^{6R} mouse is associated with both skull and vertebral column defects. This was the first study to report the involvement of *Nell1* in the development of the vertebral column. It was a novel and an unexpected finding.

***Nell1* IN CELL DIFFERENTIATION PATHWAYS:** The *Nell1* overexpression experiments conducted in both *in vivo* and *in vitro* have clearly shown that *Nell1* promotes differentiation and plays a critical role in osteoblast development (Zhang et al. 2003). The *Nell1* expression accelerated osteoblast differentiation and mineralization along with upregulation of differentiation marker genes like *Opn*, *Ocn*, and *Bmp-7*. Conversely, downregulation of *Nell1* *in vitro* reduced *Ocn* and *Opn* expression and delayed osteoblast differentiation (Zhang et al. 2002) and suggested that reduced levels of *Nell1* would promote osteoblast proliferation in calvarial bones. Additionally, other studies have reported that *Nell1* is involved in endochondral bone formation. *Nell1* accelerates chondrocyte hypertrophy and endochondral bone formation within the distracted maxillary sutures (Cowan et al. 2006) and it also induced premature hypertrophy and increased apoptosis of chondrocytes with subsequent acrania-like deformity (Zhang et al. 2006). The results of this study are consistent with these reports. The reduced expression of *Nell1* in *Nell1*^{6R} leads to decreased differentiation of chondrocytes in the vertebral column and decreased mineralization (as a result of decreased osteoblast differentiation) in both cranial and vertebral bones. The immunohistochemical analysis showed decreased *Col10* expression, a marker for chondrocyte differentiation in vertebral bodies and decreased mineralization in both calvarial and vertebral bones indicating decreased osteoblast differentiation. The histological analysis done on fetal vertebral bodies was consistent with these results. The Masson staining of the vertebral bodies showed that in mutants, cells looked less differentiated and developed compared to wild-type cells. Additionally, the enlarged and

immature bone formation in the cranial vault along with decreased ossification in the vertebral column also demonstrates that the aberrant expression of *Nell1* increases proliferation and decreases differentiation in both osteoblasts and chondrocytes. The *Nell1*-deficient mice exhibit immature and thinner bones compared to wild type. Increased proliferation and decreased differentiation of osteoblasts due to reduced expression *Nell1* accounts for the thinner, less mineralized and enlarged calvarial bones. Only the differentiated osteoblast and chondrocytes secrete ECM proteins (collagen-proteoglycan matrix) that bind calcium salts and become mineralized to produce new bone. However, due to the aberrant expression of *Nell1*, differentiation along with the secretion of ECM and subsequent mineralization process is affected. All the previous *in vitro* studies and transgenic models of *Nell1* have confirmed the role of *Nell1* in craniofacial development and osteoblast biology. However, the broader role of *Nell1* in skeletal development is revealed by the new and the first loss-of-function mouse model *Nell1*^{6R}. In particular, the alteration of spinal curvature, reduction in the intervertebral spaces and decreased bone mineralization in these mutants indicate involvement of *Nell1* in endochondral ossification and differentiation of chondrocytes.

***Nell1* CONTROLS CELL DIFFERENTIATION VIA ECM PATHWAYS:** The gene expression analysis by Real-Time qRT-PCR showed an association between the loss of *Nell1* function and reduced expression of genes for extracellular matrix proteins that are critical for chondrogenesis and osteogenesis. The majority of the genes with reduced expression encode ECM proteins such as specific collagens, thrombospondins, tenascins and matrilins. These proteins provide cell adhesion and communication, and impart strength and flexibility to tissues. This finding was further supported by the histological analysis of the fetal vertebral columns. H and E staining of mutant vertebral bodies showed lesser amount of ECM compared to wild-type. The decreased bone mineralization resulting from the loss of function of *Nell1* gene is also consistent with reduced levels of ECM detected in these mutant mice. The finding that *Nell1* directly or indirectly affects the expression of at least eight genes (*Tnxb*, *Tnc*, *Col12a1*, *Col6a1*, *Matn3*, *Bmpr1a*, *Thbs3*) that are necessary for the development of and/or are specific

constituents of the intervertebral disc matrix and vertebrae (Miller et al. 1991; Roberts et al. 1991; Nerlich et al. 1998; Gruber et al. 2002; Jackson et al. 2004; Yoon et al. 2005) provides additional support for a role for *Nell1* in early vertebral column development. This finding along with the spatio-temporal expression of PKC in vertebral bodies and intervertebral discs in both human and mice at a time when chondrogenesis and osteogenesis are initiated provides additional support for the *Nell1*'s role in the early vertebral column development. It is interesting to note that EDS-associated genes, *Tnxb*, *Col5a1* and *Col5a3* are severely reduced by the *Nell1*^{6R} mutation and one of the EDS subtype syndromes, EDS types V1, manifests spinal curvature. Based on these findings, it can be speculated that *Nell1* mutant mice may model certain forms of EDS.

REGULATORS OF *Nell1*: *NELL1* is regulated by several growth factors and transcription factors. The osteoinductive growth factors like *FGF-2*, BMPs and *TGF- β 1* stimulate *NELL1* (Zhang et al. 2002). The FGFs control bone formation by regulating the expression of various genes involved in osteoprogenitor cell proliferation, osteoblast differentiation and apoptosis via PKC and MAP kinases (ERK and p38 MAP kinases), which in turn regulate transcription factor like *OSF-2/RUNX2* and regulate the expression of target genes like *COL-1*, *IL-6*, *OCN*, *OPN*, *VEGF*, alkaline phosphatase and *NELL1* (Marie 2003; Aghaloo et al. 2006). The BMPs are known to regulate the genes involved in the differentiation of osteoprogenitor cells, endochondral ossification, chondrogenesis and apoptosis (Hay et al. 2001; Marie et al. 2002) and they are known to mediate their action through PKC and *OSF-2/RUNX2* development pathways (Hay et al. 2001; Lee et al. 2002). TGF- β , a potent regulator of osteochondroprogenitor cell migration and proliferation and differentiation of osteoblasts and chondrocytes (Mehrra et al. 2002; Rosado et al. 2002), is known to up regulate PKC and *OSF-2/RUNX2* in both osteoblasts and chondrocytes and mediate some of its biological function through activating MAP kinases via PKC and thereby regulate *OSF-2/RUNX2* and transcription of target genes (Mehrra et al. 2002; Rosado et al. 2002).

Furthermore, the *NELL1* expression is also modulated by transcription factors such as *MSX-2* and *OSF-2/RUNX2*. The *NELL1* promoter contains multiple conserved

MSX-2 and *OSF-2/RUNX2* binding sites (Lu et al. 2007; Truong et al. 2007). *NELL1* is known to bind with and become phosphorylated by specific isoforms of PKC (Kuroda et al. 1999). *NELL1* is also known to regulate the expression of several genes, which are involved in bone development. It is known to up regulate osteoblastic differentiation marker genes like *OPN*, *OCN*, *BSP* and chondrocyte differentiation marker *COL-10* (Zhang et al. 2002; Cowan et al. 2006).

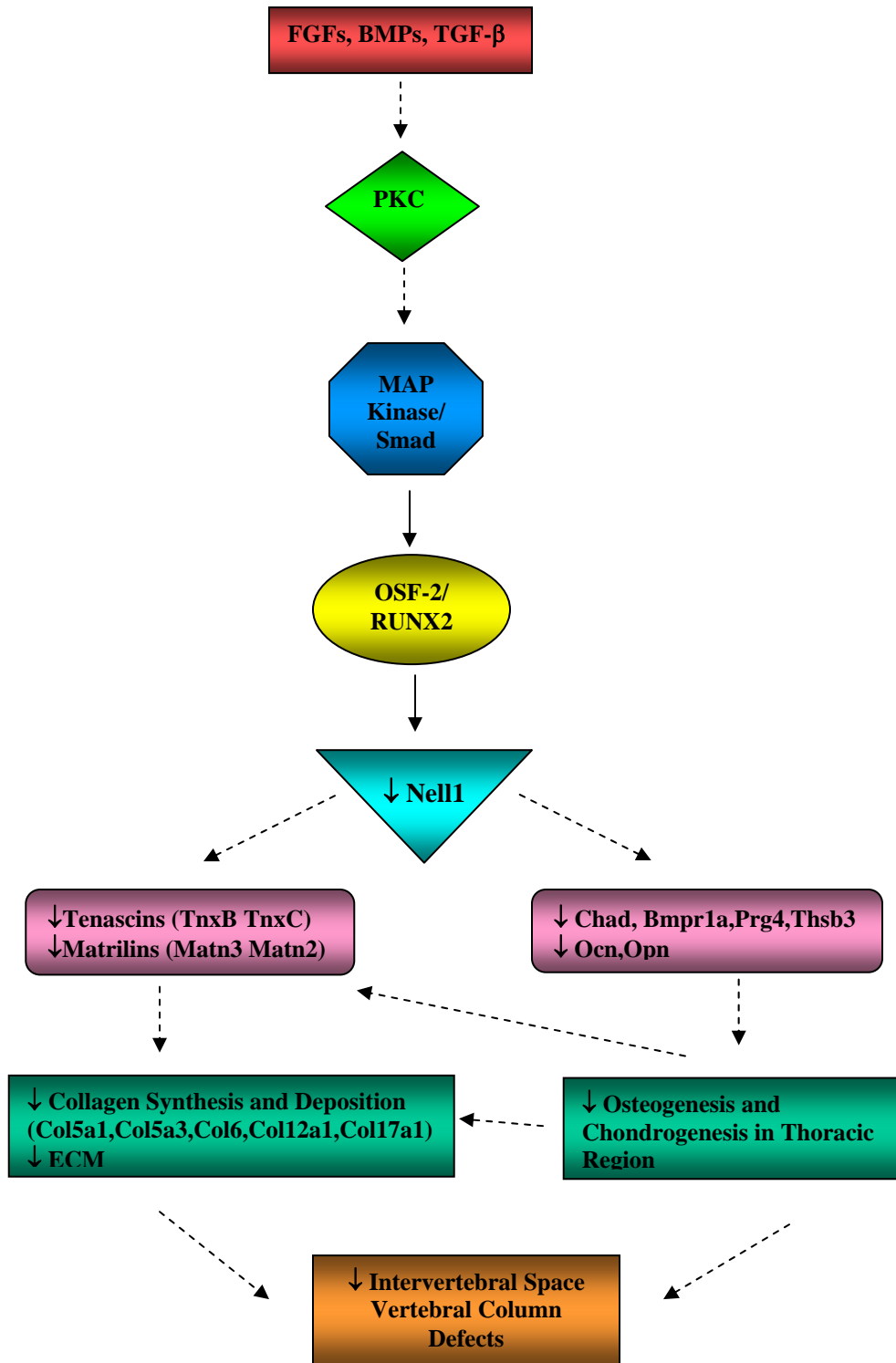
This study indicates that *Nell1* may regulate transcription of several collagenous and non-collagenous ECM proteins. Matrilins are adhesion proteins and form collagenous and non-collagenous filamentous networks (Mates et al. 2004). They are known to be involved in cell adhesion, and spreading (Makihira et al. 1999) They interact with COL-2, -6, and proteoglycans and several studies suggest that they are involved in both intramembranous and endochondral ossification (Winterbottom et al. 1992; Klatt et al. 2000; Wiberg et al. 2003). Tenascins are known to regulate cell migration, differentiation and cell and ECM interactions. TNX binds COL-6 and regulate collagen synthesis (Minamitani et al. 2004). OPN and OCN are associated with maturation and organization of the bone and cartilage ECM and prepare the matrix for mineralization (Stein et al. 1993).

Based on findings that the FGFs, BMPs, and TGF- β upregulate PKC and signal through PKC via *OSF-2/RUNX2* and regulate the genes involved in osteogenesis and chondrogenesis and the association of *NELL1* with certain PKC isoforms and its regulation by *OSF-2/RUNX2*, it is very clear that these growth factors along with the transcription factor *OSF-2/RUNX2* and *NELL*, and its down stream targets like specific collagenous (*Col12a1*, *Col6a1*, *Col5a1* and *Col5a3*, *Col X*) and non-collagenous (matrilins, tenascins, PRG 4, BMPR-1A, OPN, OCN and BSP) proteins play a major role in both intramembranous and endochondral ossification.

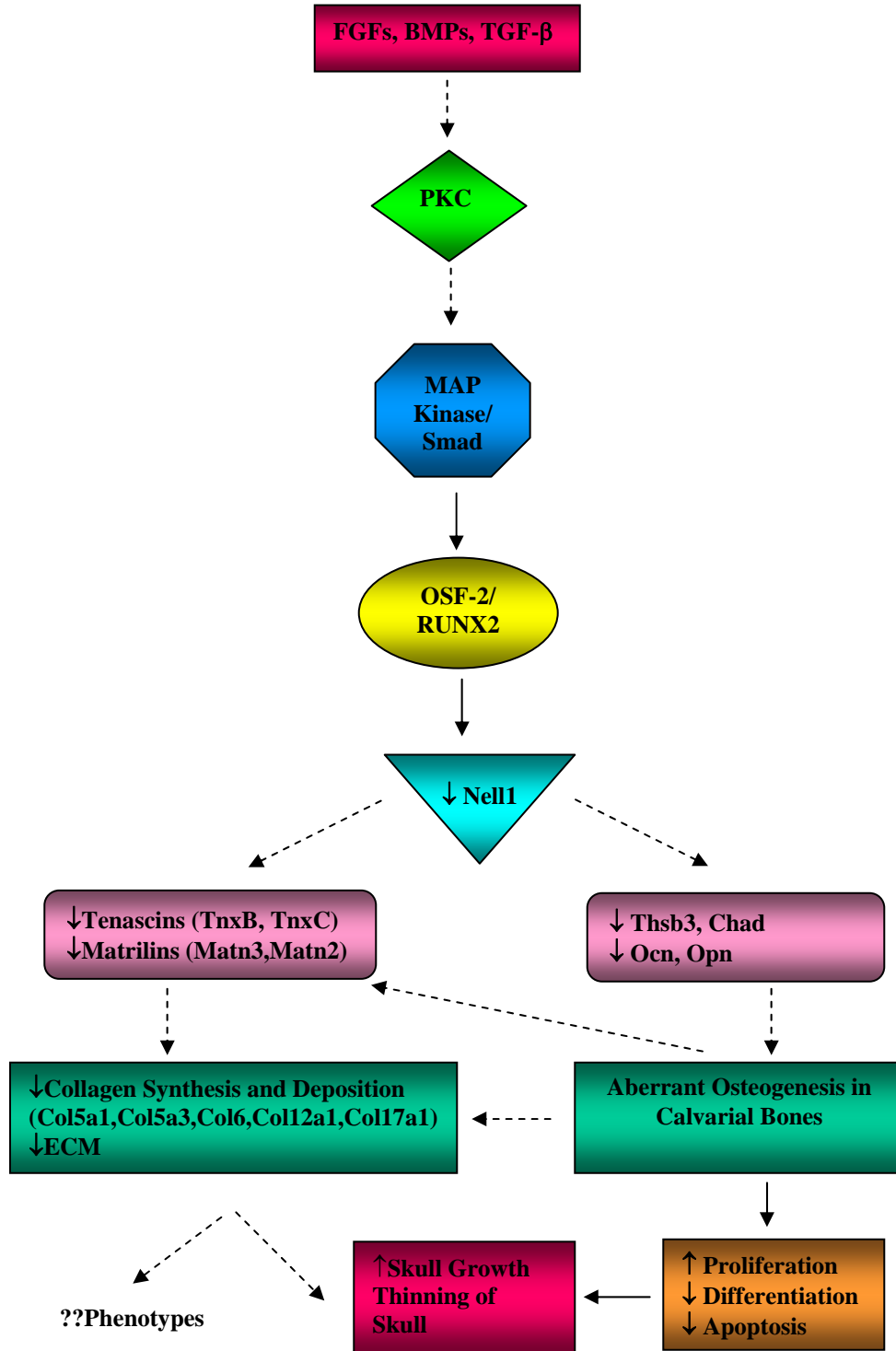
MODEL FOR *Nell1*-MEDIATED PATHWAYS. The Figure.5.1 shows the hypothetical model of *Nell1* signaling and function in both craniofacial and vertebral column development and this was based on the previously published reports and data gathered from this study. Mutation in *Nell1* might disrupt signaling by growth factors via

Figure. 5.1: The Hypothetical Model of *Nell1* Signaling Pathway. In vertebral column (A) and craniofacial (B) development. See text for details. ↓ - Decreased expression, ↑ - Increased, ↓ - Decreased.

A.



B.



PKC during osteogenesis and chondrogenesis (Fig.5.1). During the vertebral column development, reduced expression of *Nell1* may directly or indirectly decrease the expression of ECM proteins like tenascins and matrilins and this in turn may affect the synthesis and deposition of certain collagens (*Col5a1*, *Col5a3*, *Col6*, *Col12a1*, *Col15a1*, and *Col17a1*). The decreased expression of matrilins may disrupt their interaction with collagens and proteoglycans and this in turn may lead to decreased osteoblast / chondrocyte adhesion, spreading, and irregular ossification. Downregulation of tenascins and *Col X* may interfere with collagen synthesis, deposition and chondrocyte differentiation. The decreased expression of matrilins, tenascins and collagens may also lead to decreased ECM production and vertebral defects. Additionally, aberrant expression of *Nell1* may downregulate the differentiation of specific genes like *Chad*, *Prg4*, *Thsb3*, *Opn*, and *Ocn* and this in turn leads to decreased chondrogenesis and osteogenesis in the thoracic region and subsequent vertebral column defects (Fig. 5.1A).

During the craniofacial development, mutation in *Nell1* might lead to reduced expression of matrilins and tenascins and this in turn may lead to reduced synthesis and deposition of specific collagens (*Col5a1*, *Col5a3*, *Col10a1*, and *Col18a1*) which may subsequently lead to decreased ECM production, thinning of the bones and immature bone formation. Furthermore, reduced expression of *Nell1* may downregulate the differentiation of specific genes like *Opn* and *Ocn* with subsequent reduction in osteoblast differentiation and this may in turn also increase the proliferation and decrease apoptosis in osteoblasts. This in turn may lead to reduced ECM deposition by osteoblasts. Thus, the disrupted balance between proliferation, differentiation, and apoptosis along with reduction in ECM may increase skull growth and thinning of the skull bones (Fig. 5.1B).

FUTURE DIRECTIONS AND RECOMMENDATIONS

Despite the fact that understanding of *Nell1* mediated pathways is still in its infancy, the dramatic effect of the protein in bone formation has already led to promising studies that are paving the way for treating human bone disorders. *NELLI* is currently

being tested as a therapeutic agent for bone regeneration. Many craniofacial defects can be corrected with bone grafts or bone regeneration after orthopedic or surgical expansion. Although autografts have been used for a long time, they are limited by availability and injury to the donor site (Sawin et al. 1998). Therefore there is a great demand for osteoinductive therapies that will eliminate the use of autografts. Currently *BMP-2* and *-7* have been approved for human use and have been used successfully to induce bone formation in craniofacial areas of sheep (Abu-Serriah et al. 2003), mice (Matsumoto et al. 2001), and humans (van den Bergh et al. 2000). However, the BMP therapy is associated with adverse effects like ectopic bone formation, local inflammatory reaction and various non-bone specific effects (Valentin-Opran et al. 2002).

NELLI's osteoinductive properties along with its osteo-chondroprogenitor and osteoblast cell specificity and its preferential expression in skeletal tissues makes it a potential candidate for bone regeneration in craniofacial and other skeletal defects. Currently several researchers are using *Nelli* as a therapeutic agent to regenerate bone in animal models. *Nelli* was able to induce bone formation in calvarial defects in a mouse model (Aghaloo et al. 2006) and in distracted intermaxillary suture in a rat model (Cowan et al. 2006). Additionally, *Nelli* was successfully used to induce spinal fusion in rats (Lu et al. 2007). In all these animal models, *Nelli*'s osteoinductive effects were compared to *Bmp-2* and *-7* and data gathered from these studies show that *Nelli* is as potent as BMPs in inducing bone formation and exerts its effects more specifically in skeletal tissues than BMPs.

Even though in the past few years great progress has been made in delineating *Nelli* function and its mode of action, the pathway(s) utilized by *Nelli* and the other players involved in osteogenesis and chondrogenesis still largely remain unclear. The immediate upstream regulators as well as downstream targets of *Nelli* still need to be identified. In this study, impact of the loss-of-function of *Nelli* on the selected genes was examined. However, only 219 genes were assayed and there may be other genes (involved in osteoblast proliferation/differentiation, survival and signaling) that are involved in vertebral column development and are affected by aberrant expression of

Nell1. With whole genome microarray analysis many new genes, which play critical roles in endochondral ossification can be identified.

During the vertebral skeleton development, *Nell1* may mediate its actions through interacting with and regulating other genes which are critical for osteogenesis and chondrogenesis including growth factors, cytokines, extracellular matrix proteins, transcriptions factors, and genes that are involved in proliferation, differentiation and death /survival in osteoblasts and chondrocytes.

In recent years, DNA microarrays have enabled researchers to examine the consequences of loss of function of a particular gene on other genes in the entire genome. Data gathered from these experiments may aid in finding novel interactions of *Nell1* with other genes or its association with certain biological pathway (s). By identifying the genes, which are differentially regulated by loss of function of *Nell1*, we may be able to determine if *Nell1* operates upstream or downstream of these genes or which genes in osteoblast/chondrocyte growth, differentiation and death are affected. By finding the genes that are associated with, co-regulated with or regulated by *Nell1*, we may be able to better understand its role in both intramembranous and endochondral ossification. Taken as a whole, the data generated by these experiments will lead to a better understanding of the role of *Nell1* in general, consequences of its mutation and its underlying mechanisms of action in the developing vertebral skeleton. This information may also help make *Nell1* a better therapeutic agent in terms of specificity and efficacy in treating skeletal defects.

This study began with the characterization of the five mutant alleles (88SJ, 335SJ, 2038SJ and 11DSJ) of *Nell1* along with *Nell1*^{6R} (102DSJ). However, after initial phenotyping, expression and skeletal analysis, only *Nell1*^{6R} was chosen for further characterization, because *Nell1*^{6R} mice exhibited severe skeletal defects and dramatically reduced *Nell* expression levels compared to other mutant alleles. One of the other alleles, *Nell1*^{1R} (88SJ) also showed severe skeletal defects and attempts to find a mutation in that allele as well as other mutant alleles was not met with success. Mutation scanning was done on all the 20 exons and only on their flanking intron sequences (~ 40 bp upstream and downstream of each exons, where ENU is likely to induce point mutations). The mutation 88SJ and other alleles may be deep inside the intron sequences. By fully

sequencing *Nell1* genomic DNA (all the exons along with intron sequences) we may be able to identify mutation in these other alleles and see the other functional consequences of *Nell1* mutation and this may lead to a better understanding of the *Nell1* function in osteogenesis / chondrogenesis and possibly its role in other organ systems. By characterizing other alleles, we may be able to elucidate the full range of *Nell1* functions in skeletal as well as in other systems and identify other yet unknown functions of *Nell1* or defects in other organs/systems due to its mutation during the mouse development.

Mutation in *Nell1* leads to neonatal lethality, making it difficult to study its functions in the skeletal as well as other systems. To understand the role of *Nell1* in vertebral column development, conditional knockout mice can be created by using lox P and by tissue specific expression of Cre recombinase. By selectively knocking out *Nell1* in vertebral column, deleterious effects of *Nell1* mutation on survival of mice can be avoided. Mice will be born alive and are allowed to develop and thus the effect of *Nell1* in vertebral column can be studied.

Nell1 mediated signaling pathway(s) in both intramembranous and endochondral ossification can be further elucidated by conducting *in vitro* studies. The osteoblasts /chondrocytes can be isolated from the calvarial bones and vertebral column and treated with osteogenic factors like FGFs and BMPs. Upregulation of *Nell1* and activation of MAP kinases (ERK/p38/JNK) pathways can be detected by Western blot analysis.

LIST OF REFERENCES

LIST OF REFERENCES

- Abu-Serriah, M., A. Ayoub, J. Boyd, C. Paterson and D. Wray** (2003). "The role of ultrasound in monitoring reconstruction of mandibular continuity defects using osteogenic protein-1 (rhOP-1)." *Int J Oral Maxillofac Surg* 32(6): 619-27.
- Adams, J. and J. Lawler** (1993). "Extracellular matrix: the thrombospondin family." *Curr Biol* 3(3): 188-90.
- Aghaloo, T., C. M. Cowan, Y. F. Chou, X. Zhang, H. Lee, S. Miao, N. Hong, S. Kuroda, B. Wu, K. Ting and C. Soo** (2006). "Nell-1-induced bone regeneration in calvarial defects." *Am J Pathol* 169(3): 903-15.
- Ahrens, M., T. Ankenbauer, D. Schroder, A. Hollnagel, H. Mayer and G. Gross** (1993). "Expression of human bone morphogenetic proteins-2 or -4 in murine mesenchymal progenitor C3H10T1/2 cells induces differentiation into distinct mesenchymal cell lineages." *DNA Cell Biol* 12(10): 871-80.
- Alberts, B., Bray, D., Lewis, J., Raff, M., Roberts, K. and Watson, J.** (1994). *Molecular Biology Of THE CELL*, Garland Publishing, Inc. New York & London.
- Altschul, S. F., W. Gish, W. Miller, E. W. Myers and D. J. Lipman** (1990). "Basic local alignment search tool." *J Mol Biol* 215(3): 403-10.
- Anderson, P. J., C. M. Hall, R. D. Evans, R. D. Hayward, W. J. Harkness and B. M. Jones** (1997). "The cervical spine in Saethre-Chotzen syndrome." *Cleft Palate Craniofac J* 34(1): 79-82.
- Anderson, P. J., C. M. Hall, R. D. Evans, B. M. Jones, W. Harkness and R. D. Hayward** (1996). "Cervical spine in Pfeiffer's syndrome." *J Craniofac Surg* 7(4): 275-9.
- Angier** (1994). *New York Times*.
- Applied, B.** (2001). *Relative Quantitation of Gene Expression. User Bulletin 2.*
- Bandyopadhyay, A., Tsuji, K., Cox, K., Harfe, B.D., Rosen, V. and Tabin, C.J.** (2006). "Genetic Analysis of the Roles of BMP2, BMP4, and BMP7 in Limb Patterning and Skeletogenesis." *PLoS Genetics* 2(12): 2116.
- Bareggi, R., A. M. Martelli, V. Grill, M. A. Sandrucci, M. Zweyer and P. Narducci** (1995). "Protein kinase C (PKC) isoenzymes exhibit specific expression in the vertebral column of human fetuses." *Boll Soc Ital Biol Sper* 71(3-4): 83-90.
- Barry, F., R. E. Boynton, B. Liu and J. M. Murphy** (2001). "Chondrogenic differentiation of mesenchymal stem cells from bone marrow: differentiation-dependent gene expression of matrix components." *Exp Cell Res* 268(2): 189-200.
- Baur, S. T., J. J. Mai and S. M. Dymecki** (2000). "Combinatorial signaling through BMP receptor IB and GDF5: shaping of the distal mouse limb and the genetics of distal limb diversity." *Development* 127(3): 605-19.
- Beighton, P., A. De Paepe, B. Steinmann, P. Tsipouras and R. J. Wenstrup** (1998). "Ehlers-Danlos syndromes: revised nosology, Villefranche, 1997. Ehlers-Danlos National Foundation (USA) and Ehlers-Danlos Support Group (UK)." *Am J Med Genet* 77(1): 31-7.

- Bendall, A. J. and C. Abate-Shen** (2000). "Roles for Msx and Dlx homeoproteins in vertebrate development." *Gene* 247(1-2): 17-31.
- Bidanset, D. J., C. Guidry, L. C. Rosenberg, H. U. Choi, R. Timpl and M. Hook** (1992). "Binding of the proteoglycan decorin to collagen type VI." *J Biol Chem* 267(8): 5250-6.
- Bornstein, P.** (1992). "Thrombospondins: structure and regulation of expression." *Faseb J* 6(14): 3290-9.
- Bornstein, P. and E. H. Sage** (1994). "Thrombospondins." *Methods Enzymol* 245: 62-85.
- Bristow, J., W. Carey, D. Egging and J. Schalkwijk** (2005). "Tenascin-X, collagen, elastin, and the Ehlers-Danlos syndrome." *Am J Med Genet C Semin Med Genet* 139(1): 24-30.
- Bristow, J., M. K. Tee, S. E. Gitelman, S. H. Mellon and W. L. Miller** (1993). "Tenascin-X: a novel extracellular matrix protein encoded by the human XB gene overlapping P450c21B." *J Cell Biol* 122(1): 265-78.
- Burch, G. H., Y. Gong, W. Liu, R. W. Dettman, C. J. Curry, L. Smith, W. L. Miller and J. Bristow** (1997). "Tenascin-X deficiency is associated with Ehlers-Danlos syndrome." *Nat Genet* 17(1): 104-8.
- Carson, F. L.** (1990). *Histotechnology*, American Society of Clinical Pathologists Press, Chicago, USA.
- Carver, E. A., K. F. Oram and T. Gridley** (2002). "Craniosynostosis in Twist heterozygous mice: a model for Saethre-Chotzen syndrome." *Anat Rec* 268(2): 90-2.
- Chapman, K. L., G. R. Mortier, K. Chapman, J. Loughlin, M. E. Grant and M. D. Briggs** (2001). "Mutations in the region encoding the von Willebrand factor A domain of matrilin-3 are associated with multiple epiphyseal dysplasia." *Nat Genet* 28(4): 393-6.
- Chen, C. Y. and A. B. Shyu** (2003). "Rapid deadenylation triggered by a nonsense codon precedes decay of the RNA body in a mammalian cytoplasmic nonsense-mediated decay pathway." *Mol Cell Biol* 23(14): 4805-13.
- Chiquet-Ehrismann, R.** (1991). "Anti-adhesive molecules of the extracellular matrix." *Curr Opin Cell Biol* 3(5): 800-4.
- Chiquet, M. and B. Wehrle-Haller** (1994). "Tenascin-C in peripheral nerve morphogenesis." *Perspect Dev Neurobiol* 2(1): 67-74.
- Christ, B., C. Schmidt, R. Huang, J. Wilting and B. Brand-Saberi** (1998). "Segmentation of the vertebrate body." *Anat Embryol (Berl)* 197(1): 1-8.
- Cohen, M. M., Jr.** (1993). "Sutural biology and the correlates of craniosynostosis." *Am J Med Genet* 47(5): 581-616.
- Cohen, M. M., Jr.** (2006). "The new bone biology: pathologic, molecular, and clinical correlates." *Am J Med Genet A* 140(23): 2646-706.
- Cohen, M. M. a. M., R. E.** (2000). *Diagnosis, Evaluation, and Management.*, Oxford University Press, New York.
- Cowan, C. M., S. Cheng, K. Ting, C. Soo, B. Walder, B. Wu, S. Kuroda and X. Zhang** (2006). "Nell-1 induced bone formation within the distracted intermaxillary suture." *Bone* 38(1): 48-58.

- Cundy, T., M. Hegde, D. Naot, B. Chong, A. King, R. Wallace, J. Mulley, D. R. Love, J. Seidel, M. Fawkner, T. Banovic, K. E. Callon, A. B. Grey, I. R. Reid, C. A. Middleton-Hardie and J. Cornish** (2002). "A mutation in the gene TNFRSF11B encoding osteoprotegerin causes an idiopathic hyperphosphatasia phenotype." *Hum Mol Genet* 11(18): 2119-27.
- De Pollack, C., D. Renier, M. Hott and P. J. Marie** (1996). "Increased bone formation and osteoblastic cell phenotype in premature cranial suture ossification (craniosynostosis)." *J Bone Miner Res* 11(3): 401-7.
- Deak, F., R. Wagener, I. Kiss and M. Paulsson** (1999). "The matrilins: a novel family of oligomeric extracellular matrix proteins." *Matrix Biol* 18(1): 55-64.
- Deng, G., S. A. Curriden, G. Hu, R. P. Czekay and D. J. Loskutoff** (2001). "Plasminogen activator inhibitor-1 regulates cell adhesion by binding to the somatomedin B domain of vitronectin." *J Cell Physiol* 189(1): 23-33.
- Desai, J., M. E. Shannon, M. D. Johnson, D. W. Ruff, L. A. Hughes, M. K. Kerley, D. A. Carpenter, D. K. Johnson, E. M. Rinchik and C. T. Culiati** (2006). "Nell1-deficient mice have reduced expression of extracellular matrix proteins causing cranial and vertebral defects." *Hum Mol Genet* 15(8): 1329-41.
- Dewulf, N., K. Verschueren, O. Lonnoy, A. Moren, S. Grimsby, K. Vande Spiegle, K. Miyazono, D. Huylebroeck and P. Ten Dijke** (1995). "Distinct spatial and temporal expression patterns of two type I receptors for bone morphogenetic proteins during mouse embryogenesis." *Endocrinology* 136(6): 2652-63.
- Diaz, L. A., H. Ratrie, 3rd, W. S. Saunders, S. Futamura, H. L. Squiquera, G. J. Anhalt and G. J. Giudice** (1990). "Isolation of a human epidermal cDNA corresponding to the 180-kD autoantigen recognized by bullous pemphigoid and herpes gestationis sera. Immunolocalization of this protein to the hemidesmosome." *J Clin Invest* 86(4): 1088-94.
- Dodig, M., T. Tadic, M. S. Kronenberg, S. Dacic, Y. H. Liu, R. Maxson, D. W. Rowe and A. C. Lichtler** (1999). "Ectopic Msx2 overexpression inhibits and Msx2 antisense stimulates calvarial osteoblast differentiation." *Dev Biol* 209(2): 298-307.
- Dolan, K., J. Garde, J. Gosney, M. Sissons, T. Wright, A. N. Kingsnorth, S. J. Walker, R. Sutton, S. J. Meltzer and J. K. Field** (1998). "Allelotype analysis of oesophageal adenocarcinoma: loss of heterozygosity occurs at multiple sites." *Br J Cancer* 78(7): 950-7.
- Ducy, P.** (2000). "Cbfa1: a molecular switch in osteoblast biology." *Dev Dyn* 219(4): 461-71.
- Ducy, P. and G. Karsenty** (1998). "Genetic control of cell differentiation in the skeleton." *Curr Opin Cell Biol* 10(5): 614-9.
- Ducy, P., M. Starbuck, M. Priemel, J. Shen, G. Pinero, V. Geoffroy, M. Amling and G. Karsenty** (1999). "A Cbfa1-dependent genetic pathway controls bone formation beyond embryonic development." *Genes Dev* 13(8): 1025-36.
- Duprez, D., E. J. Bell, M. K. Richardson, C. W. Archer, L. Wolpert, P. M. Brickell and P. H. Francis-West** (1996). "Overexpression of BMP-2 and BMP-4 alters the size and shape of developing skeletal elements in the chick limb." *Mech Dev* 57(2): 145-57.

- Egging, D., F. van den Berkmortel, G. Taylor, J. Bristow and J. Schalkwijk** (2007). "Interactions of human tenascin-X domains with dermal extracellular matrix molecules." *Arch Dermatol Res* 298(8): 389-96.
- Eklund, L., J. Piuhola, J. Komulainen, R. Sormunen, C. Ongvarrasopone, R. Fassler, A. Muona, M. Ilves, H. Ruskoaho, T. E. Takala and T. Pihlajaniemi** (2001). "Lack of type XV collagen causes a skeletal myopathy and cardiovascular defects in mice." *Proc Natl Acad Sci U S A* 98(3): 1194-9.
- Elefteriou, F., J. Y. Exposito, R. Garrone and C. Lethias** (2001). "Binding of tenascin-X to decorin." *FEBS Lett* 495(1-2): 44-7.
- Enomoto, H., M. Enomoto-Iwamoto, M. Iwamoto, S. Nomura, M. Himeno, Y. Kitamura, T. Kishimoto and T. Komori** (2000). "Cbfa1 is a positive regulatory factor in chondrocyte maturation." *J Biol Chem* 275(12): 8695-702.
- Erlebacher, A., E. H. Filvaroff, S. E. Gitelman and R. Derynck** (1995). "Toward a molecular understanding of skeletal development." *Cell* 80(3): 371-8.
- Fawcett, D.** (1994). *A Text Book of Histology*, Chapman & Hall, New York & London.
- Foerst-Potts, L. and T. W. Sadler** (1997). "Disruption of Msx-1 and Msx-2 reveals roles for these genes in craniofacial, eye, and axial development." *Dev Dyn* 209(1): 70-84.
- Frazier, W. A.** (1991). "Thrombospondins." *Curr Opin Cell Biol* 3(5): 792-9.
- Gatalica, B., L. Pulkkinen, K. Li, K. Kuokkanen, M. Ryyanen, J. A. McGrath and J. Uitto** (1997). "Cloning of the human type XVII collagen gene (COL17A1), and detection of novel mutations in generalized atrophic benign epidermolysis bullosa." *Am J Hum Genet* 60(2): 352-65.
- Gatfield, D. and E. Izaurralde** (2004). "Nonsense-mediated messenger RNA decay is initiated by endonucleolytic cleavage in *Drosophila*." *Nature* 429(6991): 575-8.
- Geffroin, C., J. J. Garrido, L. Tremet and M. Vaiman** (1995). "Distinct tissue distribution in pigs of tenascin-X and tenascin-C transcripts." *Eur J Biochem* 231(1): 83-92.
- Geoffroy, V., M. Kneissel, B. Fournier, A. Boyde and P. Matthias** (2002). "High bone resorption in adult aging transgenic mice overexpressing cbfa1/runx2 in cells of the osteoblastic lineage." *Mol Cell Biol* 22(17): 6222-33.
- Giampietro, P. F., R. D. Blank, C. L. Raggio, S. Merchant, F. S. Jacobsen, T. Faciszewski, S. K. Shukla, A. R. Greenlee, C. Reynolds and D. B. Schowalter** (2003). "Congenital and idiopathic scoliosis: clinical and genetic aspects." *Clin Med Res* 1(2): 125-36.
- Gillison, M.** (1962). *Histology of the Body Tissues*, E & S Livingston Ltd.
- Gori, F., T. Thomas, K. C. Hicok, T. C. Spelsberg and B. L. Riggs** (1999). "Differentiation of human marrow stromal precursor cells: bone morphogenetic protein-2 increases OSF2/CBFA1, enhances osteoblast commitment, and inhibits late adipocyte maturation." *J Bone Miner Res* 14(9): 1522-35.
- Gruber, H. E., J. A. Ingram and E. N. Hanley, Jr.** (2002). "Tenascin in the human intervertebral disc: alterations with aging and disc degeneration." *Biotech Histochem* 77(1): 37-41.
- Gruber, H. E., J. A. Ingram and E. N. Hanley, Jr.** (2006). "Immunolocalization of thrombospondin in the human and sand rat intervertebral disc." *Spine* 31(22): 2556-61.

- Gulcher, J. R., D. E. Nies, M. J. Alexakos, N. A. Ravikant, M. E. Sturgill, L. S. Marton and K. Stefansson** (1991). "Structure of the human hexabrachion (tenascin) gene." *Proc Natl Acad Sci U S A* 88(21): 9438-42.
- Hagg, P. M., N. Horelli-Kuitunen, L. Eklund, A. Palotie and T. Pihlajaniemi** (1997). "Cloning of mouse type XV collagen sequences and mapping of the corresponding gene to 4B1-3. Comparison of mouse and human alpha 1 (XV) collagen sequences indicates divergence in the number of small collagenous domains." *Genomics* 45(1): 31-41.
- Hall, B. K. and T. Miyake** (1995). "Divide, accumulate, differentiate: cell condensation in skeletal development revisited." *Int J Dev Biol* 39(6): 881-93.
- Hall, B. K. and T. Miyake** (2000). "All for one and one for all: condensations and the initiation of skeletal development." *Bioessays* 22(2): 138-47.
- Hankenson, K. D., S. G. Hormuzdi, J. A. Meganck and P. Bornstein** (2005). "Mice with a disruption of the thrombospondin 3 gene differ in geometric and biomechanical properties of bone and have accelerated development of the femoral head." *Mol Cell Biol* 25(13): 5599-606.
- Hauser, N., M. Paulsson, D. Heinegard and M. Morgelin** (1996). "Interaction of cartilage matrix protein with aggrecan. Increased covalent cross-linking with tissue maturation." *J Biol Chem* 271(50): 32247-52.
- Hay, E., J. Lemonnier, O. Fromigue and P. J. Marie** (2001). "Bone morphogenetic protein-2 promotes osteoblast apoptosis through a Smad-independent, protein kinase C-dependent signaling pathway." *J Biol Chem* 276(31): 29028-36.
- Helminen, H. J., K. Kiraly, A. Peltari, M. I. Tammi, P. Vandenberg, R. Pereira, R. Dhulipala, J. S. Khillan, L. Ala-Kokko, E. L. Hume and et al.** (1993). "An inbred line of transgenic mice expressing an internally deleted gene for type II procollagen (COL2A1). Young mice have a variable phenotype of a chondrodysplasia and older mice have osteoarthritic changes in joints." *J Clin Invest* 92(2): 582-95.
- Herman, J. G. and S. B. Baylin** (2003). "Gene silencing in cancer in association with promoter hypermethylation." *N Engl J Med* 349(21): 2042-54.
- Herron, B. J., W. Lu, C. Rao, S. Liu, H. Peters, R. T. Bronson, M. J. Justice, J. D. McDonald and D. R. Beier** (2002). "Efficient generation and mapping of recessive developmental mutations using ENU mutagenesis." *Nat Genet* 30(2): 185-9.
- Hillman, R. T., R. E. Green and S. E. Brenner** (2004). "An unappreciated role for RNA surveillance." *Genome Biol* 5(2): R8.
- Hoffman, S., K. L. Crossin and G. M. Edelman** (1988). "Molecular forms, binding functions, and developmental expression patterns of cytotactin and cytotactin-binding proteoglycan, an interactive pair of extracellular matrix molecules." *J Cell Biol* 106(2): 519-32.
- Hogan, B., Beddington, R., Constantini, F. and Lacy, E.** (1994). *Manipulating the Mouse Embryo: A Laboratory Manual.* , Cold Spring Harbor Laboratory Press, New York.
- Hotten, G. C., T. Matsumoto, M. Kimura, R. F. Bechtold, R. Kron, T. Ohara, H. Tanaka, Y. Satoh, M. Okazaki, T. Shirai, H. Pan, S. Kawai, J. S. Pohl and A. Kudo** (1996). "Recombinant human growth/differentiation factor 5 stimulates

- mesenchyme aggregation and chondrogenesis responsible for the skeletal development of limbs." *Growth Factors* 13(1-2): 65-74.
- Howard, T. D., W. A. Paznekas, E. D. Green, L. C. Chiang, N. Ma, R. I. Ortiz de Luna, C. Garcia Delgado, M. Gonzalez-Ramos, A. D. Kline and E. W. Jabs** (1997). "Mutations in TWIST, a basic helix-loop-helix transcription factor, in Saethre-Chotzen syndrome." *Nat Genet* 15(1): 36-41.
- Hsia, H. C. and J. E. Schwarzbauer** (2005). "Meet the tenascins: multifunctional and mysterious." *J Biol Chem* 280(29): 26641-4.
- Hug, H. and T. F. Sarre** (1993). "Protein kinase C isoenzymes: divergence in signal transduction?" *Biochem J* 291 (Pt 2): 329-43.
- Humzah, M. D. and R. W. Soames** (1988). "Human intervertebral disc: structure and function." *Anat Rec* 220(4): 337-56.
- Ikegawa, S., M. Sano, Y. Koshizuka and Y. Nakamura** (2000). "Isolation, characterization and mapping of the mouse and human PRG4 (proteoglycan 4) genes." *Cytogenet Cell Genet* 90(3-4): 291-7.
- Imamura, Y., I. C. Scott and D. S. Greenspan** (2000). "The pro-alpha3(V) collagen chain. Complete primary structure, expression domains in adult and developing tissues, and comparison to the structures and expression domains of the other types V and XI procollagen chains." *J Biol Chem* 275(12): 8749-59.
- Imanaka-Yoshida, K., K. Matsumoto, M. Hara, T. Sakakura and T. Yoshida** (2003). "The dynamic expression of tenascin-C and tenascin-X during early heart development in the mouse." *Differentiation* 71(4-5): 291-8.
- Inada, M., T. Yasui, S. Nomura, S. Miyake, K. Deguchi, M. Himeno, M. Sato, H. Yamagiwa, T. Kimura, N. Yasui, T. Ochi, N. Endo, Y. Kitamura, T. Kishimoto and T. Komori** (1999). "Maturation disturbance of chondrocytes in Cbfa1-deficient mice." *Dev Dyn* 214(4): 279-90.
- Jackson, G. C., F. S. Barker, E. Jakkula, M. Czarny-Ratajczak, O. Makitie, W. G. Cole, M. J. Wright, S. F. Smithson, M. Suri, P. Rogala, G. R. Mortier, C. Baldock, A. Wallace, R. Elles, L. Ala-Kokko and M. D. Briggs** (2004). "Missense mutations in the beta strands of the single A-domain of matrilin-3 result in multiple epiphyseal dysplasia." *J Med Genet* 41(1): 52-9.
- Jay, G. D.** (1992). "Characterization of a bovine synovial fluid lubricating factor. I. Chemical, surface activity and lubricating properties." *Connect Tissue Res* 28(1-2): 71-88.
- Jena, N., C. Martin-Seisdedos, P. McCue and C. M. Croce** (1997). "BMP7 null mutation in mice: developmental defects in skeleton, kidney, and eye." *Exp Cell Res* 230(1): 28-37.
- Jiang, X., S. Iseki, R. E. Maxson, H. M. Sucov and G. M. Morriss-Kay** (2002). "Tissue origins and interactions in the mammalian skull vault." *Dev Biol* 241(1): 106-16.
- Jin, Z., Y. Mori, J. Yang, F. Sato, T. Ito, Y. Cheng, B. Paun, J. P. Hamilton, T. Kan, A. Olaru, S. David, R. Agarwal, J. M. Abraham, D. Beer, E. Montgomery and S. J. Meltzer** (2007). "Hypermethylation of the nel-like 1 gene is a common and early event and is associated with poor prognosis in early-stage esophageal adenocarcinoma." *Oncogene*.

- Johnson, D. K., L. J. Stubbs, C. T. Culiati, C. S. Montgomery, L. B. Russell and E. M. Rinchik** (1995). "Molecular analysis of 36 mutations at the mouse pink-eyed dilution (p) locus." *Genetics* 141(4): 1563-71.
- Justice, M. J., J. K. Noveroske, J. S. Weber, B. Zheng and A. Bradley** (1999). "Mouse ENU mutagenesis." *Hum Mol Genet* 8(10): 1955-63.
- Karsenty, G.** (2001). "Minireview: transcriptional control of osteoblast differentiation." *Endocrinology* 142(7): 2731-3.
- Kaufman, M. H. a. B., J. B. L.** (1999). *The Anatomical Basis of Mouse Development*, Academic Press.
- Kielty, C. M., S. P. Whittaker, M. E. Grant and C. A. Shuttleworth** (1992). "Type VI collagen microfibrils: evidence for a structural association with hyaluronan." *J Cell Biol* 118(4): 979-90.
- Kivirikko, K. I.** (1993). "Collagens and their abnormalities in a wide spectrum of diseases." *Ann Med* 25(2): 113-26.
- Klatt, A. R., D. P. Nitsche, B. Kobbe, M. Morgelin, M. Paulsson and R. Wagener** (2000). "Molecular structure and tissue distribution of matrilin-3, a filament-forming extracellular matrix protein expressed during skeletal development." *J Biol Chem* 275(6): 3999-4006.
- Klatt, A. R., M. Paulsson and R. Wagener** (2002). "Expression of matrilins during maturation of mouse skeletal tissues." *Matrix Biol* 21(3): 289-96.
- Knudson, A. G.** (2001). "Two genetic hits (more or less) to cancer." *Nat Rev Cancer* 1(2): 157-62.
- Ko, Y., B. Kobbe, C. Nicolae, N. Miosge, M. Paulsson, R. Wagener and A. Aszodi** (2004). "Matrilin-3 is dispensable for mouse skeletal growth and development." *Mol Cell Biol* 24(4): 1691-9.
- Kobayashi, T., K. M. Lyons, A. P. McMahon and H. M. Kronenberg** (2005). "BMP signaling stimulates cellular differentiation at multiple steps during cartilage development." *Proc Natl Acad Sci U S A* 102(50): 18023-7.
- Komori, T.** (2002). "Runx2, a multifunctional transcription factor in skeletal development." *J Cell Biochem* 87(1): 1-8.
- Komori, T., H. Yagi, S. Nomura, A. Yamaguchi, K. Sasaki, K. Deguchi, Y. Shimizu, R. T. Bronson, Y. H. Gao, M. Inada, M. Sato, R. Okamoto, Y. Kitamura, S. Yoshiki and T. Kishimoto** (1997). "Targeted disruption of *Cbfa1* results in a complete lack of bone formation owing to maturational arrest of osteoblasts." *Cell* 89(5): 755-64.
- Kuivaniemi, H., G. Tromp and D. J. Prockop** (1997). "Mutations in fibrillar collagens (types I, II, III, and XI), fibril-associated collagen (type IX), and network-forming collagen (type X) cause a spectrum of diseases of bone, cartilage, and blood vessels." *Hum Mutat* 9(4): 300-15.
- Kuroda, S., M. Oyasu, M. Kawakami, N. Kanayama, K. Tanizawa, N. Saito, T. Abe, S. Matsubashi and K. Ting** (1999). "Biochemical characterization and expression analysis of neural thrombospondin-1-like proteins NELL1 and NELL2." *Biochem Biophys Res Commun* 265(1): 79-86.
- Kuroda, S. and K. Tanizawa** (1999). "Involvement of epidermal growth factor-like domain of NELL proteins in the novel protein-protein interaction with protein kinase C." *Biochem Biophys Res Commun* 265(3): 752-7.

- Kwan, K. M., M. K. Pang, S. Zhou, S. K. Cowan, R. Y. Kong, T. Pfordte, B. R. Olsen, D. O. Sillence, P. P. Tam and K. S. Cheah** (1997). "Abnormal compartmentalization of cartilage matrix components in mice lacking collagen X: implications for function." *J Cell Biol* 136(2): 459-71.
- Lajeunie, E., H. W. Ma, J. Bonaventure, A. Munnich, M. Le Merrer and D. Renier** (1995). "FGFR2 mutations in Pfeiffer syndrome." *Nat Genet* 9(2): 108.
- Leboy, P., G. Grasso-Knight, M. D'Angelo, S. W. Volk, J. V. Lian, H. Drissi, G. S. Stein and S. L. Adams** (2001). "Smad-Runx interactions during chondrocyte maturation." *J Bone Joint Surg Am* 83-A Suppl 1(Pt 1): S15-22.
- Lee, B., K. Thirunavukkarasu, L. Zhou, L. Pastore, A. Baldini, J. Hecht, V. Geoffroy, P. Ducy and G. Karsenty** (1997). "Missense mutations abolishing DNA binding of the osteoblast-specific transcription factor OSF2/CBFA1 in cleidocranial dysplasia." *Nat Genet* 16(3): 307-10.
- Lee, K. S., S. H. Hong and S. C. Bae** (2002). "Both the Smad and p38 MAPK pathways play a crucial role in Runx2 expression following induction by transforming growth factor-beta and bone morphogenetic protein." *Oncogene* 21(47): 7156-63.
- Lee, K. S., H. J. Kim, Q. L. Li, X. Z. Chi, C. Ueta, T. Komori, J. M. Wozney, E. G. Kim, J. Y. Choi, H. M. Ryoo and S. C. Bae** (2000). "Runx2 is a common target of transforming growth factor beta1 and bone morphogenetic protein 2, and cooperation between Runx2 and Smad5 induces osteoblast-specific gene expression in the pluripotent mesenchymal precursor cell line C2C12." *Mol Cell Biol* 20(23): 8783-92.
- Lefebvre, V. and P. Smits** (2005). "Transcriptional control of chondrocyte fate and differentiation." *Birth Defects Res C Embryo Today* 75(3): 200-12.
- Lejeune, F., X. Li and L. E. Maquat** (2003). "Nonsense-mediated mRNA decay in mammalian cells involves decapping, deadenylation, and exonucleolytic activities." *Mol Cell* 12(3): 675-87.
- Lethias, C., F. Elefteriou, G. Parsiegla, J. Y. Exposito and R. Garrone** (2001). "Identification and characterization of a conformational heparin-binding site involving two fibronectin type III modules of bovine tenascin-X." *J Biol Chem* 276(19): 16432-8.
- Li, K., K. Tamai, E. M. Tan and J. Uitto** (1993). "Cloning of type XVII collagen. Complementary and genomic DNA sequences of mouse 180-kilodalton bullous pemphigoid antigen (BPAG2) predict an interrupted collagenous domain, a transmembrane segment, and unusual features in the 5'-end of the gene and the 3'-untranslated region of the mRNA." *J Biol Chem* 268(12): 8825-34.
- Li, Q., Z. Liu, H. Monroe and C. T. Cui** (2002). "Integrated platform for detection of DNA sequence variants using capillary array electrophoresis." *Electrophoresis* 23(10): 1499-511.
- Liu, Y. H., Z. Tang, R. K. Kundu, L. Wu, W. Luo, D. Zhu, F. Sangiorgi, M. L. Snead and R. E. Maxson** (1999). "Msx2 gene dosage influences the number of proliferative osteogenic cells in growth centers of the developing murine skull: a possible mechanism for MSX2-mediated craniosynostosis in humans." *Dev Biol* 205(2): 260-74.
- Lu, S. S., X. Zhang, C. Soo, T. Hsu, A. Napoli, T. Aghaloo, B. M. Wu, P. Tsou, K. Ting and J. C. Wang** (2007). "The osteoinductive properties of Nell-1 in a rat spinal fusion model." *Spine J* 7(1): 50-60.

- Luce, M. J. and P. D. Burrows** (1999). "The neuronal EGF-related genes NELL1 and NELL2 are expressed in hemopoietic cells and developmentally regulated in the B lineage." *Gene* 231(1-2): 121-6.
- Lyon, M. F., T. R. King, Y. Gondo, J. M. Gardner, Y. Nakatsu, E. M. Eicher and M. H. Brilliant** (1992). "Genetic and molecular analysis of recessive alleles at the pink-eyed dilution (p) locus of the mouse." *Proc Natl Acad Sci U S A* 89(15): 6968-72.
- Mackie, E. J., I. Thesleff and R. Chiquet-Ehrismann** (1987). "Tenascin is associated with chondrogenic and osteogenic differentiation in vivo and promotes chondrogenesis in vitro." *J Cell Biol* 105(6 Pt 1): 2569-79.
- Mackie, E. J. and R. P. Tucker** (1992). "Tenascin in bone morphogenesis: expression by osteoblasts and cell type-specific expression of splice variants." *J Cell Sci* 103 (Pt 3): 765-71.
- Maeda, K., S. Matsushashi, K. Tabuchi, T. Watanabe, T. Katagiri, M. Oyasu, N. Saito and S. Kuroda** (2001). "Brain specific human genes, NELL1 and NELL2, are predominantly expressed in neuroblastoma and other embryonal neuroepithelial tumors." *Neurol Med Chir (Tokyo)* 41(12): 582-8; discussion 589.
- Makihira, S., W. Yan, S. Ohno, T. Kawamoto, K. Fujimoto, A. Okimura, E. Yoshida, M. Noshiro, T. Hamada and Y. Kato** (1999). "Enhancement of cell adhesion and spreading by a cartilage-specific noncollagenous protein, cartilage matrix protein (CMP/Matrilin-1), via integrin alpha1beta1." *J Biol Chem* 274(16): 11417-23.
- Malfait, F. and A. De Paepe** (2005). "Molecular genetics in classic Ehlers-Danlos syndrome." *Am J Med Genet C Semin Med Genet* 139(1): 17-23.
- Mansson, B., C. Wenglen, M. Morgelin, T. Saxne and D. Heinegard** (2001). "Association of chondroadherin with collagen type II." *J Biol Chem* 276(35): 32883-8.
- Mao, J. R. and J. Bristow** (2001). "The Ehlers-Danlos syndrome: on beyond collagens." *J Clin Invest* 107(9): 1063-9.
- Mao, J. R., G. Taylor, W. B. Dean, D. R. Wagner, V. Afzal, J. C. Lotz, E. M. Rubin and J. Bristow** (2002). "Tenascin-X deficiency mimics Ehlers-Danlos syndrome in mice through alteration of collagen deposition." *Nat Genet* 30(4): 421-5.
- Marcelino, J., J. D. Carpten, W. M. Suwairi, O. M. Gutierrez, S. Schwartz, C. Robbins, R. Sood, I. Makalowska, A. Baxevanis, B. Johnstone, R. M. Laxer, L. Zemel, C. A. Kim, J. K. Herd, J. Ihle, C. Williams, M. Johnson, V. Raman, L. G. Alonso, D. Brunoni, A. Gerstein, N. Papadopoulos, S. A. Bahabri, J. M. Trent and M. L. Warman** (1999). "CACP, encoding a secreted proteoglycan, is mutated in camptodactyly-arthropathy-coxa vara-pericarditis syndrome." *Nat Genet* 23(3): 319-22.
- Marie, P. J.** (2003). "Fibroblast growth factor signaling controlling osteoblast differentiation." *Gene* 316: 23-32.
- Marie, P. J., F. Debais and E. Hay** (2002). "Regulation of human cranial osteoblast phenotype by FGF-2, FGFR-2 and BMP-2 signaling." *Histol Histopathol* 17(3): 877-85.
- Marvulli, D., D. Volpin and G. M. Bressan** (1996). "Spatial and temporal changes of type VI collagen expression during mouse development." *Dev Dyn* 206(4): 447-54.
- Mates, L., C. Nicolae, M. Morgelin, F. Deak, I. Kiss and A. Aszodi** (2004). "Mice lacking the extracellular matrix adaptor protein matrilin-2 develop without obvious abnormalities." *Matrix Biol* 23(3): 195-204.

- Matsuda, A., A. Yoshiki, Y. Tagawa, H. Matsuda and M. Kusakabe** (1999). "Corneal wound healing in tenascin knockout mouse." *Invest Ophthalmol Vis Sci* 40(6): 1071-80.
- Matsubishi, S., S. Noji, E. Koyama, F. Myokai, H. Ohuchi, S. Taniguchi and K. Hori** (1995). "New gene, nel, encoding a M(r) 93 K protein with EGF-like repeats is strongly expressed in neural tissues of early stage chick embryos." *Dev Dyn* 203(2): 212-22.
- Matsumoto, A., K. Yamaji, M. Kawanami and H. Kato** (2001). "Effect of aging on bone formation induced by recombinant human bone morphogenetic protein-2 combined with fibrous collagen membranes at subperiosteal sites." *J Periodontal Res* 36(3): 175-82.
- Matsumoto, K., Y. Saga, T. Ikemura, T. Sakakura and R. Chiquet-Ehrismann** (1994). "The distribution of tenascin-X is distinct and often reciprocal to that of tenascin-C." *J Cell Biol* 125(2): 483-93.
- Mehrrara, B. J., J. A. Spector, J. A. Greenwald, H. Ueno and M. T. Longaker** (2002). "Adenovirus-mediated transmission of a dominant negative transforming growth factor-beta receptor inhibits in vitro mouse cranial suture fusion." *Plast Reconstr Surg* 110(2): 506-14.
- Miller, R. R. and C. A. McDevitt** (1991). "Thrombospondin in ligament, meniscus and intervertebral disc." *Biochim Biophys Acta* 1115(1): 85-8.
- Minamitani, T., H. Ariga and K. Matsumoto** (2004). "Deficiency of tenascin-X causes a decrease in the level of expression of type VI collagen." *Exp Cell Res* 297(1): 49-60.
- Minamitani, T., T. Ikuta, Y. Saito, G. Takebe, M. Sato, H. Sawa, T. Nishimura, F. Nakamura, K. Takahashi, H. Ariga and K. Matsumoto** (2004). "Modulation of collagen fibrillogenesis by tenascin-X and type VI collagen." *Exp Cell Res* 298(1): 305-15.
- Mishina, Y., A. Suzuki, N. Ueno and R. R. Behringer** (1995). "Bmpr encodes a type I bone morphogenetic protein receptor that is essential for gastrulation during mouse embryogenesis." *Genes Dev* 9(24): 3027-37.
- Mizuno, M., R. Fujisawa and Y. Kuboki** (1996). "Bone chondroadherin promotes attachment of osteoblastic cells to solid-state substrates and shows affinity to collagen." *Calcif Tissue Int* 59(3): 163-7.
- Mori, Y., K. Cai, Y. Cheng, S. Wang, B. Paun, J. P. Hamilton, Z. Jin, F. Sato, A. T. Berki, T. Kan, T. Ito, C. Mantzur, J. M. Abraham and S. J. Meltzer** (2006). "A genome-wide search identifies epigenetic silencing of somatostatin, tachykinin-1, and 5 other genes in colon cancer." *Gastroenterology* 131(3): 797-808.
- Muenke, M., K. W. Gripp, D. M. McDonald-McGinn, K. Gaudenz, L. A. Whitaker, S. P. Bartlett, R. I. Markowitz, N. H. Robin, N. Nwokoro, J. J. Mulvihill, H. W. Losken, J. B. Mulliken, A. E. Guttmacher, R. S. Wilroy, L. A. Clarke, G. Hollway, L. C. Ades, E. A. Haan, J. C. Mulley, M. M. Cohen, Jr., G. A. Bellus, C. A. Francomano, D. M. Moloney, S. A. Wall, A. O. Wilkie and et al.** (1997). "A unique point mutation in the fibroblast growth factor receptor 3 gene (FGFR3) defines a new craniosynostosis syndrome." *Am J Hum Genet* 60(3): 555-64.
- Mundlos, S., L. F. Huang, P. Selby and B. R. Olsen** (1996). "Cleidocranial dysplasia in mice." *Ann N Y Acad Sci* 785: 301-2.

- Myllyharju, J. and K. I. Kivirikko** (2004). "Collagens, modifying enzymes and their mutations in humans, flies and worms." *Trends Genet* 20(1): 33-43.
- Nagy, E. and L. E. Maquat** (1998). "A rule for termination-codon position within intron-containing genes: when nonsense affects RNA abundance." *Trends Biochem Sci* 23(6): 198-9.
- Nah, H. D. and W. B. Upholt** (1991). "Type II collagen mRNA containing an alternatively spliced exon predominates in the chick limb prior to chondrogenesis." *J Biol Chem* 266(34): 23446-52.
- Nakao, N., N. Hiraiwa, A. Yoshiki, F. Ike and M. Kusakabe** (1998). "Tenascin-C promotes healing of Habu-snake venom-induced glomerulonephritis: studies in knockout congenic mice and in culture." *Am J Pathol* 152(5): 1237-45.
- Natali, P. G., M. R. Nicotra, A. Bigotti, C. Botti, P. Castellani, A. M. Risso and L. Zardi** (1991). "Comparative analysis of the expression of the extracellular matrix protein tenascin in normal human fetal, adult and tumor tissues." *Int J Cancer* 47(6): 811-6.
- Nerlich, A. G., N. Boos, I. Wiest and M. Aebi** (1998). "Immunolocalization of major interstitial collagen types in human lumbar intervertebral discs of various ages." *Virchows Arch* 432(1): 67-76.
- Nishizuka, Y.** (1988). "The molecular heterogeneity of protein kinase C and its implications for cellular regulation." *Nature* 334(6184): 661-5.
- Noveroske, J. K., J. S. Weber and M. J. Justice** (2000). "The mutagenic action of N-ethyl-N-nitrosourea in the mouse." *Mamm Genome* 11(7): 478-83.
- Oh, S. P., M. L. Warman, M. F. Seldin, S. D. Cheng, J. H. Knoll, S. Timmons and B. R. Olsen** (1994). "Cloning of cDNA and genomic DNA encoding human type XVIII collagen and localization of the alpha 1(XVIII) collagen gene to mouse chromosome 10 and human chromosome 21." *Genomics* 19(3): 494-9.
- Opperman, L. A., K. Adab and P. T. Gakunga** (2000). "Transforming growth factor-beta 2 and TGF-beta 3 regulate fetal rat cranial suture morphogenesis by regulating rates of cell proliferation and apoptosis." *Dev Dyn* 219(2): 237-47.
- Otto, F., A. P. Thornell, T. Crompton, A. Denzel, K. C. Gilmour, I. R. Rosewell, G. W. Stamp, R. S. Beddington, S. Mundlos, B. R. Olsen, P. B. Selby and M. J. Owen** (1997). "Cbfa1, a candidate gene for cleidocranial dysplasia syndrome, is essential for osteoblast differentiation and bone development." *Cell* 89(5): 765-71.
- Pacifici, M.** (1995). "Tenascin-C and the development of articular cartilage." *Matrix Biol* 14(9): 689-98.
- Pacifici, M., M. Iwamoto, E. B. Golden, J. L. Leatherman, Y. S. Lee and C. M. Chuong** (1993). "Tenascin is associated with articular cartilage development." *Dev Dyn* 198(2): 123-34.
- Peters, H., B. Wilm, N. Sakai, K. Imai, R. Maas and R. Balling** (1999). "Pax1 and Pax9 synergistically regulate vertebral column development." *Development* 126(23): 5399-408.
- Pourquie, O.** (2003). "The segmentation clock: converting embryonic time into spatial pattern." *Science* 301(5631): 328-30.
- Prockop, D. J. and K. I. Kivirikko** (1995). "Collagens: molecular biology, diseases, and potentials for therapy." *Annu Rev Biochem* 64: 403-34.

- Qabar, A. N., Z. Lin, F. W. Wolf, K. S. O'Shea, J. Lawler and V. M. Dixit** (1994). "Thrombospondin 3 is a developmentally regulated heparin binding protein." *J Biol Chem* 269(2): 1262-9.
- Ramchandran, R., M. Dhanabal, R. Volk, M. J. Waterman, M. Segal, H. Lu, B. Knebelmann and V. P. Sukhatme** (1999). "Antiangiogenic activity of restin, NC10 domain of human collagen XV: comparison to endostatin." *Biochem Biophys Res Commun* 255(3): 735-9.
- Reardon, W., R. M. Winter, P. Rutland, L. J. Pulleyn, B. M. Jones and S. Malcolm** (1994). "Mutations in the fibroblast growth factor receptor 2 gene cause Crouzon syndrome." *Nat Genet* 8(1): 98-103.
- Rhee, D. K., J. Marcelino, M. Baker, Y. Gong, P. Smits, V. Lefebvre, G. D. Jay, M. Stewart, H. Wang, M. L. Warman and J. D. Carpten** (2005). "The secreted glycoprotein lubricin protects cartilage surfaces and inhibits synovial cell overgrowth." *J Clin Invest* 115(3): 622-31.
- Rinchik, E. M.** (2000). "Developing genetic reagents to facilitate recovery, analysis, and maintenance of mouse mutations." *Mamm Genome* 11(7): 489-99.
- Rinchik, E. M. and D. A. Carpenter** (1999). "N-ethyl-N-nitrosourea mutagenesis of a 6- to 11-cM subregion of the Fah-Hbb interval of mouse chromosome 7: Completed testing of 4557 gametes and deletion mapping and complementation analysis of 31 mutations." *Genetics* 152(1): 373-83.
- Rinchik, E. M., D. A. Carpenter and D. K. Johnson** (2002). "Functional annotation of mammalian genomic DNA sequence by chemical mutagenesis: a fine-structure genetic mutation map of a 1- to 2-cM segment of mouse chromosome 7 corresponding to human chromosome 11p14-p15." *Proc Natl Acad Sci U S A* 99(2): 844-9.
- Roberts, S., S. Ayad and P. J. Menage** (1991). "Immunolocalisation of type VI collagen in the intervertebral disc." *Ann Rheum Dis* 50(11): 787-91.
- Rosado, E., Z. Schwartz, V. L. Sylvia, D. D. Dean and B. D. Boyan** (2002). "Transforming growth factor-beta1 regulation of growth zone chondrocytes is mediated by multiple interacting pathways." *Biochim Biophys Acta* 1590(1-3): 1-15.
- Roth-Kleiner, M., E. Hirsch and J. C. Schittny** (2004). "Fetal lungs of tenascin-C-deficient mice grow well, but branch poorly in organ culture." *Am J Respir Cell Mol Biol* 30(3): 360-6.
- Rozen, S. and H. Skaletsky** (2000). "Primer3 on the WWW for general users and for biologist programmers." *Methods Mol Biol* 132: 365-86.
- Saga, Y., T. Tsukamoto, N. Jing, M. Kusakabe and T. Sakakura** (1991). "Murine tenascin: cDNA cloning, structure and temporal expression of isoforms." *Gene* 104(2): 177-85.
- Saga, Y., T. Yagi, Y. Ikawa, T. Sakakura and S. Aizawa** (1992). "Mice develop normally without tenascin." *Genes Dev* 6(10): 1821-31.
- Sahlman, J., M. T. Pitkanen, D. J. Prockop, M. Arita, S. W. Li, H. J. Helminen, T. K. Langsjo, K. Puustjarvi and M. J. Lammi** (2004). "A human COL2A1 gene with an Arg519Cys mutation causes osteochondrodysplasia in transgenic mice." *Arthritis Rheum* 50(10): 3153-60.
- Sakou, T.** (1998). "Bone morphogenetic proteins: from basic studies to clinical approaches." *Bone* 22(6): 591-603.

- Salmivirta, M., K. Elenius, S. Vainio, U. Hofer, R. Chiquet-Ehrismann, I. Thesleff and M. Jalkanen** (1991). "Syndecan from embryonic tooth mesenchyme binds tenascin." *J Biol Chem* 266(12): 7733-9.
- Sambrook, J., Fritsch, E. F. and Maniatis, T.** (1989). *Molecular Cloning: A Laboratory Manual*, Cold Spring Harbor Laboratory Press, New York, USA.
- Sandell, L. J., N. Morris, J. R. Robbins and M. B. Goldring** (1991). "Alternatively spliced type II procollagen mRNAs define distinct populations of cells during vertebral development: differential expression of the amino-propeptide." *J Cell Biol* 114(6): 1307-19.
- Sasaki, T., H. Larsson, D. Tisi, L. Claesson-Welsh, E. Hohenester and R. Timpl** (2000). "Endostatins derived from collagens XV and XVIII differ in structural and binding properties, tissue distribution and anti-angiogenic activity." *J Mol Biol* 301(5): 1179-90.
- Satokata, I., L. Ma, H. Ohshima, M. Bei, I. Woo, K. Nishizawa, T. Maeda, Y. Takano, M. Uchiyama, S. Heaney, H. Peters, Z. Tang, R. Maxson and R. Maas** (2000). "Msx2 deficiency in mice causes pleiotropic defects in bone growth and ectodermal organ formation." *Nat Genet* 24(4): 391-5.
- Sawin, P. D., V. C. Traynelis and A. H. Menezes** (1998). "A comparative analysis of fusion rates and donor-site morbidity for autogeneic rib and iliac crest bone grafts in posterior cervical fusions." *J Neurosurg* 88(2): 255-65.
- Schalkwijk, J., M. C. Zweers, P. M. Steijlen, W. B. Dean, G. Taylor, I. M. van Vlijmen, B. van Haren, W. L. Miller and J. Bristow** (2001). "A recessive form of the Ehlers-Danlos syndrome caused by tenascin-X deficiency." *N Engl J Med* 345(16): 1167-75.
- Schwarze, U., M. Atkinson, G. G. Hoffman, D. S. Greenspan and P. H. Byers** (2000). "Null alleles of the COL5A1 gene of type V collagen are a cause of the classical forms of Ehlers-Danlos syndrome (types I and II)." *Am J Hum Genet* 66(6): 1757-65.
- Semba, I., K. Nonaka, I. Takahashi, K. Takahashi, R. Dashner, L. Shum, G. H. Nuckolls and H. C. Slavkin** (2000). "Positionally-dependent chondrogenesis induced by BMP4 is co-regulated by Sox9 and Msx2." *Dev Dyn* 217(4): 401-14.
- Sertie, A. L., V. Sossi, A. A. Camargo, M. Zatz, C. Brahe and M. R. Passos-Bueno** (2000). "Collagen XVIII, containing an endogenous inhibitor of angiogenesis and tumor growth, plays a critical role in the maintenance of retinal structure and in neural tube closure (Knobloch syndrome)." *Hum Mol Genet* 9(13): 2051-8.
- Shen, Z., S. Gantcheva, B. Mansson, D. Heinegard and Y. Sommarin** (1998). "Chondroadherin expression changes in skeletal development." *Biochem J* 330 (Pt 1): 549-57.
- Shiraishi, M., A. Sekiguchi, M. J. Terry, A. J. Oates, Y. Miyamoto, Y. H. Chuu, M. Munakata and T. Sekiya** (2002). "A comprehensive catalog of CpG islands methylated in human lung adenocarcinomas for the identification of tumor suppressor genes." *Oncogene* 21(23): 3804-13.
- Shirakabe, K., K. Terasawa, K. Miyama, H. Shibuya and E. Nishida** (2001). "Regulation of the activity of the transcription factor Runx2 by two homeobox proteins, Msx2 and Dlx5." *Genes Cells* 6(10): 851-6.

- Shum, L. and G. Nuckolls** (2002). "The life cycle of chondrocytes in the developing skeleton." *Arthritis Res* 4(2): 94-106.
- Simmons, P. J., J. P. Levesque and D. N. Haylock** (2001). "Mucin-like molecules as modulators of the survival and proliferation of primitive hematopoietic cells." *Ann N Y Acad Sci* 938: 196-206; discussion 206-7.
- Sofaer, J. A.** (1985). "Developmental stability in the mouse vertebral column." *J Anat* 140 (Pt 1): 131-41.
- Soini, Y., D. Kamel, M. Apaja-Sarkkinen, I. Virtanen and V. P. Lehto** (1993). "Tenascin immunoreactivity in normal and pathological bone marrow." *J Clin Pathol* 46(3): 218-21.
- Solloway, M. J., A. T. Dudley, E. K. Bikoff, K. M. Lyons, B. L. Hogan and E. J. Robertson** (1998). "Mice lacking Bmp6 function." *Dev Genet* 22(4): 321-39.
- Sparrow, D. B., G. Chapman, M. A. Wouters, N. V. Whittock, S. Ellard, D. Fatkin, P. D. Turnpenny, K. Kusumi, D. Silence and S. L. Dunwoodie** (2006). "Mutation of the LUNATIC FRINGE gene in humans causes spondylocostal dysostosis with a severe vertebral phenotype." *Am J Hum Genet* 78(1): 28-37.
- Stefansson, S. E., H. Jonsson, T. Ingvarsson, I. Manolescu, H. H. Jonsson, G. Olafsdottir, E. Palsdottir, G. Stefansdottir, G. Sveinbjornsdottir, M. L. Frigge, A. Kong, J. R. Gulcher and K. Stefansson** (2003). "Genomewide scan for hand osteoarthritis: a novel mutation in matrilin-3." *Am J Hum Genet* 72(6): 1448-59.
- Stein, G. S. and J. B. Lian** (1993). "Molecular mechanisms mediating proliferation/differentiation interrelationships during progressive development of the osteoblast phenotype." *Endocr Rev* 14(4): 424-42.
- Svensson, K., R. Zeidman, U. Troller, A. Schultz and C. Larsson** (2000). "Protein kinase C beta1 is implicated in the regulation of neuroblastoma cell growth and proliferation." *Cell Growth Differ* 11(12): 641-8.
- Takeda, S., J. P. Bonnamy, M. J. Owen, P. Ducy and G. Karsenty** (2001). "Continuous expression of Cbfa1 in nonhypertrophic chondrocytes uncovers its ability to induce hypertrophic chondrocyte differentiation and partially rescues Cbfa1-deficient mice." *Genes Dev* 15(4): 467-81.
- Tamaoki, M., K. Imanaka-Yoshida, K. Yokoyama, T. Nishioka, H. Inada, M. Hiroe, T. Sakakura and T. Yoshida** (2005). "Tenascin-C regulates recruitment of myofibroblasts during tissue repair after myocardial injury." *Am J Pathol* 167(1): 71-80.
- Tanaka, T., K. Ikari, K. Furushima, A. Okada, H. Tanaka, K. Furukawa, K. Yoshida, T. Ikeda, S. Ikegawa, S. C. Hunt, J. Takeda, S. Toh, S. Harata, T. Nakajima and I. Inoue** (2003). "Genomewide linkage and linkage disequilibrium analyses identify COL6A1, on chromosome 21, as the locus for ossification of the posterior longitudinal ligament of the spine." *Am J Hum Genet* 73(4): 812-22.
- ten Dijke, P., H. Yamashita, H. Ichijo, P. Franzen, M. Laiho, K. Miyazono and C. H. Heldin** (1994). "Characterization of type I receptors for transforming growth factor-beta and activin." *Science* 264(5155): 101-4.
- Thesleff, I., T. Kantomaa, E. Mackie and R. Chiquet-Ehrismann** (1988). "Immunohistochemical localization of the matrix glycoprotein tenascin in the skull of the growing rat." *Arch Oral Biol* 33(6): 383-90.

- Thomas, J. T., S. Ayad and M. E. Grant** (1994). "Cartilage collagens: strategies for the study of their organisation and expression in the extracellular matrix." *Ann Rheum Dis* 53(8): 488-96.
- Thorogood, P., J. Bee and K. von der Mark** (1986). "Transient expression of collagen type II at epitheliomesenchymal interfaces during morphogenesis of the cartilaginous neurocranium." *Dev Biol* 116(2): 497-509.
- Ting, K., H. Vastardis, J. B. Mulliken, C. Soo, A. Tieu, H. Do, E. Kwong, C. N. Bertolami, H. Kawamoto, S. Kuroda and M. T. Longaker** (1999). "Human NELL-1 expressed in unilateral coronal synostosis." *J Bone Miner Res* 14(1): 80-9.
- Truong, T., X. Zhang, D. Pathmanathan, C. Soo and K. Ting** (2007). "Craniosynostosis-associated gene nell-1 is regulated by runx2." *J Bone Miner Res* 22(1): 7-18.
- Tsuji, K., Y. Ito and M. Noda** (1998). "Expression of the PEBP2alphaA/AML3/CBFA1 gene is regulated by BMP4/7 heterodimer and its overexpression suppresses type I collagen and osteocalcin gene expression in osteoblastic and nonosteoblastic mesenchymal cells." *Bone* 22(2): 87-92.
- Tucker, R. P., K. Drabikowski, J. F. Hess, J. Ferralli, R. Chiquet-Ehrismann and J. C. Adams** (2006). "Phylogenetic analysis of the tenascin gene family: evidence of origin early in the chordate lineage." *BMC Evol Biol* 6: 60.
- Tucker, R. P., C. Hagios, R. Chiquet-Ehrismann and J. Lawler** (1997). "In situ localization of thrombospondin-1 and thrombospondin-3 transcripts in the avian embryo." *Dev Dyn* 208(3): 326-37.
- Tucker, R. P., J. Spring, S. Baumgartner, D. Martin, C. Hagios, P. M. Poss and R. Chiquet-Ehrismann** (1994). "Novel tenascin variants with a distinctive pattern of expression in the avian embryo." *Development* 120(3): 637-47.
- Valentin-Opran, A., J. Wozney, C. Csimma, L. Lilly and G. E. Riedel** (2002). "Clinical evaluation of recombinant human bone morphogenetic protein-2." *Clin Orthop Relat Res*(395): 110-20.
- van den Bergh, J. P., C. M. ten Bruggenkate, H. H. Groeneveld, E. H. Burger and D. B. Tuinzing** (2000). "Recombinant human bone morphogenetic protein-7 in maxillary sinus floor elevation surgery in 3 patients compared to autogenous bone grafts. A clinical pilot study." *J Clin Periodontol* 27(9): 627-36.
- van der Rest, M. and R. Garrone** (1991). "Collagen family of proteins." *Faseb J* 5(13): 2814-23.
- Van Klinken, B. J., J. Dekker, H. A. Buller and A. W. Einerhand** (1995). "Mucin gene structure and expression: protection vs. adhesion." *Am J Physiol* 269(5 Pt 1): G613-27.
- Vandesompele, J., K. De Preter, F. Pattyn, B. Poppe, N. Van Roy, A. De Paepe and F. Speleman** (2002). "Accurate normalization of real-time quantitative RT-PCR data by geometric averaging of multiple internal control genes." *Genome Biol* 3(7): RESEARCH0034.
- Vos, H. L., S. Devarayalu, Y. de Vries and P. Bornstein** (1992). "Thrombospondin 3 (Thbs3), a new member of the thrombospondin gene family." *J Biol Chem* 267(17): 12192-6.

- Warman, M. L., M. Abbott, S. S. Apte, T. Hefferon, I. McIntosh, D. H. Cohn, J. T. Hecht, B. R. Olsen and C. A. Francomano** (1993). "A type X collagen mutation causes Schmid metaphyseal chondrodysplasia." *Nat Genet* 5(1): 79-82.
- Watanabe, T. K., T. Katagiri, M. Suzuki, F. Shimizu, T. Fujiwara, N. Kanemoto, Y. Nakamura, Y. Hirai, H. Maekawa and E. Takahashi** (1996). "Cloning and characterization of two novel human cDNAs (NELL1 and NELL2) encoding proteins with six EGF-like repeats." *Genomics* 38(3): 273-6.
- Watanabe, Y., D. Duprez, A. H. Monsoro-Burq, C. Vincent and N. M. Le Douarin** (1998). "Two domains in vertebral development: antagonistic regulation by SHH and BMP4 proteins." *Development* 125(14): 2631-9.
- Weber, P., U. Bartsch, M. N. Rasband, R. Czaniera, Y. Lang, H. Bluethmann, R. U. Margolis, S. R. Levinson, P. Shrager, D. Montag and M. Schachner** (1999). "Mice deficient for tenascin-R display alterations of the extracellular matrix and decreased axonal conduction velocities in the CNS." *J Neurosci* 19(11): 4245-62.
- Wiberg, C., A. R. Klatt, R. Wagener, M. Paulsson, J. F. Bateman, D. Heinegard and M. Morgelin** (2003). "Complexes of matrilin-1 and biglycan or decorin connect collagen VI microfibrils to both collagen II and aggrecan." *J Biol Chem* 278(39): 37698-704.
- Wilkie, A. O.** (1997). "Craniosynostosis: genes and mechanisms." *Hum Mol Genet* 6(10): 1647-56.
- Wilkie, A. O., Z. Tang, N. Elanko, S. Walsh, S. R. Twigg, J. A. Hurst, S. A. Wall, K. H. Chrzanowska and R. E. Maxson, Jr.** (2000). "Functional haploinsufficiency of the human homeobox gene *MSX2* causes defects in skull ossification." *Nat Genet* 24(4): 387-90.
- Winterbottom, N., M. M. Tondravi, T. L. Harrington, F. G. Klier, B. M. Vertel and P. F. Goetinck** (1992). "Cartilage matrix protein is a component of the collagen fibril of cartilage." *Dev Dyn* 193(3): 266-76.
- Wolfman, N. M., G. Hattersley, K. Cox, A. J. Celeste, R. Nelson, N. Yamaji, J. L. Dube, E. DiBlasio-Smith, J. Nove, J. J. Song, J. M. Wozney and V. Rosen** (1997). "Ectopic induction of tendon and ligament in rats by growth and differentiation factors 5, 6, and 7, members of the TGF-beta gene family." *J Clin Invest* 100(2): 321-30.
- Wozney, J. M., V. Rosen, A. J. Celeste, L. M. Mitsock, M. J. Whitters, R. W. Kriz, R. M. Hewick and E. A. Wang** (1988). "Novel regulators of bone formation: molecular clones and activities." *Science* 242(4885): 1528-34.
- Yang, R. S., C. H. Tang, Q. D. Ling, S. H. Liu and W. M. Fu** (2002). "Regulation of fibronectin fibrillogenesis by protein kinases in cultured rat osteoblasts." *Mol Pharmacol* 61(5): 1163-73.
- Yeowell, H. N. and L. C. Walker** (2000). "Mutations in the lysyl hydroxylase 1 gene that result in enzyme deficiency and the clinical phenotype of Ehlers-Danlos syndrome type VI." *Mol Genet Metab* 71(1-2): 212-24.
- Yoon, B. S., D. A. Ovchinnikov, I. Yoshii, Y. Mishina, R. R. Behringer and K. M. Lyons** (2005). "*Bmpr1a* and *Bmpr1b* have overlapping functions and are essential for chondrogenesis in vivo." *Proc Natl Acad Sci U S A* 102(14): 5062-7.
- Yoshizawa, T., F. Takizawa, F. Iizawa, O. Ishibashi, H. Kawashima, A. Matsuda, N. Endo and H. Kawashima** (2004). "Homeobox protein *MSX2* acts as a molecular

- defense mechanism for preventing ossification in ligament fibroblasts." *Mol Cell Biol* 24(8): 3460-72.
- Young, A. A., S. McLennan, M. M. Smith, S. M. Smith, M. A. Cake, R. A. Read, J. Melrose, D. H. Sonnabend, C. R. Flannery and C. B. Little** (2006). "Proteoglycan 4 downregulation in a sheep meniscectomy model of early osteoarthritis." *Arthritis Res Ther* 8(2): R41.
- Zelzer, E. and B. R. Olsen** (2003). "The genetic basis for skeletal diseases." *Nature* 423(6937): 343-8.
- Zhang, X., D. Carpenter, N. Bokui, C. Soo, S. Miao, T. Truong, B. Wu, I. Chen, H. Vastardis, K. Tanizawa, S. Kuroda and K. Ting** (2003). "Overexpression of *Nell-1*, a craniosynostosis-associated gene, induces apoptosis in osteoblasts during craniofacial development." *J Bone Miner Res* 18(12): 2126-34.
- Zhang, X., C. M. Cowan, X. Jiang, C. Soo, S. Miao, D. Carpenter, B. Wu, S. Kuroda and K. Ting** (2006). "*Nell-1* induces acrania-like cranioskeletal deformities during mouse embryonic development." *Lab Invest* 86(7): 633-44.
- Zhang, X., S. Kuroda, D. Carpenter, I. Nishimura, C. Soo, R. Moats, K. Iida, E. Wisner, F. Y. Hu, S. Miao, S. Beanes, C. Dang, H. Vastardis, M. Longaker, K. Tanizawa, N. Kanayama, N. Saito and K. Ting** (2002). "Craniosynostosis in transgenic mice overexpressing *Nell-1*." *J Clin Invest* 110(6): 861-70.
- Zheng, Q., G. Zhou, R. Morello, Y. Chen, X. Garcia-Rojas and B. Lee** (2003). "Type X collagen gene regulation by *Runx2* contributes directly to its hypertrophic chondrocyte-specific expression in vivo." *J Cell Biol* 162(5): 833-42.
- Zweers, M. C., W. B. Dean, T. H. van Kuppevelt, J. Bristow and J. Schalkwijk** (2005). "Elastic fiber abnormalities in hypermobility type Ehlers-Danlos syndrome patients with tenascin-X mutations." *Clin Genet* 67(4): 330-4.

VITA

Jayashree Desai was born in Belgaum, India. She received a Bachelor of Science degree in Microbiology in 1994 from the University of Tennessee at Knoxville TN. She then worked in Dr. Donald Torry's laboratory, Department of Obstetrics and Gynecology, Graduate School of Medicine Knoxville, TN. In August 1997, she reentered the University of Tennessee to pursue the Master of Science degree in Comparative and Experimental Medicine. The Master of Science degree was received in December 1999. Her thesis work was entitled the "Molecular and Cellular Responses of Normal Human Trophoblast to Vascular Endothelial Growth Factor and Placenta Growth Factor" She then worked as a senior research associate in Dr. Torry's laboratory at the University of Tennessee Medical Center and then as a senior research assistant in Dr. Cymbeline Culiati's laboratory at the Oak Ridge National Laboratory. Later she reentered the University of Tennessee in 2003 to pursue her Doctorate in Life Sciences with a concentration in Genome Science and Technology. She worked on her doctoral research project under the guidance of Dr. Cymbeline Culiati at the Oak Ridge National Laboratory. She graduated with a Ph.D in 2007. She is planning to continue her career as a research scientist and is currently perusing her research options.